A MOLECULAR MECHANISM FOR DEPTOR IN THE CONTROL OF CELLULAR METABOLISM AND DISEASE

A Dissertation

by

JOHN WILLIAM DEAVER

Submitted to the Office of Graduate and Professional Studies of
Texas A&M University
in partial fulfillment of the requirements for the degree of

DOCTOR OF PHILOSOPHY

Chair of Committee,	James D. Fluckey
Committee Members,	J. Timothy Lightfoot
	Michael Massett
	Penny K. Riggs
Head of Department,	Melinda Sheffield-Moore

December 2020

Major Subject: Kinesiology

ABSTRACT

One of the main hubs of cellular metabolic integration is the mechanistic target of rapamycin, or mTOR. In normal, healthy cells, mTOR helps to regulate and balance cellular growth and proliferation against metabolic conservation and maintenance. However, when cellular conditions deteriorate due to environmental stressors or genetic mutations, mTOR's contribution towards normal cellular metabolism can become dysregulated, leading to a number of disease states in different tissues, including type 2 diabetes, a large percentage of human cancers, Parkinson's disease, Alzheimer's disease, cancer cachexia, and many effects of ageing. One of the primary regulators of mTOR activation is DEPTOR, a potent endogenous inhibitor of mTOR. The purpose of this dissertation is to mechanistically define the role of DEPTOR protein expression in regulating cellular metabolism under various conditions. While the direct relationship between DEPTOR and mTOR has been explored under some steady state conditions, there are only a handful of studies that have explored the use of directed changes in DEPTOR protein content as a means to regulate mTOR activity. By taking advantage of recently developed precision gene editing technologies, we have shown that the chronic and constitutively active expression of DEPTOR protein can act as a potent regulator of cellular anabolism through mTOR in both the normal, healthy C2C12 murine myoblast, and in MCF7 human epithelial cancer cells. This approach offers a number of benefits over pharmacological inhibition of mTOR or of upstream signaling proteins, as those strategies often suffer from a lack of specificity, have inherent cytotoxic properties, or

eventually become ineffective due to altered feedback mechanisms. The current experiments are the first to demonstrate a causative relationship between DEPTOR expression, the resultant mTOR activity, and eventual downstream anabolic function. In addition, the outcomes contained within this dissertation indicate the possibility that certain anabolically aggressive diseases may be treated through directed changes in DEPTOR protein content.

DEDICATION

To the love of my life, Ali Walsh. This would not have been possible without your love, encouragement, and steadfast example of hard work and dedication. You are an inspiration to me and continue to be the greatest thing that has ever happened to me. I don’t know exactly where life will take us, but I am very excited to find out together.

ACKNOWLEDGEMENTS

From the bottom of my heart, I would like to thank everyone that has been a part of this journey through graduate school. Dr. Fluckey, your mentorship and guidance have had an enormous impact on my professional and personal development in your laboratory. I will always cherish our debates and discussions that left us in the laboratory conference room many hours after we intended to go home.

Dr. Riggs, Dr. Lightfoot, and Dr. Massett, your input, encouragement, and guidance have helped craft this dissertation. Not only have you been invaluable assets to me in performing this dissertation project, but I asked you to be on my committee with Dr. Fluckey because you all represent exactly what I hope to achieve professionally. I look up to each of you more than you can know, and I appreciate all of your help in getting me to this point. Thank you to Dr. Susan Bloomfield for taking a chance on me and encouraging me to pursue a master's degree at Texas A&M, I honestly do not have any idea what my life would look like without that guidance.

Thank you, Dr. Peter Nghiem and Dr. Sara Mata Lopez. You were both instrumental in crafting this dissertation, and I appreciate all of the help that you have both provided. Your feedback was always spot on, and I truly appreciate your willingness to hear our laboratory's crazy ideas! Thank you Dr. Riechman for your help in these projects and others. Thank you to Dr. Corrine Metzger and Dr. Heather Allaway for your help with my initial efforts in fluorescence microscopy. I could not have done it without your help.

To my current lab mates: I told you that I wouldn't say goodbye to you, because I know that you will all continue to be a part of my life for as long as I live. Your contributions to this dissertation are far too numerous to list. Colleen, you have been a stalwart companion in the Muscle Biology Lab. When Kevin graduated, he deemed me a successor of sorts and left the day to day operations of the lab in my hands. Now, I can proudly and confidently say the same to you (not that you weren't already basically running the place), and I know that the lab will continue to grow with you as the senior Ph.D. student. Take care of Gary and Maude, they still need close supervision. Pat and Selina, I know that you are both destined for great things in our field. Keep working hard, and keep asking great questions, and it will all pay off in the end. Now, hurry up and graduate so that we can collaborate!

To my former lab mates: thank you for giving me the tools to succeed. Kevin, you taught me how to western blot, how to operate the GC-MS, and how to grow cultured cells. More importantly, you have been an invaluable friend. You saw potential in me and helped me become the scientist that I am today. Amanda, your dedication to your work and to your family is an absolute case study in professional balance, and I hope that I can learn from your example with my current and future family.

As far as family goes, I have been extremely fortunate to have parents that have supported me in everything that I have ever set out to do. Brian and Sherron Deaver deserve more than I can ever repay for their unending love and support. In addition, Ali's parents, Nic and Wendy Walsh, have been an incredible source of love and support. Thank you Nic and Wendy for all that you have done to help get me to this

point. I have been fortunate to be a part of a very large extended family, and they have all given me their continued love and support. Thank you so much to my grandparents and all of my aunts and uncles that have encouraged me throughout my entire life. Your love is incredible.

Finally, thank you Ali. I have said it a million times, and I will say it many millions more: you are the best thing to ever happen to me. You are the hardest working person I have ever met, and you are always pushing yourself to new heights. I could not have done this without your love, your encouragement, or your example.

CONTRIBUTORS AND FUNDING SOURCES

Contributors

This work was supervised by a dissertation committee consisting of Dr. James D. Fluckey (Advisor), Dr. J. Timothy Lightfoot, and Dr. Michael P. Massett of the Department of Health and Kinesiology, and Dr. Penny K. Riggs of the Department of Animal Science.

The fluorescent imaging in Chapters 4 and 5 was obtained with the help of Dr. Corinne Metzger, Dr. Heather Allaway, and Patrick Ryan. Development of new GCMS methods was done with the help of Colleen O'Reilly. Dr. Sara Mata Lopez aided in multiple analyses of genomic DNA. All other work conducted for this dissertation was completed by the student independently.

Funding Sources

This work was made possible in large part by funding from The Sydney & J.L. Huffines Institute for Sports Medicine & Human Performance in the form of a graduate student research award. In addition, this work was funded by multiple graduate research grant awards from the College of Education and Human Development, and a Student Research Development Award from the Texas Chapter of the American College of Sports Medicine. This dissertation's contents are solely the responsibility of the authors and do not necessarily represent the official views of the aforementioned funding sources. Graduate study was supported through graduate teaching assistantships and one

year of a graduate research assistantship through the Department of Health and Kinesiology.

NOMENCLATURE

mTOR	Mechanistic target of rapamycin
DEPTOR	DEP domain containing target of rapamycin
CRISPR	Clustered regularly interspaced short palindromic repeats
NHEJ	Non-homologous end joining
HDR	Homology directed repair
HR	Homologous recombination
HA	Homology arms
GCMS	Gas Chromatograph Mass Spectrometer
FSR	Fractional synthesis rate
MPE	Moles percent excess
GM	Growth media
DM	Differentiation media
FBS	Fetal bovine serum
PBS	Phosphate buffered saline

TABLE OF CONTENTS

Page

LIST OF FIGURES

Page

1. INTRODUCTION

Despite the incredible diversity of life on this planet, there exists a surprising level of consistency in some of the core biological processes. For example, in virtually all organisms capable of aerobic metabolism, there exists a remarkably well preserved citric acid cycle (26, 55). The complex evolution of this system has served as the cornerstone for the development of aerobic respiration for billions of years (88). A much more recent development (relatively) is the appearance of the mechanistic Target of Rapamycin, or mTOR (32, 95). mTOR regulates cellular metabolism from a complex nexus of signaling integration that has been present since before the Last Eukaryotic Common Ancestor, and has been highly conserved across all eukaryotes, while also gaining in complexity through the addition of multiple signaling inputs throughout animal evolution (5, 95). This metabolic regulation allows for the precise promotion of anabolism and limiting of catabolism when cellular conditions are right for growth (50).

However, the same regulatory pathways that allow for such precise control are also prone to dysregulation. Disrupted or dysregulated signaling, both upstream and downstream from mTOR can lead to a variety of human diseases including metabolic diseases, neurodegenerative diseases, cancer, and even ageing (50). Incredibly, mTOR hyperactivation (through various mechanisms) is present in up to 80% of all human cancers (57). This makes mTOR, and both the upstream and downstream associated proteins, extremely popular regulatory targets for manipulation of cellular metabolism under a variety of conditions. Although, many pharmacological agents that have been

directed against the mTOR kinase have proven to be non-specific, cytotoxic, or ineffective at suppressing mTOR activity when used chronically (50).

One of the more recently discovered mTOR-associated proteins is known as the DEP domain-containing mTOR-interacting protein (DEPTOR), and is an intrinsic inhibitor of the mTOR kinase (7, 67). Being an intrinsic inhibitor of mTOR, DEPTOR has been implicated as a possible causative factor in some instances of mTOR dysregulation (7, 8, 10, 16, 39, 41, 45, 56, 60, 96, 98, 99). However, it has also been noted that due to the complex nature of the mTOR-DEPTOR relationship, some of these apparently causative mechanisms may actually be a result of mTOR's direct role in initiating DEPTOR's degradation (7). One potential avenue for determination of the causative nature of the mTOR-DEPTOR interaction would be through the use of experiments designed manipulate that interaction through chronic and constitutive overexpression of DEPTOR and/or the use of pharmacologies designed to prevent that interaction. To our knowledge, no studies exist that have directly assessed the impact of DEPTOR expression and its interaction with mTOR on cellular anabolic/proliferative capacity. To complete these studies, we designed and implemented unique precision gene editing technologies to overexpress DEPTOR protein, which to date has not been previously used in any model, regardless of the cell type.

1.1. Aims of the Experiments

The primary purpose of this dissertation was to explore the causative role of DEPTOR expression on the reduced activation of mTOR and downstream cellular

metabolism. ***The overarching hypothesis for these experiments was that directed changes to DEPTOR will directly translate to a modulation of mTOR activity, thus altering anabolic rates and cellular proliferation.*** The following experiments were used to elucidate the role of modified DEPTOR protein content on cellular metabolism and mTOR activation. As such, this dissertation sought to address three specific aims.

(Specific Aim 1 - SA 1): Investigate the extent of mTOR activation on downstream signaling with directed changes of DEPTOR protein content. Our first hypothesis was that the insertion of our designed gene would upregulate DEPTOR expression in mammalian cells. Further, due to previous work, a second hypothesis was that the cellular overexpression of DEPTOR protein content would reduce native mTOR activation, subsequent downstream signaling, and overall protein synthesis rates.

(Specific Aim 2 - SA 2): Identify the impact of directed changes in DEPTOR levels on rates of cellular proliferation. We hypothesized that directed changes in DEPTOR protein content would have a profound impact on cellular mitotic capacity and differentiation.

(Specific Aim 3 - SA 3): Elucidate the contribution of DEPTOR protein to downstream cellular anabolism through pharmacological inhibition of the DEPTOR-mTOR interaction, with or without DEPTOR overexpression. We hypothesized that the pharmacological prevention of DEPTOR binding to mTOR would completely reverse the impact of DEPTOR overexpression on downstream metabolic effectors, with little to no impact on non-overexpressing cells.

While these specific aims are addressed primarily in Chapter 4 and Chapter 5, the following Chapter 2 serves as a literature review of cellular metabolism with a specific focus on protein translation. In addition, Chapter 3 serves as an extended background relating to the technologies that have made this dissertation possible, with a specific focus on how this laboratory has adapted them for our specific purposes.

2. REGULATION OF CELLULAR ANABOLISM: OR HOW I LEARNED TO STOP WORRYING AND LOVE TRANSLATION

2.1. Introduction

Over the past 15 years, great strides have been made in describing the complex mechanisms that regulate growth in eukaryotic cells. Often, at the center of these discussions is the mechanistic target of rapamycin, or mTOR. This protein and its associated complexes sit at a focal point of anabolic and catabolic regulation. By integrating the input from a number of upstream signals, mTOR is responsible for regulating many aspects of growth in the cell based on nutrient availability, energy status, inflammation, genotoxic stress, oxidative stress, and multiple growth factors (3, 32, 35, 46, 50, 73). However, there exist a number of signaling cascades that can occur alongside canonical mTOR signaling, with some of them being regulated independently of mTOR but able to effect similar downstream metabolic changes (21, 25, 49, 53, 72, 89, 92). The purpose of this review is to describe in detail the role of mTOR-dependent and -independent signaling pathways in the regulation of cellular metabolism, with a considerable focus on mRNA translation.

2.2. Background

Our understanding of the mechanisms regulating mRNA translation, or protein synthesis, have been constantly evolving since the discovery of mRNA and polysomes in the 1960s. One area of research that has gained popularity in recent years is that

pertaining to the control of non-canonical methods of protein synthesis. The traditional view of mRNA translation has involved a very strict environment of upstream signaling emanating from or arising through the mTOR kinase, ultimately leading to the activation of specific initiation factors; the ribosomal binding to the mRNA mediated through the 7-methylguanosine cap (m7G) and eIF2; the subsequent scanning for an AUG start codon downstream from an appropriate Kozak sequence, and the binding of the methionine initiator tRNA (Met-tRNAi) to begin the translational process (38, 70, 87). While these steps represent a standardized dogma, our current understanding of translation initiation now includes alternative processes for each of these previously mentioned steps.

2.3. mTOR Structure and Function

A central feature of anabolic regulation involves the mTOR kinase. mTOR was formally "discovered" in 1994 by three independent laboratories, namely Stuart L. Schreiber, David M. Sabatini, and Robert T. Abraham (4, 74, 75). However, the mechanistic *target of rapamycin* has been known to exist in some form since the discovery of Rapamycin from soil bacterium on Easter Island in the 1960's (81). Since that time, mTOR has been afforded much scientific inquiry and fanfare. mTOR exists in mammalian cells as a 289 kDa serine/threonine protein kinase of the PI3K-related Kinases (PIKK) family, and forms three distinct protein complexes known as mTOR complex 1 (mTORC1), mTOR complex 2 (mTORC2) and the recently discovered mTOR complex 3 (mTORC3) (34, 43, 50). Although the mTOR kinase is the common

feature among all three, these protein complexes differ in their binding partners, upstream input, and downstream targets.

mTORC1 is defined by its interaction with the regulatory-associated protein of mTOR (RAPTOR), a scaffolding protein that is critical to mTOR's subcellular localization to the lysosome and in mediating mTOR's interaction with other mTORC1 associated subunits (33, 50). RAPTOR also mediates the interaction of the proline rich AKT substrate 40 kDa (PRAS40) endogenous mTORC1 inhibitor. mTORC2 is defined by its interaction with the rapamycin-insensitive companion of mTOR (RICTOR), which may aid in mTOR's subcellular localization to the plasma membrane, and in mediating mTOR's interaction with other mTORC2-associated subunits (50, 77). RICTOR also mediates the binding of the MAPK-interacting protein 1 (mSIN1), which may aid in mTORC2 interactions with the plasma membrane (104). Both complexes contain the mammalian lethal with SEC13 protein 8 (mLST8), which appears to stabilize the kinase domain of both complexes, but ablation of this protein inhibits the structure and function of mTORC2, while mTORC1 downstream substrates appear to remain unaffected (50). In both of these complexes, mTOR directly interacts with an inhibitory protein, DEP-domain containing mTOR-interacting protein (DEPTOR), and plays a critical role in the regulation of both mTOR complexes through multiple complex feedback mechanisms that are only incompletely understood (9, 18, 41, 56, 67). The mTORC3 complex was only recently discovered, and very little is known about its downstream targets or its binding partners beyond ETV7, a transcription factor commonly upregulated with many types of cancer (34).

While each of the mTOR complexes respond to different inputs and have different downstream targets, these functions are much better defined for mTORC1 than mTORC2, and we know considerably more about mTORC2 when compared to mTORC3. mTORC1 is sensitive to signaling input along the IRS-1/PI3K/AKT signaling axis, and is responsible for the regulation of a number of critical cellular functions including protein synthesis, lipid synthesis and metabolism, nucleotide synthesis, energy homeostasis, autophagy, mitochondrial biogenesis, and mitochondrial metabolism (46, 50, 73, 100). In contrast, mTORC2 appears to play important roles in the organization of the cellular cytoskeleton, and in complex interactions with AKT that may serve to reinforce cross-talk between mTORC1 and mTORC2, but the nature and our understanding of these relationships are far from complete (19).

2.3.1. DEPTOR

One of the more interesting and understudied mTOR complex components is a protein known as DEPTOR, which is an endogenous inhibitor of mTOR, regardless of complex, through direct binding to the mTOR kinase. While DEPTOR is bound to mTOR, the mTOR kinase exhibits reduced kinase activity as measured through the phosphorylation of downstream targets, and DEPTOR depletion leads to a promotion of mTORC1 activity (41, 67). Through a complex relationship, DEPTOR and mTOR reciprocally inhibit each other, generating double-negative feedback loops (18). Once activated via upstream signaling, mTOR is able to auto-phosphorylate the bound DEPTOR protein, triggering it’s release from mTOR, enabling subsequent

phosphorylation by the constitutively active Casein Kinase I (CKI), and ultimately the ubiquitination and degradation via the $SCF^{\beta\text{-}TRCP}$ E3 ubiquitin ligase complex in a β-TRCP dependent fashion (18, 22). This degradative process is dependent upon mTOR activation, and the availability of SCFβ-TRCP complex, as the initial phosphorylation events may not be sufficient to remove the inhibitory effect of DEPTOR on mTOR, but serve to enable further protein modifications by CKI and β-TRCP.

In some contexts, DEPTOR can act as an oncogene, and in others, a tumor suppressor (9, 67). Some have speculated that in some cases, increased DEPTOR levels can relieve the negative feedback from p70 S6 kinase on IRS-1, allowing for increased signal transduction through the IRS/AKT/mTOR signaling axis (7). Decreased DEPTOR levels would simply allow for a lower threshold of upstream signal to activate mTOR and downstream anabolic targets. This presents an extremely complicated relationship, that is compounded by the fact that each of the mTOR complexes appear to compete for DEPTOR binding, with RAPTOR being a preferred binding partner than RICTOR (67). Recent computational modeling of this complex interaction has revealed that the mTOR/DEPTOR relationship can form a wide range of nonlinear dynamics, and can transition between these multiple behaviors through the modulation of a single factor, such as DEPTOR protein expression (96). Varusai et al. indicated that there may be a "therapeutic window" of DEPTOR overexpression that can serve to suppress mTORC1/2 activation, while also inhibiting AKT activation (96). In addition, they also indicated that the stability of the rapidly changing system is improved with longer

timescales, and are ultimately dependent upon the rate of synthesis and degradation of DEPTOR (96).

Changes in the capacity of a cell to express DEPTOR protein have been reported in some studies as a potential causative factor for altered anabolic signaling (41), while others have suggested that these outcomes could be a consequence of changes in mTOR activity, ultimately leading to changes in the expression of DEPTOR (7). Caron et al. noted in a comprehensive review that reductions in DEPTOR protein are generally a direct result of mTOR activation, but do not exclude DEPTOR's role in inhibiting mTOR (7). While both arguments have merit, due to the complexities of the interaction between these two proteins, the positive and negative feedback loops associated with this pathway, and the fact that mTOR's activation could play an important role in the translation of DEPTOR mRNA, it seems difficult to assess this cause and effect relationship without the stable and long-term overexpression of DEPTOR protein, independent of mTORC1/2's significant role in reducing DEPTOR expression when activated. This sentiment is mirrored by Caron et al., stating that DEPTOR silencing or overexpression is likely required to determine the true effects of any treatment on anabolic signaling through DEPTOR-mTOR (7).

2.4. Protein Synthesis

Within eukaryotic cells, messenger RNA (mRNA) is translated into proteins via a number of different mechanisms that are subject to overlapping, but often independent, cellular regulation processes. The translational process employed by the cell is largely

dictated by the mRNA characteristics that determine which pieces of cellular machinery are required to take part in peptide-chain initiation, translation, or termination, but can also be defined by the subcellular compartment in which it takes place (e.g. the mitochondria). In addition to differences in cellular machinery, these specific translational processes can be subject to drastic differences in regulation and control that not only influence the ultimate rate of protein synthesis within the cell, but also determine the type of mRNAs that will be prioritized for translation. From subtle differences in transcripts due to the heterogeneity of transcription start sites, to the vast differences in 5' UTR sequence and secondary structure, the manufacture of a given protein is regulated post-transcriptionally based on the configuration of the mRNA and/or the specific translational processes available at the time (38, 42, 52). Aside from the energy status of the cell, translation initiation is widely considered to be the rate limiting step for protein synthesis and is a critical control point to determine not only what transcripts have access to the anabolic apparatus, but their affinity to anabolic machinery and the ease by which they are translated. All protein coding transcripts within eukaryotic cells fall under two, often overlapping, categories: Cap-Dependent (CD), and Cap-Independent (CI) (38). Previously thought to only occur during times of great cellular stress, cap-independent translation of particular mRNA transcripts is now believed to occur simultaneously with cap-dependent translation in virtually all eukaryotic cells, albeit with notable differences in priority and efficiency depending on the nature of the specific transcript (42). Classically categorized by their dependency on 7-methylguanosine cap (m7G) binding initiation factors, many of these transcripts are

now known to exhibit properties of both classifications and can take part in translation through a variety of processes, under a variety of conditions (53, 101). One such mRNA is that of mTOR, possessing both CD and CI elements, ensuring that it can be translated under normal conditions, and during times of great cellular stress (53). However, cap-independent transcripts are likely largely unidentified due to the dramatic variations in the 5' UTR primary and secondary structure that play an important role in their translation (53). Identifying and quantifying the contribution of CD and CI translation initiation to overall protein synthesis, and to the synthesis of specific proteins will be of the utmost importance in developing a complete understanding of the human translatome.

2.4.1. Basic Overview

From the most basic perspective, protein synthesis is the process of converting mRNA transcripts into usable proteins within the cell. Generally, it is described as being a three-part process, consisting of initiation, elongation, and termination. Each of these steps is carried out by complex ribonucleoproteins consisting of dozens of proteins and multiple RNA molecules that form the different subunits comprising a fully formed ribosome. The exact composition and size of the ribosomal subunits will depend upon the location of translation, but there are always two ribosomal subunits, one large, and one small. If translation is occurring in the cytosol, the small (40S) subunit and the large (60S) subunit together form the 80S ribosome (52). If translation is occurring inside the

mitochondria, the 28S small subunit (mt-SSU) and the 39S large subunit (mt-LSU) together form the 55S mitoribosome (30).

In addition to the location within the cell, different types of translation can occur based on the sequence and secondary structure of mRNA transcripts. Not only do these different mechanisms of translation operate through different collections of translational machinery, they occur at different efficiencies, are subject to different upstream signaling input, and are ultimately responsible for the translation of specific subsets of mRNA transcripts within the cell.

2.4.2. Cap-Dependent Translation Initiation

The most common type of translation that takes place in eukaryotic cells is known as cap-dependent translation. As such, it will also serve as the basis for comparison when discussing other types or variations of translation. Cap-dependent translation is so named due to the sequence and structure of the 5' untranslated region (UTR) of this class of transcripts. Specifically, the 7-methylguanosine cap (m7G) of cap-dependent transcripts require the binding of eukaryotic initiation factor 4E (eIF4E) as part of the eukaryotic initiation factor 4F (eIF4F) complex, to enable the mRNA to interface with the 40S small ribosomal subunit, to form the 43S preinitiation complex (43S PIC) (38). For eIF4E to be made available, 4E-binding protein 1 (4E-BP1) must be deactivated through phosphorylation to cause dissociation with eIF4E. Of the four relevant 4E-BP1 phosphorylation sites, mTORC1 is known to phosphorylate Thr 37 and Thr 46, which is not independently sufficient to release 4E-BP1 from eIF4E, but rather

appears to prime 4E-BP1 for phosphorylation at Ser 65 and Thr 70 (27). It is believed that phosphorylation at Ser 65 and Thr 70 may be required for full deactivation and complete dissociation from eIF4E, although the specific kinase responsible for this phosphorylation is unknown, some sources point to mTOR or an mTOR complex-associated protein (28).

The vast majority of mRNA within a normal, healthy cell contains a 7-methylguanosine cap (m7G) at the 5' end that facilitates interaction with eukaryotic initiation factor 4E (eIF4E), which ultimately allows for coupling of the mature transcript with the small ribosomal subunit as part of the 43S pre-initiation complex (PIC) (38). This new complex consisting of the 43S PIC and transcript form the 48S PIC. The binding of eIF4E to the 5' m7G cap structure is generally considered to be the overall rate-limiting step of translation under most circumstances. Due to binding at the cap structure, often significantly upstream from a start codon, ATP-dependent eIF4A helicase is required to unwind any secondary structures present in the downstream 5' untranslated region (UTR) to enable efficient scanning for an appropriate start codon (generally AUG) within a Kozak sequence (44). When the appropriate start codon is encountered, the methionine tRNA initiator (Met-tRNAi) anticodon in the ribosomal P site, binds to the mRNA start codon, facilitated by eIF5 in the PIC by hydrolyzing a GTP bound to eIF2 (38). This is marked by a conformational change in the PIC, enabling it to bind to the 60S large ribosomal subunit to form the 80S ribosomal complex and enter the elongation phase of protein translation (38).

As the 80S ribosomal unit moves along the transcript during the elongation phase, newly formed 40S subunits, guided by eIF4e, can bind to the 5’ m7G cap, and begin scanning for a start codon (38). These mRNA with multiple ribosomal units engaging in simultaneous translation are referred to as polysomes.

2.4.2.1. 5’ TOP mRNA

There is a subset of cap-dependent transcripts that contain a 5’ terminal oligopyrimidine (5’ TOP) motif, which encode many of the growth-related proteins, including many of the translation factors and nearly all ribosomal proteins. LARP1 was recently shown to be involved in the binding of these specialized 5’TOP mRNAs in an mTORC1 activation-dependent manner (89). LARP1 associates with mTORC1 via RAPTOR, and upon mTORC1 inhibition, is liberated and able to bind 5’TOP mRNA to repress their expression (21). This interaction occurs competitively with eIF4E, but may occur alongside eIF4A, and likely eIF4G (89). In addition, LARP1, in conjunction with the poly-A binding protein (PABP) and eIF4G, is able to bind to the 40S ribosomal subunit, by creating an alternative “48S”-like complex that is able to stabilize the 5’TOP mRNA, but not allowing for its expression (25). This indicates a dynamic relationship between mTORC1 activity and the preferential expression of critical components of the anabolic machinery required to translate mRNA into proteins. This ultimately serves two purposes. One, the cell is able to preferentially halt the expansion of anabolic machinery very quickly upon mTORC1 inhibition, and two, is able to preserve the mRNA coding for the same anabolic machinery through a stabilizing complexation through LARP1 in

the face of halted anabolism. In addition to LARP1, there have been a number of mRNA cap-binding proteins identified that have opened the door to the possibility of further sub-classifications of mRNA that may receive preferential treatment during translation (89).

2.4.2.2. Alternative Cap-Dependent Translation Initiation

In roughly 20% of cap-dependent mRNAs, eIF4E is not required to initiate translation, but is done in a way that still requires the 5' cap structure. DAP5, an eIF4GI homologue, can utilize eIF3d to facilitate direct binding of the PIC to the 5' m7G cap to enable translation initiation independently of eIF4E availability or 4E-BP1 activation through mTORC1 (14). These transcripts do not contain cap-independent internal ribosome entry site elements (IRES), although DAP5 is capable of promoting the translation initiation of a fair number of mRNAs containing IRESs as well (14). Genome-wide translation profiling has revealed that DAP5 is critically important in the cap-independent (IRES-mediated) translation of proteins involved in cell differentiation, cell cycle progression, apoptosis, and metastasis. Some of these proteins include Bcl-2, Apaf-1, cIAP1, CDK1, and p53 (3). Interestingly, the genome-wide transcriptome and translatome profiling revealed highly DAP5-dependent mRNAs involved in many cell functions, including cell death, cell proliferation, cell mobility, DNA damage and repair, and translation initiation, that do not contain IRES elements, and are translated in a cap-dependent, but eIF4E independent fashion. The authors report that all in all, the translation of roughly 20% of all mRNAs was found to be highly dependent on the

expression of DAP5 and eIF3d (14). While this mechanism occurs independently of eIF4E canonical cap-binding, it is still entirely dependent upon cap-binding processes and is therefore still technically cap-dependent.

2.4.3. Cap-Independent Translation Initiation

In contrast to the eIF4E cap-dependent mechanisms described above, cap-independent translation occurs independently of m7G cap binding, and instead relies upon the presence of 5’ or 3’ UTR elements that directly interface with elements of the translation apparatus. This subset of translation initiation is extremely varied, and much less well-defined when compared to cap-dependent translation initiation. The recruitment of mRNAs to the 40S ribosomal subunit using a cap-independent process can occur through the direct binding of specialized mRNA sequences to ribosomal subunits or translation initiation factors (38, 52). These specialized mRNA sequences often feature complex secondary RNA structures in the 5’ and/or 3’ UTRs of certain transcripts. Many of these sequences enable the direct binding of the 40S subunit just upstream or directly at the start codon sequence via specific internal ribosome entry site (IRES) elements (11). In some mRNAs, specifically under apoptotic conditions, translation can occur through a 5’ end-dependent scanning mechanism, in what is known as a cap-independent translational enhancer (CITE) (11). Transcripts that contain these cap-independent regions are often related to growth, programmed cell death, and stress response, including many that have been classified as oncogenes (52).

It should be noted that these cap-independent motifs containing mRNAs also contain a m7G cap, as are all cellular RNA polymerase II-transcribed mRNAs (68). Therefore, transcripts that contain both cap-dependent and cap-independent elements can be translated through multiple independently regulated mechanisms. Although the importance of why a transcript would contain both cap-dependent and -independent sequence motifs is not completely understood, it suggests that mRNA translation by one mechanism or the other is largely dependent on whether mTORC1 is on or off (53). In other words, although cap-independent translation does not require mTORC1 activity, translation may largely occur for those transcripts only when mTORC1 is not active, as elevated activity of mTORC1 may preferentially direct cap-dependent sequences to the anabolic apparatus at the expense of the available cap-independent transcripts. Alternatively, having cap-independent sequences may allow for translation of those transcripts whether mTORC1 is active or not. As noted earlier, one such transcript is the human mTOR transcript (53). It's 5' UTR forms a highly folded RNA scaffold that enables it to bind to the 40S subunit with high affinity, thereby enabling some basal amount of mTOR mRNA translation regardless of upstream signaling conditions within the cell (53). While cap-dependent translation is never completely halted, the affinity of the translational machinery towards particular mRNA elements can be dramatically altered (83). Having both cap-dependent and -independent translation sequences may be critical for progression of certain phases of the cell cycle, and the maintenance of normal cellular functions under various stress conditions.

2.4.4. MicroRNA

One of the more recent developments in characterizing translational regulation pertains to microRNA, or miRNA. These very short (~22 nucleotides in length) RNA molecules are transcribed from DNA, and often undergo multiple processing steps to become mature miRNA. These mature miRNA sequences are able to bind with mRNA to induce a variety of downstream effects, including the induction of mRNA degradation and translational repression (62). However, depending on where the miRNA interacts with the mRNA, they can also activate translation, or through interaction with gene promoters, can regulate transcription (62). In most cases, translational repression occurs via binding to the 3' UTR of transcripts, and translational activation is most often associated with miRNA binding to the 5' UTR. The effect can depend on a variety of factors, including subcellular location of the miRNA species, abundance of both miRNA and target mRNA, and a variety of other factors (62). Not only does this effect take place inside the cytoplasm of cells, but miRNA can be released from cells to act extracellularly, or their transport out of the cell can be mediated by vesicles to act as an effector inside of other cells. Some species of miRNA can exert a control over both the transcription and translation of certain genes (58), and in some rare cases, viral transcripts have evolved to take advantage of miRNA translational promotion (79).

With specific regard to the control of protein synthesis, there have been investigations into specific miRNA species that are associated with key regulators of these signaling processes. Overexpression of miRNA-16 (miR-16) in C2C12 myotubes was associated with reductions in protein synthesis, while miR-16 inhibition was

associated with increases in rates of protein synthesis (47). This observation is consistent with observations that miR-16 is aggressively released from contracting skeletal muscle, possibly enabling post contraction-mediated increases in anabolism. In addition, miR-16 appears to be capable of reducing the proliferation of other types of cells once released from skeletal muscle. This appears to be accomplished through the packaging of miR-16 rich vesicles during skeletal muscle contractions. Skeletal muscle-derived miR-16 induced inhibition of anabolism extends to cultured MFC7 human epithelial breast cancer cells, effecting changes across tissue types as well as species (29).

2.5. Anabolic Regulation

Historically, the regulation of anabolism, including protein synthesis, has fallen under two distinct categories that define their signaling pathways: rapamycin-sensitive, and rapamycin-insensitive (2, 20, 34, 51). The former refers to signaling pathways the converge on mTORC1 (including insulin sensitive IRS-1/PI3K/AKT signaling, energy sensitive AMPK signaling, amino acid sensitive signaling through GATOR1/2, and mechanotransduction signaling through PLD1 mediated phosphatidic acid (PA) production), while the latter refers to all other signaling that is independent of the rapamycin-induced inhibition of mTORC1. We should note, however, that this nomenclature has been revised somewhat, as mTORC1 phosphorylation of 4E-BP1 at Thr46 is sufficient to prevent some level eIF4E:4E-BP1 binding and can occur in a rapamycin-insensitive manner (51).

Both mTOR complexes are subject to multiple regulatory mechanisms that range from upstream signal transduction, self-limiting inhibition, and downstream negative feedback through changes in both transcription and translation. As the aptly named target of rapamycin, mTORC1 is inhibited by direct binding of rapamycin to mTOR and subsequently partially occluding substrate entry into the mTOR kinase domain. However, mTORC2 is not subject to direct binding by rapamycin, and as a result, not acutely impacted by treatment with rapamycin. Although, it should be noted here that long-term treatment of rapamycin ultimately influences mTORC2 activity through alterations in feedback from the direct inhibition of mTORC1 (76). This section will focus on anabolism through the rapamycin-sensitive and -insensitive pathways.

2.5.1. Rapamycin-Sensitive Anabolic Pathway

2.5.1.1. mTORC1

Under normal conditions, mTORC1 is sensitive to a number of upstream inputs in the cell, and most serve to monitor intracellular and extracellular markers whose signals are “summed” at the mTORC1 nexus to modulate its kinase activity, and ultimately anabolic activity. One of the most commonly studied mTORC1 signaling inputs is the IRS-1/PI3K/AKT signaling axis. This signaling pathway is sensitive to both insulin, and the insulin-like growth factor 1 (IGF-1), through IRS-1 bound to the insulin receptor (IR) (31, 91). This receptor has two splice variants, IR-A and IR-B (11). Although insulin binds to both splice variants fairly equally, IGF-1 has a strong preference for IR-A and is not expressed as highly in skeletal muscle as the IR-B

receptor. Upon activation of the IR, IRS-1 is phosphorylated on a number of tyrosine residues, which creates a number of potential binding sites for proteins that contain an SH2 domain, including phosphatidylinositol 3-kinase (PI3K). Recruitment and activation of PI3K allows for the interaction and conversion of phosphatidylinositol (3,4)-bisphosphate (PIP2) lipids to phosphatidylinositol (3,4,5)-trisphosphate (PIP3). The formation of PIP3 is then able to mediate interaction between the constitutively active 3-phosphoinositide-dependent protein kinase-1 (PDK1) and AKT through recruitment to the membrane. PDK1 then phosphorylates AKT at Thr 308, which at least partially activates the kinase. In addition, atypical PKC isoforms lambda/iota and zeta can be recruited to the membrane and phosphorylated in a similar manner on the kinases Thr 410/403 sites. When phosphorylated at Thr 308, AKT is able to regulate the activity of a number of downstream targets, including TSC2, PRAS40, GSK3, and FOXO3. Through inhibitory phosphorylation of TSC2, there is relief of the TSC1/2 complex's inhibitory action of mTORC1. Similarly, AKT phosphorylates the mTORC1 inhibitor PRAS40, inducing its release from the mTORC1 complex.

In addition to IRS-1/PI3K/AKT signaling, a number of membrane receptors (including the IR) are able to bind the GRB2/SOS complex, which is then able to remove the GDP from the small GTPase Ras, allowing it to bind to GTP and subsequently trigger a phosphorylation cascade through Raf, MEK, and ultimately, ERK1/2 and RSK1. These phosphorylation events enable ERK1/2 and RSK1 to join AKT in TSC2 inhibition at different phosphorylation sites. mTORC1 is also sensitive to extracellular inflammation through activation of IKK beta, and subsequent inhibitory

phosphorylation of TSC1. This event, in conjunction with inhibition by phosphorylation via ERK1/2, RSK1, and AKT represent the primary upstream events that lead to the activation of mTORC1.

Conversely, TSC2 can also undergo phosphorylation events leading to activation of the TSC1/2 complex, increasing the inhibitory capability of the complex on its downstream target Rheb. These events can be mediated by a constitutively active GSK3, or an active AMPK, as both of these kinases serve to monitor energy status within the cell, and serve to inhibit mTORC1 during a lack of upstream activation, or during times of energy stress respectively. TSC1/2 have been described in the literature as a molecular "switchboard" regulating mTORC1 activity, and the aforementioned phosphorylation of various residues on the complex exist in a complex equilibrium that incrementally regulate the overall inhibitory activity toward the Rheb GTPase. Through the withdrawal of TSC1/2 inhibitory stimulus on the Rheb GTPase, Rheb is able to bind directly to mTOR on mTORC1, distally from the kinase site, leading to a conformational change of mTORC1 that allows for accelerated catalysis at the mTOR kinase site (100).

The relief of Rheb inhibition and the resultant allosterically improved kinase activity of mTOR leads to the phosphorylation of multiple downstream mTORC1 targets. These include DEPTOR, p70 S6K-1, p70 S6K-2, 4E-BP1, 4E-BP2, and 4E-BP3. However, as noted previously, the phosphorylation of Thr46 on 4E-BP1 has been shown to occur in a rapamycin-insensitive manner, and is sufficient to at least partially prevent eIF4e:4E-BP1 binding (51). The S6 kinases have multiple downstream phosphorylation targets, including rpS6, and eIF4B. Phosphorylated ribosomal protein S6 is an important

component of the 40S ribosomal subunit, and is critical for the binding of the 40S subunit to the 5' m7G cap of mRNA. On the other hand, eIF4B has a much more nuanced role in the translation of cap-dependent transcripts. eIF4B enhances the activity of the ATPase and helicase, eIF4A, and is thought to facilitate attachment of the PIC to mRNA containing cap-proximal secondary RNA structures (82). In addition, the activation of eIF4B enables the translation of "eIF4B-hyperdependent" transcripts that feature atypically long sequences, and higher propensities for secondary structure (82).

2.5.2. Rapamycin-Insensitive Anabolic Pathway

2.5.2.1. mTORC2

While the presence of mTORC2 has been known for some time, it is much less well characterized than mTORC1. The specific mechanisms relating to mTORC2 activation remains unknown, but is thought to be primarily regulated by growth factors through PI3K (50). However, it is known that mTORC2 can be activated through a similar mechanism by which PIP3 and PDK1 recruit and phosphorylate AKT at the plasma membrane. This localization to the plasma membrane is mediated by binding of the mTORC2 complex protein mSIN1 to PIP3, thereby removing inhibition of the mTOR kinase, and enabling mTORC2 to phosphorylate AKT at Ser473.

2.5.2.2. ERK

The Ras/Raf/MEK/ERK signaling pathway can be activated alongside the IRS-1/PI3K/AKT/mTOR pathway, but can also act independently, while still influencing the

activity of some of the same downstream effectors. Broadly, this pathway can be activated by a variety of extracellular stimuli occurring through G-coupled protein receptors and receptor tyrosine kinases (including the insulin receptor, and various integrin transmembrane receptors). Once activated, this signaling pathway plays an important role in the regulation of the cell cycle, apoptosis, growth, and cellular differentiation.

When an extracellular mitogen binds and activates an appropriate membrane receptor, the small GTP binding protein, Ras, is liberated from its bound GDP molecule, allowing it to bind to a new GTP. This activated form of Ras, is capable of hydrolyzing the bound GTP to recruit and phosphorylate multiple downstream targets, including the protein kinase Raf. Raf is then able to promote the activity of MEK1/2 protein kinases through the phosphorylation of serine/threonine residues, which are ultimately responsible for the phosphorylation and activation of ERK1/2. The ERK1/2 proteins are responsible for the phosphorylation of at least 160 downstream targets, including various transcription factors and cytosolic signaling enzymes (78). Of particular note is the downstream target RSK (ribosomal S6 kinase), which then activates ribosomal protein S6 (rpS6) a component of the 40S ribosomal subunit. Leading to its recruitment to the m7G cap structure, and the formation of the 43S pre-initiation complex required for cap-dependent translation (72). This can occur cooperatively and/or independently of the activation of p70S6 kinase by the rapamycin sensitive mTORC1 pathway.

2.5.2.3. mTORC3

Proposed in 2018 as a third complex containing mTOR, this newly discovered complex interacts with the E26 transformation-specific (ETS) transcription factor ETV7, and is capable of forming a distinct third mTOR complex upon ETV7 expression (34). To date, there have been no other investigations related to this potential third mTOR complex. However, the compelling evidence provided by Harwood et al. (34) indicated that mTORC3 can operate in a rapamycin-insensitive manner, while being capable of phosphorylating mTORC1 and mTORC2 downstream targets independently of RAPTOR or RICTOR complexation. Expression of the ETS transcription factors help to regulate many essential cellular processes, and their overexpression has been associated with tumor initiation, progression, and metastasis, making them popular targets for novel cancer treatments (37).

2.5.2.4. AKT

Represented by three different isoforms in human tissues, AKT is a potent regulator of many cellular processes. AKT1 and AKT2 are expressed in all known tissue types, and are extremely similar proteins, being 480 and 481 amino acids in length, respectively (36). AKT3 is less defined, but in adult tissues is highly expressed in the brain, lung, and kidney, and to a lesser extent in the heart, testes, and liver (102). Between AKT1 and AKT2, approximately 82% of amino acid identities are conserved through the protein sequence, and approximately 70% of the differing residues are physiologically conservative substitutions, resulting in ~92% positive overlap between

the two proteins. Two of the most relevant phosphorylation sites on AKT1 are Thr 308, and Ser 473 (3, 36). On AKT2, these sites and their surrounding regions are extremely well conserved, and are represented at Thr 309, and Ser 474.

Despite the presence of two similar, but physiologically distinct isoforms of AKT in all human tissues, it has often been treated as a single entity in the literature. Despite their sequence similarities, these two protein kinases have been shown to have distinct signaling differences and are often diametrically opposed to the function of the other. This problem has been conflated by the simple fact that most commercially available primary antibodies targeting the AKT phosphorylation sites have significant cross reactivity between AKT1 and AKT2. Due in part to the complex relationship between these two enzymes and their respective signaling pathways, and also due to the cross reactivity of phospho-antibodies, there has been a considerable amount of scientific debate as to which phosphorylation events are required for full activation of these proteins. Delving through the literature concerning AKT activation can become a daunting task in light of these realities, but it becomes abundantly clear that some of the conclusions that have been made about these proteins, their post-translational modifications, and their subsequent activity, have been mired by a lack of accurate tool-sets employed for the task.

2.6. Dysregulation and Disease

While metabolic dysregulation is associated with many human diseases, it is not always clear if the dysregulation in a certain tissue is driving the progression of the

disease, or if the dysregulation is a byproduct of cellular attempts at homeostasis in the face of abnormal extracellular conditions. While distinguishing between the two may appear to resemble debates of causality akin to certain poultry and their ovum, the distinction in this case is neither semantic, nor arbitrary. In some cases, this relationship is fairly straightforward. In many human cancers, a single mutation can lead to myriad cellular signaling dysregulation that can have devastatingly lethal effects. Often times, these mutations have dramatic effects on signaling through the IRS-1/PI3K/AKT/mTOR signaling axis. In fact, in most human cancers, DEPTOR expression is low (67), and in some cancers, DEPTOR downregulation is an indicator of poor prognosis (39).

On the other hand, some neurodegenerative diseases can be characterized by disrupted anabolic or catabolic signaling, with some occurring in mTOR dependent signaling pathways. For example, the accumulation of amyloid-β plaques in the precentral gyrus, postcentral gyrus and occipital lobe of Alzheimer's patients has been associated with a marked decrease in DEPTOR protein content when compared to the same regions from healthy brain tissue (13). In addition, it has been shown that mTOR inhibition can be neuroprotective against the toxic effects of amyloid-β plaques (13). However, it is unclear if this effect plays a role in driving the progression of the disease or of it is merely a consequence thereof. There is also an increasing amount of evidence that indicates that the dysregulation of mTOR and autophagy are critical to the pathogenesis of Parkinson's Disease (107).

Further, DEPTOR and mTOR dysregulation appears to play an important role in the progression insulin resistance in type 2 diabetes. Skeletal muscle is particularly

sensitive to insulin signaling and metabolic disorders, and is generally serves as one of the first indicators of insulin resistance (15). It has also been shown that decreased DEPTOR levels in obese Zucker rats contribute to increased levels of basal protein synthesis, despite reduced muscle mass when compared to their non-obese litter mates (60). In addition, this effect may contribute to an overall resistance to the anabolic effects of exercise in muscle, which in turn can reduce the effectiveness of exercise as a means of treating type 2 diabetes.

2.7. Conclusions

Cellular anabolism and the control of translation is an extremely complex process, with new layers of complexity being uncovered routinely. The central nature of mTOR to these processes make it an enticing target to manipulate as a means to many different ends. However, the complexity of mTOR's many positive and negative feedback mechanisms can make achieving these ends extremely difficult. The recent development of second-generation mTOR kinase inhibitors, such as Torin-1, is extremely exciting, and has shown promising new possibilities for strategies designed to regulate this pathway. Other examples may include the tissue specific delivery of advanced pharmacological inhibitors, mRNA of intrinsic inhibitors, or specific miRNA species, all of which may offer incredible opportunities to mitigate the effects of many diseases that suffer from dysregulation of these pathways. Given that the startling prevalence of common dysregulation involving mTOR pathways in various anabolically

aggressive diseases, a fundamental understanding of mTOR-centric regulation may offer interesting opportunities for potential common treatments.

3. DEVELOPING NEW APPROACHES TO OLD PROBLEMS

3.1. Introduction

The experiments described in this dissertation would not have been possible without a number of new methodological approaches developed by the Muscle Biology Laboratory. As with many examples in science and engineering, it is not always about the technology, but more so in how said technology was applied to a particular problem. The following chapter will highlight the incredible technologies that have made this dissertation possible, with a specific focus on how this laboratory has adapted them for our specific purposes.

3.2. Gene Editing

3.2.1. Background

The current CRISPR/Cas9 gene editing technologies have been developed by many scientists around the world over the past number of years. At its core, Cas9 is simply an endonuclease that is capable of creating extremely precise double stranded breaks in DNA, guided by specialized single-stranded guide RNAs (sgRNA or gRNA) that are complementary to the target DNA sequence (69). While specific gene targeting endonucleases have been in use for several decades, the TALEN and CRISPR/Cas9 systems have brought to bear an entirely unprecedented precision that has increased the ease and reduced the time to develop novel site-specific nucleases from weeks to

months, to less than a week, and in many cases, can now be commercially purchased as an “off the shelf” product (69).

The most common application of CRISPR/Cas9 is to induce a double stranded break (DSB) of DNA at a specific location within a genome of interest. Generally, this is done within the open reading frame of a protein coding region with the gene, downstream of the AUG start codon. In response to the DSB, the cell will employ a repair process known as non-homologous end joining (NHEJ), which is often error prone in the repair of DSBs, leading to the introduction of insertions or deletions (indels) in the resulting “repaired” DNA (12, 69). Ultimately, this leads to a significant chance of introducing a frameshift mutation in the repaired open reading frame (54). However, because of the lower percentage chance that a repair is performed accurately, the Cas9 nuclease is able to bind, and cleave the DNA a second time, or rather, as many times as necessary to induce DNA changes sufficient to inhibit binding of Cas9 to the target location. Conversely, the more dramatic the change in DNA from the original sequence the more dramatically it reduces the likelihood of further DSBs by Cas9, as the sgRNAs are extremely specific (12, 69). This process is an extremely quick and a relatively easy way to develop genetic knockout models for essentially any gene of interest.

However, using Cas9 to create a knock-in of a gene, termed an overexpressor model, is a significantly more complex process. Rather than relying on the error prone NHEJ to repair a DSB, it is possible to provide a “template” to direct the repair at the DSB induced by Cas9. This process is known as homologous directed repair (HDR) and can provide a number of advantages for overexpressing a gene of interest in the cell (12).

Figure 3.1 provides a simplified visual depiction of both NHEJ and HDR mechanisms (94). While promising, the complex nature of this process often requires the use of viral vectors or multiple plasmids to initiate or transform the cell.

By providing a repair template in the form of a double stranded DNA plasmid (dsDNA), the genomic DNA is able to recognize regions of sequence homology found on the donor plasmid (~1 kb) for each portion of DNA flanking the DSB (69). In contrast to NHEJ, when cellular repair machinery responds to the DSB, they are able to use these homology arms as a template to synthesize a complimentary sequence inside the gap created by the DSB. This process allows for the insertion of large transgenes into a precise location within the genome. By including various selection markers to be expressed alongside the gene of interest, additional steps can be taken to either select for positive responding cells, or against negative responding cells, depending on the nature of the experiment.

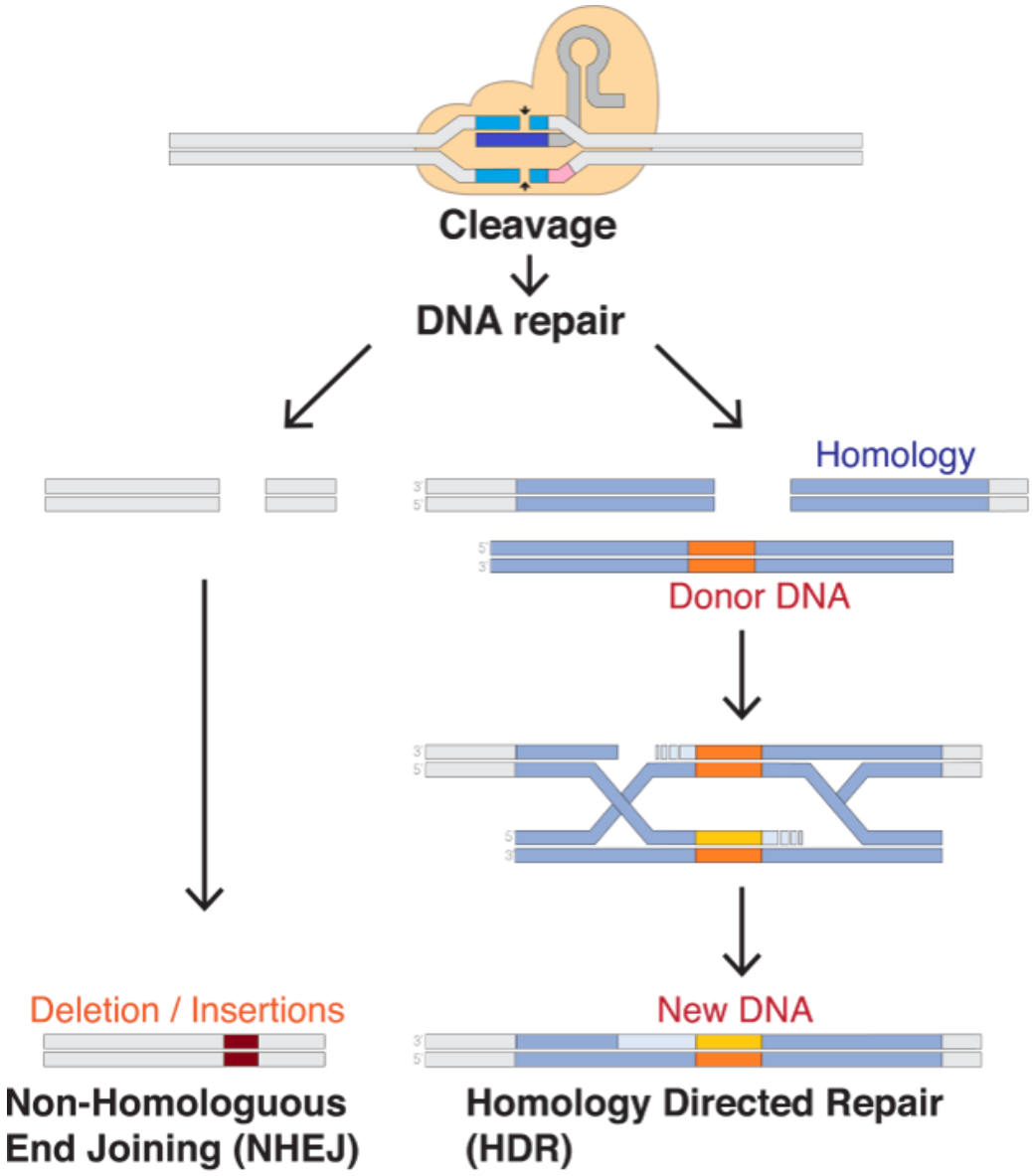

Figure 3.1 DNA repair by NHEJ vs HDR. Reprinted from Wikimedia Digital Commons (94).

3.2.2. Rationale

Based on a number of experiments from our lab and considerable debate with regard to the many iterations of plans for genetic modification of possible cell lines, it was decided that we would undertake multiple genetic modifications in different cell lines to try and understand the effect of altered DEPTOR protein levels on cellular metabolism. The C2C12 and MCF7 cell lines were chosen, in part due to our extensive experience with these cell lines, their robust growth potential, and their relatively hardy nature. These characteristics, coupled with being representative of both murine and human immortalized cell lines, have made them ideal candidates for precision genetic editing.

Current standards for stable transgene expression typically involve the use of gamma-retroviral and lentiviral vectors. A strength of these viral approaches is that they are capable of inserting large sequences of DNA into the host's genome. However, a drawback to these vectors is that they affect their actions on the genome randomly (105). This random integration of transgenes can lead to 'off-target' consequences and dramatically interfere with the normal operation of the cell. An additional concern is that because of the nature of viral transductions, a balance must be struck between introducing a sufficient number of viral particles to effectively transduce a large number of cells while limiting the average number of transgene insertions per cell during a transduction, as these random integrations can occur many times within a host genome. Thus, the current experiments would require a strategy to greatly enhance our precision of inserting the gene of interest to maximize its expression without affecting otherwise

normal functions in the cell. To accomplish this task, we would need to use methodologies that eliminated random integration and minimize the potential for 'off-target' consequences.

By utilizing the aforementioned CRISPR/Cas9 technology, coupled with a suitable HDR repair template, we chose to insert a transgene at a genomic "safe-harbor" site for each species. These are known as the AAVS1 Safe-Harbor site in the human genome, and the ROSA26 Safe-Harbor site in the mouse genome. The safe-harbor sites are somewhat of an evolutionary oddity and allow for the insertion of large transgenes without the use of viral vectors, or the disruption of normal gene expression (63, 64). In contrast to the more random viral vector approaches, our experiments capitalized on the knowledge that safe-harbor sites exist in regions of the genome that do not interfere with expression of native genes, and afford very consistent expression of transgenes due to the open chromatin structure of the surrounding DNA. The nature of this type of gene edit allows for the constitutive expression of large transgene inserts, without interfering in the expression of other native genes, while affording the convenience of multiple selection markers to "weed out" cells that are not responsive to the therapy.

For this type of gene edit, cultured cells are subjected to a simultaneous co-transfection in an effort to reduce the size of the overall 'package' being delivered to the cell. One plasmid containing an expression cassette for the Cas9 endonuclease and the sgRNA targeting the specific safe-harbor site, and a second plasmid that contained the open reading frame (ORF) for the species-specific native DEPTOR gene, an ORF for an enhanced green fluorescent protein (GFP), as well as the ORF for puromycin N-

acetyltransferase, and enzyme that confers cellular resistance to the antibiotic puromycin. Additional groups were subjected to the same treatments, with the only difference being in a substitution of a red fluorescent protein (RFP) marker in lieu of the DEPTOR transgene. In all cases, the second plasmid containing the genes of interest to be inserted, had these regions flanked by very specific nucleotide sequences to serve as homology arms (HA) to aid in the homologous recombination (HR) that occurs as a part of the homologous directed repair.

Following co-transfection of the two plasmids, cellular machinery are able to express the Cas9 nuclease and specific sgRNA, enabling Cas9 to bind to a very specific area of the safe-harbor site, and induce a DSB. The second plasmid, with specific HA's that serve as complementary sequences to the newly exposed broken DNA, is able to bind and serve as a repair template. In effect, by providing a DNA template with sequence homology to the exposed ends of the DSB, the repair template is able to 'trick' the cell into repairing the break with a much longer DNA sequence. However, depending on cellular conditions at the time, this repair may favor NHEJ as opposed to our intended HDR approach. In the instance that NHEJ occurs and completes a successful repair (a repair of the original sequence), Cas9 will simply be able to bind the region again and perform another DSB. However, it should be noted that if NHEJ occurs and induces alterations in the safe-harbor region, those alterations may be sufficient to prevent Cas9 from binding, and it will be then unlikely that this cell will receive the intended gene edit. However, in a subset of cells, HDR will occur, and depending on the cell cycle phase, can use sister chromatin strands as a repair template, or the exogenous DNA

repair template provided. If sister chromatin strands are used for a successful repair, Cas9 can induce another DSB and try again. If our exogenous repair template is used, then we have successfully edited the genome of our targeted cells.

By including GFP and puromycin N-acetyltransferase in the transgene edit, we were able to almost immediately begin artificial selection for positive responding cells following the co-transfections. Twenty-four hours following co-transfection, cells are subjected to media enriched with 1g/ml of the antibiotic puromycin. Puromycin is toxic to both eukaryotic and prokaryotic cells by imitating tRNA and interrupting the synthesis of new proteins by being utilized as a pseudo-tRNA and halting the peptide-chain elongation process. Through successful incorporation of our genes, we give the newly transformed cells the ability to manufacture a puromycin N-acetyltransferase enzyme, which converts puromycin to N-acetyl puromycin, which is ineffective in halting peptide-chain elongation. By subjecting cells to 14 days of puromycin selection, non-responders to gene editing treatments are quickly eliminated (>99% in <3 days) and responders are allowed to continue to grow. Further confirmation of gene editing is performed via live fluorescence microscopy for the presence of GFP in the DEPTOR over-expressors, as well as GFP and RFP co-expression in the RFP expressor groups.

3.2.3. Additional Benefits Over Alternative Methods

Not only does this transgenic model for DEPTOR overexpression allow for increased DEPTOR protein content (see results sections), it does so in a fashion that is independent of the many complex regulatory mechanisms that are normally present for

expression of the native wild-type DEPTOR gene. This type of expression from the safe-harbor site effectively bypasses most forms of transcriptional regulation and does not rely on post-transcriptional modifications, such as splicing, as the expression product is already an ORF (64). In addition, possessing an engineered 5' UTR sequence that is used for the sole purpose of leading to high levels of protein expression for a given ORF, aids in bypassing many of the mRNA translation initiation regulatory mechanisms mentioned previously. Specifically, unpublished data from our laboratory have indicated the possibility that DEPTOR translation may be contingent upon either cap-independent translation mechanisms, and/or possibly, a suppression of some non-canonical cap-dependent mechanisms. During periods of mTOR activation, DEPTOR mRNA has been significantly depressed. This phenomenon has also been observed *in vivo* by our laboratory in a rodent model of obesity and insulin resistance, where reduced DEPTOR content, and high levels of mTOR activation (60), were associated with reduced DEPTOR mRNA compared to non-obese control animals (see Figure 4.1), strongly suggesting an mTOR negative feedback mechanism. By utilizing a species-specific DEPTOR clone with a modified 5' UTR that is not subject to the same pre-translational regulation, we have sought to uncouple this negative feedback and allow for the stable and constitutive expression of DEPTOR protein. This approach has allowed us to investigate the effects of stable DEPTOR overexpression in human cancer epithelial cells and murine myoblasts and monitor these effects over periods that would be impossible with only transient overexpression.

3.2.4. Potential Drawbacks

As with many experiments that focus on alterations in the expression of specific physiologically relevant proteins, there exists an enormous uncertainty in the full scope of consequences within the cellular environment. This is especially true for the manipulation of proteins that are key regulators of many cellular functions. DEPTOR and mTOR sit at a nexus of a multiple regulatory pathways that help to control many aspects of day to day cellular processes, including the regulation of protein synthesis and protein degradation, mitochondrial biogenesis, lipid synthesis, cytoskeletal organization, and even in the regulation of cell cycle progression (50). Directly manipulating these key regulatory proteins could have many unintended consequences for the cell that would make long term study highly impractical, if not impossible. One such specific concern was that constitutive DEPTOR overexpression would severely impair cellular function to such an extent that it would be unavoidably lethal. With regard to the C2C12 myoblasts, it was a distinct possibility that DEPTOR overexpression would interfere with the maintenance of the cell cycle progression in a way that made differentiation into myotubes either unavoidable, or impossible. However, at this point in time, no such drawbacks have been identified in either the C2C12 or MCF7 DEPTOR overexpressing cells.

3.3. GCMS

3.3.1. Background

One of the defining features of the Muscle Biology Laboratory lies in the popularization of utilizing the stable heavy isotope of hydrogen, deuterium, in physiologically relevant metabolic labeling studies. While the foundations for this technique have origins dating back to the early 1940's, it did not gain popularity for a variety of reasons, including a scarcity of deuterium due to appropriation by governments for use in weapons development, and a lack of sufficiently sensitive detecting equipment. However, advances in mass spectrometry allowed for the detection of deuterium enriched isotopomers at much lower levels and enabled the use of heavy-water (D_2O) stable isotope labeling studies to occur in subjects ranging from cell culture, to rodents, and even humans.

The basis for measuring protein synthesis rates with stable deuterium isotope tracers is very similar to other stable isotope tracer techniques but offers a number of benefits. Heavy water, when used as a tracer, can be administered via bolus injections, infusions, and even orally. When administered, heavy water equilibrates extremely rapidly with the existing water inside the body. Virtually all water containing compartments within the body will equilibrate with administered heavy water generally in around 20 minutes. Not only does heavy water equilibrate rapidly with body water, but the deuterium ions within the heavy water exist in a dynamic equilibrium with hydrogen ions in normal water. For example, if equal parts of water, and heavy water are mixed, they very rapidly equilibrate to being 50% semi-heavy water (HDO), 25% water

(H_2O), and 25% heavy water (D_2O). This dynamic equilibrium and rapid exchange of hydrogen and deuterium ions allows for the exchange of existing hydrogen ions on various amino acids with deuterium ions during transamination processes with the cytosol of cells within the body. This process is, in effect, using the cell's native biological processes to create stably labeled amino acids within the cell, bypassing traditional difficulties in delivering pre-labeled exogenous amino acids to the intracellular environments throughout the body. This labeling strategy bypasses some of the pitfalls of traditional stable isotope labeling methods that can be delivered to the intracellular environment unevenly, based on tissue differences in blood flow, or in differences in intracellular active amino acid transport.

Although all amino acids can become deuterated through transamination at their alpha carbon, alanine offers multiple advantages over many other amino acids. Alanine undergoes rapid transamination, and in addition to the single alpha carbon bound hydrogen, it possesses 3 beta carbon bound hydrogens that can be deuterated as well. This relationship between [heavy-water]:[water]:[deuterated-alanine] ensures an extremely stable labeling of alanine, that is directly proportional to the percent enrichment of the total body water. Once labeled, ^{2}H-Alanine is available to the cell to be incorporated into proteins, and while incorporated, the deuterium labeled sites cannot be exchanged with unlabeled protons. Another advantage of this labeling technique is that unlike traditional stable isotope 'fixed' labeling schemes, if free un-labeled alanine is introduced into this system through absorption through the gut, protein breakdown, or *de novo* alanine synthesis, it will rapidly equilibrate with existing deuterated water as

well. This equilibration allows for tremendous advantages regarding the maintenance of the labeled precursor pool, even with food consumption or periods of protein breakdown.

Gas chromatography-mass spectrometry (GC-MS) is extremely well suited for measuring the enrichment of both protein derived amino acids and body water. By measuring the total abundance of the tracer (^{2}H-Alanine) and the total abundance of the tracee (Alanine), we are able to calculate the moles percent excess (MPE), or the enrichment in excess of naturally occurring isotopes of a given sample. This is done for both Alanine, and water derived from blood plasma or culture media. With both of these measurements, the fractional synthesis rate (FSR) can be calculated from the following equation:

$$FSR = ((MPE_{Tissue}) * (MPE_{Plasma\ Water} \times 3.7 \times Time)^{-1}) \times 100$$

where MPE_{Tissue} is the mole percent excess (MPE) of the proteins within a tissue, $MPE_{Plasma\ Water}$ is the MPE of water within circulating plasma, and 3.7 is a corrective factor based on the likelihood of enrichment at multiple hydrogen sites on a given alanine molecule. In an extremely abbreviated overview, liquid samples are injected into the gas chromatography unit, and are quickly vaporized into gas and swept into a glass capillary tube by a helium carrier gas. Molecules within the gaseous sample will travel through the capillary tube at different rates depending on a number of chemical properties that determine how strongly the sample is able to interact with the chemically coated inner surface of the capillary column. The temperature of the column is manipulated in a very precise manner to aid in the separation of analytes within the

column. Upon traveling the complete length of the 30-meter capillary column, the analytes are ejected into a very low-pressure vacuum chamber, directly into the path of an ionizing filament situated between electromagnets. The filament is able to fragment the analytes, and strip them of a small number of electrons, imparting a slight positive charge to the molecules. Once fragmented and charged, electromagnets divert the samples 90 degrees, where they immediately pass through a quadrupole mass filter that only allows for the passage of molecules that possess a very specific mass to charge ratio (m/z). For our purposes, the m/z representing unlabeled alanine is 99, and labeled alanine is 100. These are often referred to as m+0 and m+1, respectively. These specific m/z fragments are finally subjected to another 90 degree turn with an extremely precise magnetic field where they impact a detector at different locations, depending on the m/z and how far each m/z is deflected based on the magnetic field diverting them into the detector. This detection method is incredibly accurate, and coupled with the analyte separation from gas chromatography, can be an extremely powerful tool in the quantification of known or unknown analytes.

However, there are a number of internal and external factors that can influence the measurement of the sample MPE. The measure of 99 m/z and 100 m/z for a given sample must be compared to a set of standards run on the GCMS. Typically, standards represent different enrichment levels of alanine, while maintaining a similar total concentration of alanine, and ideally, would encompass the range of enrichments present in the samples to be compared against. For this reason, our standards range from 0% MPE enrichment (or only naturally occurring background enrichment) up to 4% MPE (a

level of enrichment that exceeds even the fastest growing cell culture samples).

While this method is extremely complicated, and this description barely scratches the surface of the complexity of this machine, it has been extremely important for adapting our GCMS methods to this dissertation. While there are a number of factors that can influence the overall accuracy of the GCMS (such as tuning conditions, detector nonlinearity, integration errors, and isotope effects during ion fragmentation), the primary concern for accuracy lies in the ionization process being concentration-dependent. In short, the ionization and fragmentation pattern for a given sample, will vary based on the total abundance of the sample injected. This problem invalidates the assumption that the measured ion abundance ratios equate to the true isotopomer ratios. Historically, this problem is side-stepped by attempting to match standard abundances with sample abundances, thereby 'leveling the playing field', so to speak, and subjecting each analyte run to very similar ionizing environments. This is typically very easy to do when working with large tissue samples from rodents or humans, as the sample preparation can be done by tissue weight, and consistent sample concentrations can be achieved. This preparation may require multiple runs of standards to match abundances sufficiently, but this is easily accomplished, and may only add 12 - 24 hours of GCMS run time on to the 72 - 96 hours of GCMS run time for a typical study of a few dozen samples run in triplicate.

However, for tissues harvested from cell culture the total protein content of the samples were not only orders of magnitude lower, but the protein content discrepancies among treatment groups could be, and as it were, massive. The typical method of

abundance matching samples to standards could take far, far longer, as some samples would require their own set of 6 to 8 standards to be run! These new problems required new solutions.

3.3.2. Trace Analyte Analysis

The majority of samples analyzed in our laboratory via GCMS have been animal or human tissue that was prepped from whole skeletal muscle tissue (e.g. animal tissue harvest, or human muscle biopsy). Having access to many milligrams of tissue affords a lot of flexibility in the preparation of GCMS samples, and in the execution of the analysis. Measuring FSR via GCMS from tissues prepped in this manner is akin to using a surgical scalpel to chisel through a large boulder. Oftentimes, the injected sample is so abundant (1 μL injection containing ~20 μg of amino acids), that 95% of the vaporized sample is ejected from the machine via the helium carrier gas, so that the sample does not overwhelm the detection capabilities of the mass spectrometer. However, as our laboratory has delved into the realm of measuring FSR in cultured cells, this approach is no longer feasible. When the entire contents of a culture plate represent, in the absolute best scenario, an order of magnitude less protein content compared to a whole muscle preparation, ejecting 95% of the analyte from the machine was no longer required, or feasible for accurate analysis.

As a result, we have crafted a number of new analytical methods specifically tailored for the analysis of extremely low abundances of alanine and deuterated alanine in cell culture tissues. This new approach utilizes a number of different injection and

analysis parameters that now enable the detection of accurate tracer to tracee ratios in samples containing just a few nanograms of amino acids, representing an increase in the lower detection limit of the GCMS by multiple orders of magnitude. These new methods can be found in Appendix B.

3.3.3. Improved Integration and Second-Order Regression of GCMS Standards

When the analytical method for GCMS detection of deuterated alanine was developed for our laboratory in conjunction with Dr. Stephen Previs (23, 24), much of the GCMS method was adapted from an analytical method developed by Dr. Previs for the quantification of deuterated glucose (40). This method was formulated to combat difficulties in performing repeatable and accurate integration calculations to determine the area under the curve for a given ion chromatogram. The ultimate goal is to measure the area under the curve for both the fragment ion of choice, m+0 (99 m/z) as well as m+1 (100 m/z). As seen in Figure 3.2, a sample tracing for deuterated alanine showing m+0 in blue and m+1 in red, alanine and deuterated alanine elute just after ~9 minutes under these particular conditions.

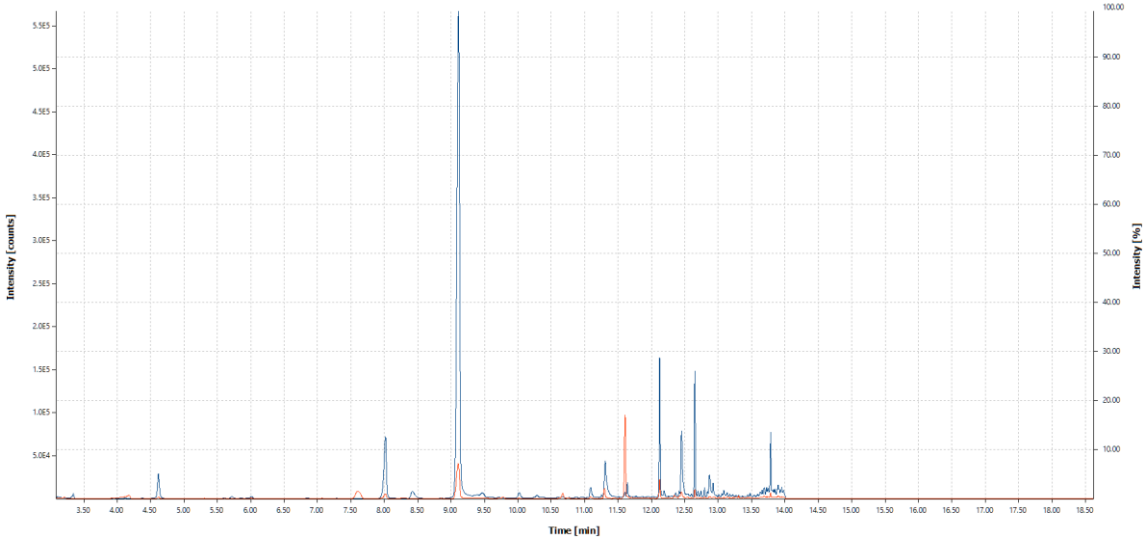

Figure 3.2 Sample MS Extracted Chromatogram. 99m/z in Blue, and 100 m/z in Red.

To combat the computational difficulties of measuring the area under the curve for both m+0 and m+1, it was determined that measuring the abundance of each ion between 25% and 50% of the peak height, was the most reliable method for determining enrichment. While this method is accurate and has the potential to be very reproducible, it is extremely time consuming, and is very dependent upon the level of training and motivation of the operator.

As a progression of this method, we have developed an automated method that completely removes the potential for operator bias and training level as confounding factors in enrichment measurements. Through the utilization of an algorithmic approach, software driven integration can reliably and accurately measure the areas under the curve for both m+0 and m+1 simultaneously, under a variety of machine conditions, including

those with variable preceding and tailing baseline measures. This area under the curve, adjusted for variable baseline isotope measures is referred to as the "corrected area under the curve", or commonly "corrected area". While this method improves upon ease of use and reproducibility, it is profoundly sensitive to the previously mentioned isotope abundance dependent ionization. Therefore, the abundances of samples and standards must be very tightly matched to maintain accurate enrichment measurement. While this may sound like a fairly straightforward problem, but in reality the amount of time it can take to accurately match samples to standards (or *vice versa*) typically takes many times longer than the initial run of samples and standards in triplicate. This can equate to hundreds of additional GCMS runs over a number of days, just to end up with imperfect standards with an acceptable predictive power. To overcome this problem, we have been forced to adapt our approach yet again.

We sought to model the abundance dependent ionization relationship between m+0 and m+1. By analyzing a set of seven standards (ranging from 0% MPE, to 4% MPE) at various preparation dilutions, injection amounts, and injection split-ratios (e.g. how much samples is ejected from the machine), we were able to model an extremely strong linear relationship between m+0 and m+1 for each standard within the set (r^2 ranging from 0.9979 to 0.9998). In effect, for a given abundance of m+0 in a standard, we are able to predict, with remarkable accuracy, the associated m+1 for each level of standard. By applying a second regression analysis to the m+0 to m+1 ratio predicted in the first regression, we are able to create a linear model that can serve as a model to predict the MPE of any m+1 for a given m+0.

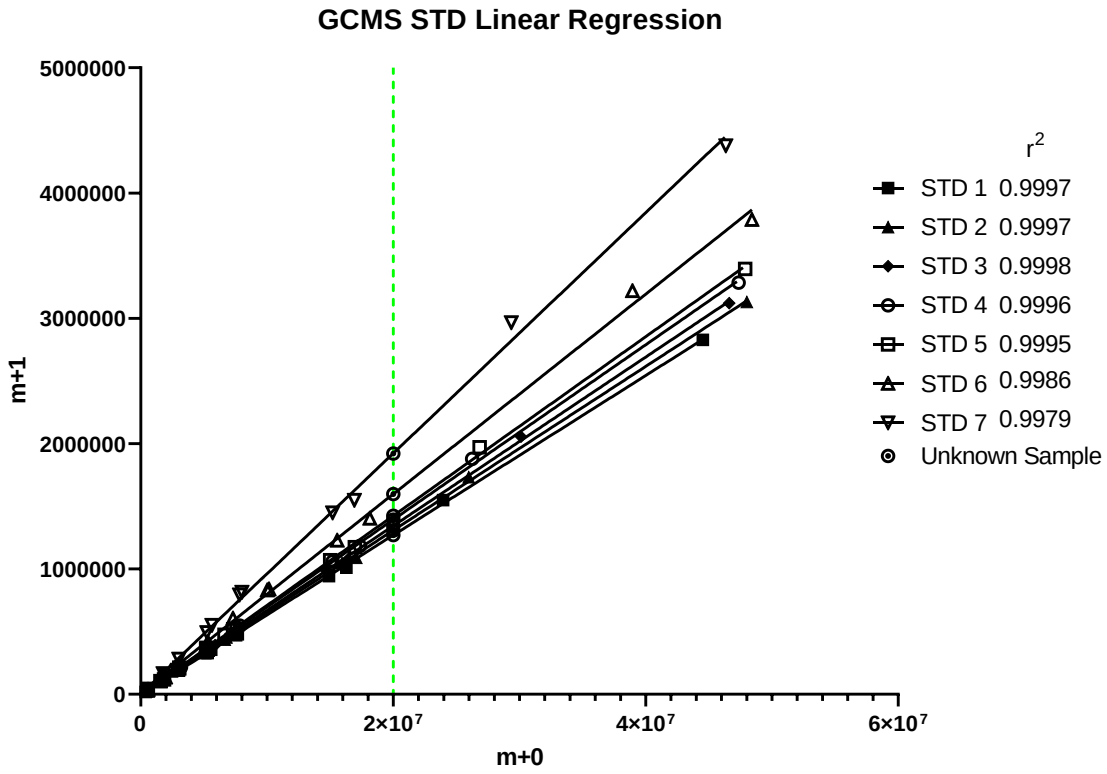

Figure 3.3 GCMS STD Regression.

As shown in Figure 3.3, for a given m+0 (shown by the vertical dotted line at $2x10^7$), we can predict a precise m+1 value for each of the seven standard levels. By running a second regression analysis with the derived m+1 values against the known MPE of each standard, we are able to predict the MPE for any m+1. In effect, we are able to produce an "ideal" set of standards based on the m+0 of any unknown sample.

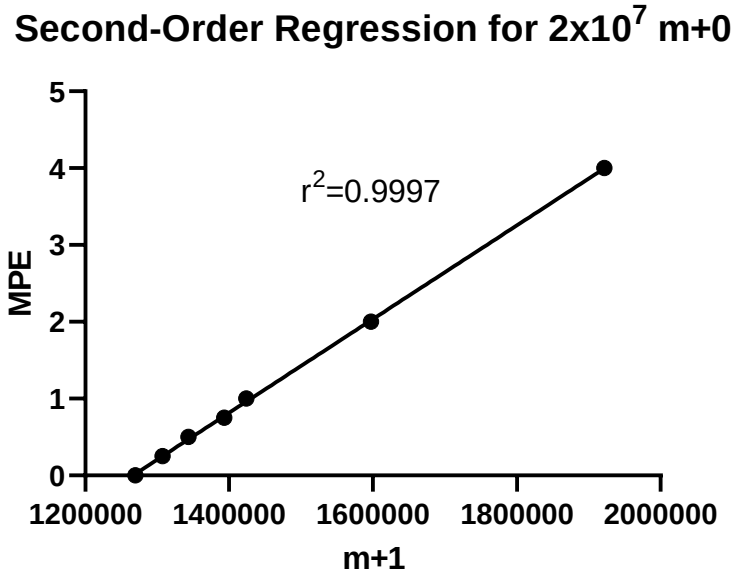

Figure 3.4 GCMS STD Second-Order Regression.

This is best visualized in Figure 3.4. As shown in Figure 3.4, the predictive ability of this model is extremely accurate for a given m+0, and affords an enormous amount of flexibility in the accurate determination of MPE regardless of the abundance dependent ionization effects inherent to the machine. After establishing this method as the *de facto* standard for analyzing deuterated alanine samples via GCMS we were both thrilled, and disappointed, to discover that a very similar method was developed for $^{2}H_{2}$-palmitate, $^{15}N_{2}$-urea, and ^{13}C-leucine by Patterson et al. over twenty years ago (65). Our contribution is that this analysis can be extended to alanine, which, since our initial efforts in this area, has become the preferred amino acid for the assessment of protein synthesis using deuterium methodologies worldwide.

With the new analysis methods, coupled with the second-order regression analysis of standards and samples, we are able to accurately measure FSR in sample amounts that would have been previously impossible. The entire contents of a 10 cm culture dish (~56 cm^2) were, at one point, pushing the reliable limits of measuring FSR. Now we have the capability to measure FSR in the partial contents of a single well on a 24-well plate (1.9 cm^2) amounting to no more than a few micrograms of tissue and representing a GCMS sample injection of ~150 nanograms of amino acids. We feel that this greatly expands the capacity to use GCMS instrument for extremely low abundances that would otherwise require more sensitive equipment that is ultimately cost prohibitive for most labs.

4. C2C12 DEPTOR OVEREXPRESSION

4.1. Introduction

There have been ongoing efforts to study the mechanisms of cellular growth for hundreds of years, and while we may have good idea of the overall process, there are many gaps in the understanding of cellular physiology. It has been estimated that there are over 10,000 different proteins that comprise the human proteome (1). However, if one considers the sum total of the different protein variations and modifications that can arise from the products of a single gene, the total number of different proteins in the human body quickly reaches into the billions (86). Cellular regulation of the production and modification of these protein products is an extremely varied and complex process that can occur at many points of control between the genomic DNA and the ultimate protein product. Our interest in this study lies in the expression (and ultimately, overexpression) of a single but powerful protein product called the DEP Domain-Containing MTOR-Interacting Protein or DEPTOR. DEPTOR acts as a cellular endogenous inhibitor of mTOR, a protein that sits "the nexus of nutrition, growth, ageing and disease" (50).

Since the discovery of DEPTOR in 2009, the relationship between DEPTOR and mTOR has slowly come to light, revealing a highly complex and dynamic double-negative feedback mechanism in which each protein exhibits negative control over the other, and sometimes in multiple ways. When DEPTOR is bound to mTOR, either in mTOR complex 1 (mTORC1) or mTOR complex 2 (mTORC2), the kinase activity of

mTOR is completely inhibited (7). However, the upstream activation of mTOR leads to the autophosphorylation of the bound DEPTOR molecule, weakening its binding to mTOR, ultimately leading to DEPTOR's degradation (18, 22). Our lab has previously found that the metabolic regulation of protein synthesis in skeletal muscle was strongly and inversely proportional to the DEPTOR content in the cell. During periods of muscle growth, as what occurs following resistance exercise, protein synthesis was relatively high while DEPTOR expression was low (60). Alternatively, when rates of synthesis were relatively low, such as what occurs with the reduction of muscle mass with hind limb unloading, DEPTOR content was high (85). We believe that this inverse relationship between rates of synthesis and DEPTOR is based on the interaction between mTOR activity (a potent regulator of muscle mass) and DEPTOR. However, it was unclear if the resultant FSR that was associated with differences in DEPTOR content were due to an altered synthesis of the DEPTOR molecule and/or the altered degradation of DEPTOR via environment-induced changes of upstream mTOR activation. Nor did we know if this relationship was causal or merely concomitant and is the underlying aim of this dissertation.

That said, recent advances have shown that the relationship between DEPTOR and mTOR is of critical importance to the normal function of mTOR, which is responsible for the regulation of cellular metabolism by modulating both protein synthesis and autophagy (32, 50, 73). Dysregulation of mTOR signaling has been implicated as a possible culprit in the onset and progression of metabolic disorders, cancer, neurodegeneration, and ageing (6, 7, 31, 50, 93). Our research has shown that a

possible culprit for metabolic syndrome and anabolic resistance may arise because of dysregulated protein metabolism (60). In that study, we found that one feature of anabolic syndrome was an uncontrolled elevation of mTORC1 activity, and this was strongly associated with reduced DEPTOR expression. This 'constitutive' dysregulation and hyperactivity of mTOR was either due to a relentless upstream signal activation of mTOR leading to the constant destruction of DEPTOR and/or an inability to manufacture DEPTOR under metabolic syndrome conditions. While the former possibility was more plausible, we conducted further study in muscle collected from Nilsson et al. (60) in order to assess mRNA content of DEPTOR (Figure 4.1) and mTOR associated proteins (not presented). Our findings demonstrate that DEPTOR mRNA is significantly reduced in response to resistance exercise and with metabolic syndrome, where we see a concomitant reduction of DEPTOR mRNA at times where DEPTOR expression is low. This strongly suggests that not only does the degradation of DEPTOR lead to the hyperactivity of mTOR, but also that the inability to manufacture the protein under some metabolic conditions allows for mTOR to remain active. This may be an important consideration for a variety conditions involving dysregulated protein metabolism, such as occurs with diabetes (60) and a host of DEPTOR-deficient cancers.

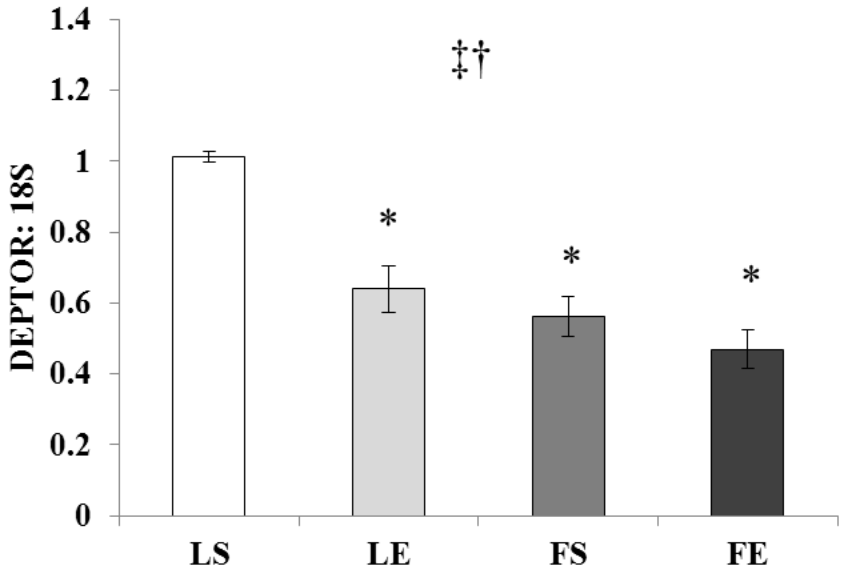

Figure 4.1 DEPTOR mRNA Content is Significantly Reduced with Exercise and Metabolic Syndrome. LS, lean sedentary (n=6); LE, lean exercised (n=6); FS, fatty sedentary (n=6); FE, fatty exercised (n=6). Data are presented as group mean ± SEM. ‡main effect of exercise ($p<0.001$); †main effect of phenotype ($p<0.001$); *different from LS ($p<0.05$). Reprinted from "Protein Degradative Processes Associated with Anabolic Dysregulation in Diabetic Skeletal Muscle" by Jackie Perticone, 2014 (66).

Based on previous experiments suggesting that the manufacture of DEPTOR may be a strong consideration for various disease states, the purpose of this study was to determine if the aforementioned DEPTOR over-expression strategy using precision edits is capable of impacting protein synthesis in skeletal muscle myotubes, in culture. Our underlying hypothesis was that the enhanced expression of DEPTOR would reduce protein synthesis in stably expressed muscle myoblasts but not interfere with cell differentiation into myotubes. This study represents a proof-of-concept first-step for the overarching goals of this dissertation. The present experiments have taken advantage of

new precision gene editing technologies to create a stable and constitutively active expression of the DEPTOR gene at the ROSA26 Safe-Harbor locus in an effort to further characterize its relationship with mTOR in the control of cellular anabolism.

4.2. Materials and Methods

4.2.1. Cell Culture, Transfection, and Differentiation

C2C12 murine myoblasts were chosen as gene editing targets for a variety of reasons but were of special interest in this case due to their rapid growth and capacity for differentiation into myotubes. Their robust growth and general hardy nature make them ideal candidates for genetic manipulation. In this study we have genetically modified the C2C12 myoblasts to contain a second copy of the DEPTOR open-reading frame (ORF) that is not only constitutively expressed but may be expressed independently of existing pre-translational regulation. We hypothesized that the stable overexpression of DEPTOR protein would be sufficient to negatively regulate anabolic markers downstream of mTOR.

C2C12 myoblasts were obtained from ATCC (Manassas, VA, CRL-1772), and were cultured in 10 cm plasma treated culture plates with Dulbecco's modified essential media (DMEM) with 20% fetal bovine serum (Avantor 1500-500), and 1% penicillin and streptomycin (Lonza 17-602F), referred to as growth media (GM). Cultured cells were grown at 37°C and 5% CO2 and were fed with fresh GM every 48 hours. Cells were grown to an appropriate level of confluency (<75%), and then passaged using a

trypsin/EDTA solution (0.25% w/v) into 6-well plates (2 x 10^4/cm^2) for transfections as described by Lee et al. (47), with a few minor modifications to the protocol.

Following 24-hours of recovery from passaging, MCP-ROSA26-CG01 vector was transfected into C2C12 cells in a single transfection (negative control), as well as with DC-Mm25645-SH02 (DEPTOR donor), and DC-SH358-SH02 (RFP donor positive control). Medium was replaced approximately 24 hours later, and cells were maintained for an additional 24 hours to recover before puromycin was added. To study the effect of DEPTOR gene overexpression on the anabolic profile of C2C12s, DEPTOR-overexpressing cells (DEP, n=5) and RFP expressing cells (RFP, n=5), were seeded at the same density (5x10^4 cells/cm^2) in 10 cm plates. 24-hours following attachment of cells, media was replaced with a differentiation media (DM) containing DMEM, 5% heat-inactivated horse serum, 1% penicillin/streptomycin, and supplemented with Insulin (5ug/ mL), Transferrin (5ug/ mL), and Selenious Acid (5ng/ mL) (Corning, Manassas, VA) and replaced daily for 7 days. For the assessment of protein synthesis rates, media was supplemented with 99.8% deuterium heavy water to a final media enrichment of 4% ^2H_2O.

4.2.2. Creation of DEPTOR overexpressing C2C12 cells by CRISPR/Cas9

A DEPTOR overexpressing C2C12 cell line was created by inserting a DEPTOR transgene expression cassette into the ROSA26 locus using the CRISPR/Cas9 system. This was accomplished by transfecting the MCP-ROSA26-CG01 vector into C2C12 cells with the DC-Mm25645-SH02 (DEPTOR donor), and DC-SH358-SH02 (RFP

donor), respectively (Genecopoeia, Rockville, MD). MCP-ROSA26-CG01 allows for the expression of Cas9 endonuclease, as well as single-guide RNA (sgRNA) designed for targeting the ROSA26 Safe-Harbor locus. Upon successful creation of a double-stranded break (DSB) at the ROSA26 site, the accompanying co-transfected vector (either the DEPTOR or RFP donor) are able to serve as DNA repair templates due to the presence of large areas of sequence homology with the areas upstream and downstream of the ROSA26 DSB. Through the innate homology directed repair mechanisms within the cell, the transgene sequence on the repair template, between the left and right ROSA26 homology arms, is effectively inserted into the ROSA26 locus. The DEP and RFP repair templates also include the ORF for a green fluorescent protein, and puromycin n-acetyl transferase.

4.2.3. Identification of DEPTOR Overexpressing C2C12 Cell Lines

Determination of transgene expression in DEP and RFP groups was accomplished in multiple ways. Firstly, following transfections, all groups of cells (Cas9 negative control, DEP, RFP positive control, and lipofectamine negative control) were subjected to a 14-day puromycin selection. Following selection, monoclonal cell lines were created through serial dilutions of positive responders. Secondly, appropriate cellular fluorescence (GFP for DEP cells; GFP and RFP for RFP cells) was confirmed via confocal fluorescence microscopy (Olympus FluoView 300, Tokyo, Japan) on live undifferentiated cells grown on glass coverslips as described by Fischer et. al 2008 (8).

4.2.4. Protein Fractional Synthesis Rates

Protein FSR was assessed using the deuterium stable isotope method as described previously (61). C2C12 myotubes (n=5 per group), were grown in media enriched with 99.8% deuterium heavy water (Cambridge Isotope Laboratories, Tewksbury, MA, #DLM-408-HP-PK) for a total enrichment of 4% $^{2}H_2O$, for a 24-hour period preceding tissue harvest. The myofibrillar rich cell fraction was isolated from the whole cell lysate, and analyzed via GC-MS as described previously (61).

4.2.5. Statistical Analyses

The effect of CRISPR/Cas9 mediated overexpression of DEPTOR gene on the rates of protein synthesis in C2C12 myotubes was assessed by independent t tests. Statistical significance was set at $P \leq 0.05$ (denoted in all figures by *). All data are presented as means ± standard error.

4.3. Results

4.3.1. Puromycin Selection and Fluorescence Microscopy

Of the C2C12 myoblasts that underwent co-transfections and single transfections, only the DEP and RFP groups contained cells that survived the 14-day puromycin selection. All groups experienced massive cell death at the onset of puromycin selection (<48 hours), but the DEP and RFP groups both contained colonies of surviving cells that were not only able to survive in the 1 µg/ml puromycin enriched media, but proliferate under the adverse conditions.

Following the Puromycin selection, surviving cells grown on glass coverslips were assessed for appropriate fluorescent protein expression. As shown in Figure 4.2, Figure 4.3, and Figure 4.4, DEP cells exhibit GFP expression and no detectable RFP expression (data not shown), and RFP cells exhibit both GFP and RFP expression.

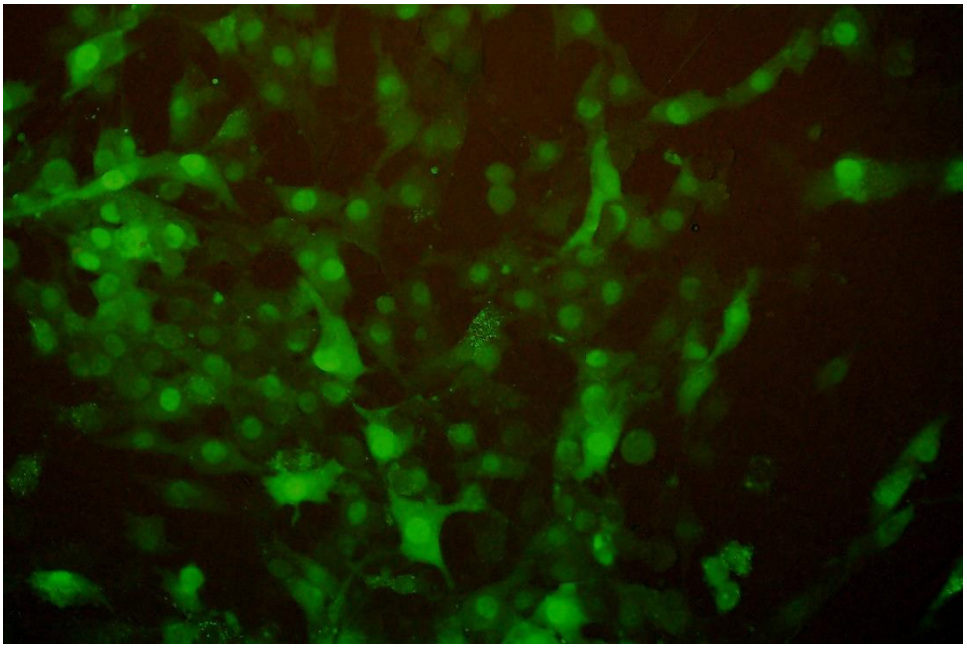

Figure 4.2 C2C12 DEP Cells GFP Expression.

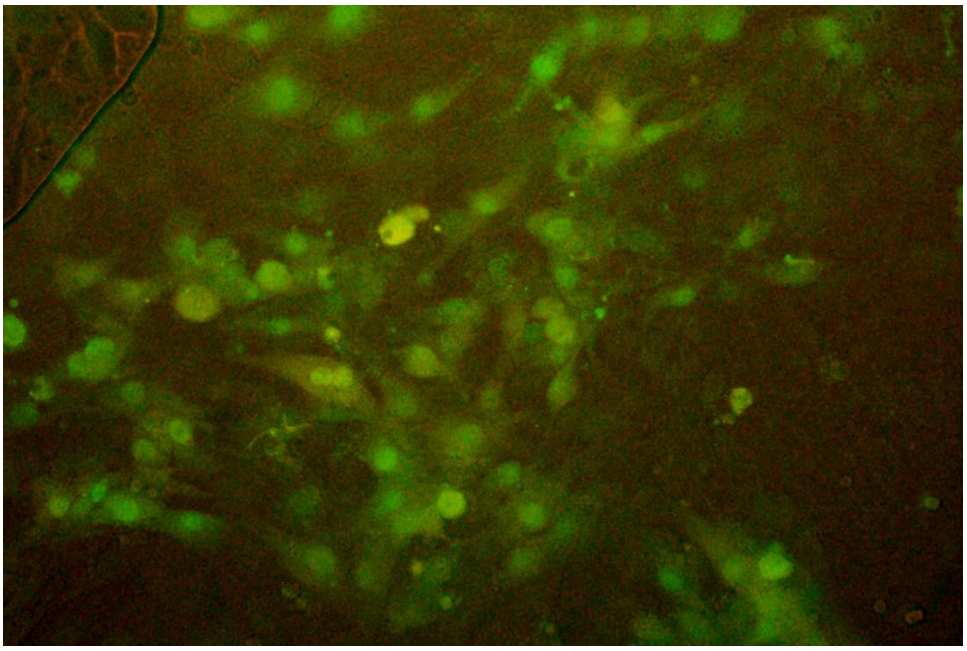

Figure 4.3 C2C12 RFP Cells expressing GFP.

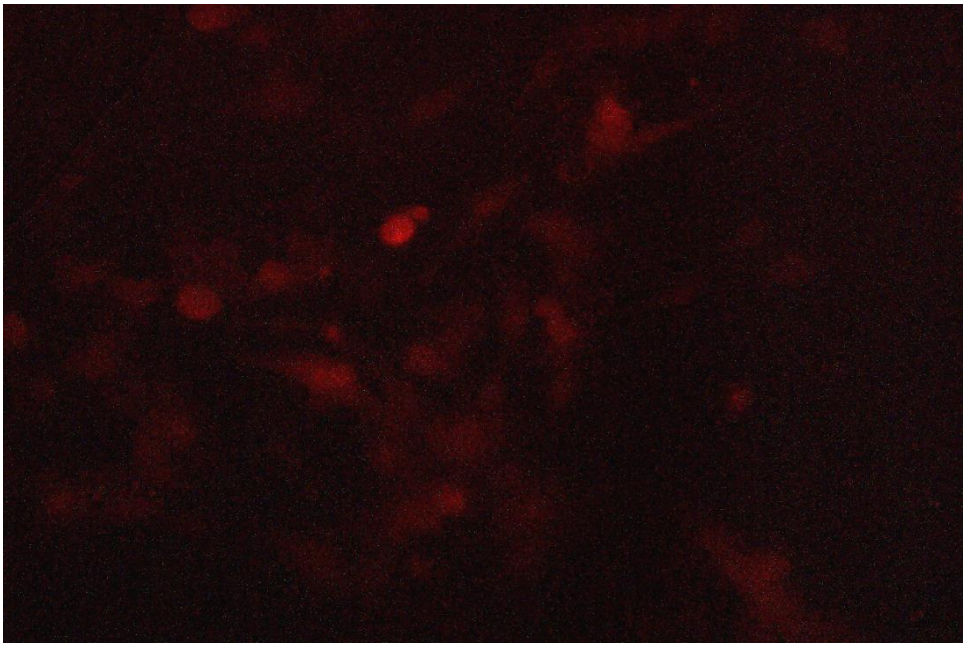

Figure 4.4 C2C12 RFP Cells Expressing RFP.

4.3.2. Fractional Synthesis Rates

Fractional synthesis rates of myofibrillar proteins were significantly lower in the DEP group (0.6155 ± 0.1791%) compared to the RFP group (1.215 ± 0.1093%) *P=0.0004.

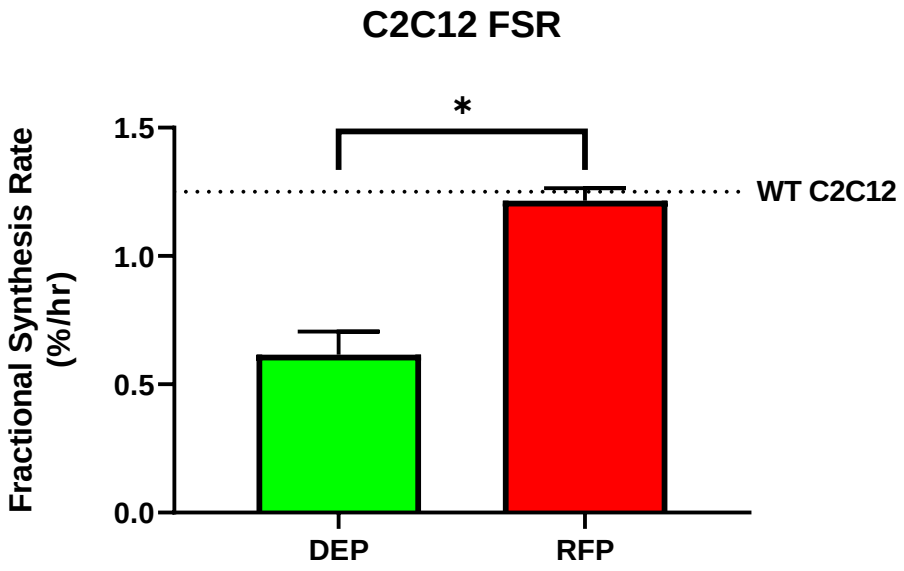

Figure 4.5 C2C12 DEP and RFP FSR. DEP (0.6155 ± 0.1791%) significantly lower than RFP (1.215 ± 0.1093%) *P=0.0004.

4.4. Discussion

Manipulated DEPTOR protein expression in C2C12 cells has shown promise in a previous investigation as a potent regulator of mTOR (41). However, that particular investigation utilized a transient knockdown of DEPTOR protein content using a short-hairpin RNA (shRNA), and is to the best of our knowledge, the only study in skeletal muscle that has utilized a direct manipulation of DEPTOR protein content. However, in

the past 2 years, there have been a number of investigations in other tissues and disease models that have also emphasized reductions in DEPTOR protein content for various outcomes (10, 16). Regardless of manipulated DEPTOR protein content, many investigations have shown that DEPTOR levels are very strongly inversely correlated with markers of cellular growth (10, 13, 16, 41, 56), and a lack of DEPTOR expression leading to rapid cell growth is a prominent feature in numerous cancers (67).

While this DEPTOR-deficient feature appears to be consistent across many tissues and diseases, we should note that there are a very few, but notable exceptions (67). In a subset of multiple myeloma cancer, overexpression of DEPTOR has been linked to increased cell survival through the suppression of apoptotic mechanisms, possibly through the relief of negative feedback stemming from mTOR activation (through p70S6 kinase on IRS-1). By suppressing mTOR activation these cells are able to, almost paradoxically, maintain anabolic signaling through PI3K and AKT, likely through an autophagic process that is often capable of protecting the cell from its extracellular environment (17). In fact, the overexpression of DEPTOR in multiple myeloma is considered largely responsible for the protection of these cancer cells during chemotherapy, preventing the drug from entering the cell. Studies have shown that the prevention of DEPTOR expression forces the cell to bring in extracellular substrates, enabling the entry of chemotherapeutic agents (17).

In addition to altered levels of anabolism and cell survival, DEPTOR protein content may be of vital importance in glucose homeostasis and in the expansion of white adipose tissue, albeit in different ways. DEPTOR protein content in adipocytes has been

shown to be strongly associated with BMI, with a 3.4 fold increase in expression found in BMI>30 compared to BMI<30 (45). However, in the skeletal muscle of a rodent model of obesity and type 2 diabetes, DEPTOR protein content is significantly diminished and associated with elevated rates of protein synthesis (60). While this may prompt one to think that the heightened anabolic responses in diabetic muscle would lead to larger muscle mass, the constitutively active mTOR actually leads to a reduction of muscle mass, likely because chronic mTOR activity suppresses the expression of specific proteins that are necessary for the maintenance of muscle mass over time (80). Furthermore, a DEPTOR deficient state in skeletal muscle may also lead, at least in part, to the insulin resistance observed in skeletal muscle with metabolic syndrome. This is likely due to constitutively active downstream targets of mTORC1, which have been shown to disrupt upstream signals leading to insulin mediated glucose uptake (45, 90, 93). Although beyond the context of the present study, successful use of precision gene edits may ultimately lead to a therapeutic intervention to normalize muscle function with insulin resistance.

Here, we have shown that C2C12 cells treated to stably overexpress the DEPTOR gene result in a significant reduction in the protein synthesis rates compared to RFP control cells. We should note that the RFP-expressing control cells exhibited similar FSR of protein when compared to WT C2C12 cells. In addition, following the gene editing of these C2C12 cells, it was markedly apparent that the DEPTOR overexpressing cell lines were expanding at a dramatically diminished rate when compared to the RFP and wild-type C2C12s (data not shown), yet they were ultimately

able to differentiate into myotubes. While this observation is anecdotal, it appeared to be extremely consistent across passages and seeding densities.

In summary, this investigation serves as an initial view into the effects of DEPTOR overexpression on the regulation of cellular metabolism, specifically as it relates to rates of protein synthesis. This study is the first to show that directed DEPTOR overexpression may have a causative effect of diminished mTOR-driven mRNA translation and may have profound implications in the treatment and/or control of a number of disease states. Future investigations should be directed to examine the effects of DEPTOR overexpression on glucose uptake, glucose metabolism, and cell survival.

5. STABLE DEPTOR OVEREXPRESSION REDUCES ANABOLIC CAPACITY OF MCF7 BREAST CANCER

5.1. Introduction

The regulation of cellular anabolism through the various mTOR complexes has been an extremely enticing prospect for the treatment of a variety of human diseases. This has been due in large part to mTOR's central location in the cellular signaling networks that control a variety of anabolic and catabolic processes inside of effectively every cell in the body. However, finding mechanisms to manipulate mTOR's signaling control has proven to be difficult due to their broad cellular effects. One avenue of research into mTOR modulation has focused on the intrinsic inhibitor, DEPTOR, a component of both mTORC1 and mTORC2. DEPTOR protein content has been strongly associated with changes in mTOR activity (41, 45, 60, 67). However, due to mTOR's role in both the degradation of DEPTOR, and in suppressing DEPTOR expression when activated, it can be difficult to assert whether changes in DEPTOR levels are leading to changes in mTOR activity, or if changes in mTOR activity are driving changes in DEPTOR levels (9, 22). As a result, there have been a number of investigations into this relationship by modulating the expression of DEPTOR protein through transient overexpression, RNA silencing, or through manipulation of DEPTOR degradation mechanisms (18, 22, 41, 67). While these transient expression experiments have yielded valuable information about the nature of DEPTOR's acute role in anabolic and catabolic

processes, they are also unable to ascertain the nature of chronic changes in the face of permanently altered DEPTOR expression.

To evaluate the relationship of DEPTOR overexpression on mTOR activity, we have previously and successfully utilized the CRISPR/Cas9 system to create a stable DEPTOR protein in mouse muscle cell lines in an effort to control fractional synthesis rates of the cells through mTOR inhibition. The purpose of this set of experiments was to expand on our prior work by stably overexpressing DEPTOR in a breast cancer MCF7 cell line, which has been characterized as a 'DEPTOR-deficient cancer'. We hypothesized that the overexpression of DEPTOR will restore control over mTOR activity and attenuate the prolific growth rates of these cells. This series of experiments was accomplished through the addition of a second copy of the human DEPTOR gene to the AAVS1 human genomic safe harbor (GSH) site (64). The benefits of this approach are two-fold. One, it allows for constitutively active transcriptional expression, and two, it reduces the likelihood of native pre-translational regulatory mechanisms from controlling the expression of DEPTOR protein. Unpublished data from our laboratory have indicated the possibility that DEPTOR translation may be dependent upon cap-independent translation mechanisms, or possibly, a suppression of some cap-dependent mechanisms. By utilizing a human DEPTOR clone with a modified 5' UTR that is dependent upon cap-dependent translation mechanisms, we have sought to uncouple this negative feedback and allow for the constitutive expression of DEPTOR protein. This approach has allowed us to investigate the effects of stable DEPTOR overexpression in human cancer and monitor these effects over periods that would be impossible with

transient overexpression. While there have been a small number of investigations that have sought to stably overexpress DEPTOR protein (8, 39, 45, 99, 103), all of these studies have utilized viral vectors or other stable integration techniques that rely upon non-specific integration into the host genome that can result in varying copy numbers, or the approaches used caused direct interference with the expression of other genes. To our knowledge, no studies exist that have utilized precision gene editing technologies to overexpress DEPTOR protein in any model, studying any tissue.

5.2. Materials and Methods

5.2.1. Cell Culture, Transfections, and Microscopy

MCF7 human epithelial breast cancer cells were obtained from ATCC (HTB-22) and cultured in Dulbecco's modified essential media (DMEM) with 20% fetal bovine serum (Avantor 1500-500), and 1% penicillin and streptomycin (Lonza 17-602F). Cultured cells were grown at 37°C and 5% CO2 and were fed with fresh GM every 48 hours. Cells were grown to an appropriate level of confluency (<75%) in 10 cm culture plates, and then passaged using a trypsin/EDTA solution (0.25% w/v) into 12-well culture plates for transfection and co-transfection procedures consistent with procedures described previously by Lee et. al 2015, with minor modifications (47).

Following 24-hours of recovery from passaging, HCP-AAVS1-CG02 vector was transfected into MCF7 cells in a single transfection (negative control), as well as with DC-A4329-SH01 (DEPTOR donor), and DC-RFP-SH01 (RFP donor positive control). Medium was replaced approximately 24 hours later, and cells were maintained for an

additional 24 hours to recover before puromycin was added. To study the effect of DEPTOR gene overexpression on the anabolic profile of MCF7 cells, DEPTOR-overexpressing cells (DEP, n=6) and RFP expressing cells (RFP, n=6), were seeded at the same density ($5x10^4$ cells/cm2) in 10 cm plates for evaluation of protein synthesis rates and immunoblotting. For the assessment of protein synthesis rates, media was supplemented with 99.8% deuterium heavy water to a final media enrichment of 4% 2H2O. In addition, DEP and RFP cells were also plated on 24-well culture plates for the evaluation of proliferation over an 8-day period with harvests at 1, 2, 4, and 8 days (n=6/group/day).

5.2.2. Creation of DEPTOR Overexpressing MCF7 Cells

A DEPTOR overexpressing MCF7 cell line was created by inserting a human DEPTOR transgene expression cassette into the AAVS1 GSH locus using the CRISPR/Cas9 system. This was accomplished by transfecting the HCP-AAVS1-CG02 vector into MCF7 cells with the DC-A4329-SH01 (DEPTOR donor), and DC-RFP-SH01 (RFP donor), respectively (Genecopoeia, Rockville, MD). HCP-AAVS1-CG02 allows for the expression of Cas9 endonuclease, as well as single-guide RNA (sgRNA) designed for targeting the AAVS1 GSH locus. Upon successful creation of a double-stranded break (DSB) at the AAVS1 site, the accompanying co-transfected vector (either the DEPTOR or RFP donor) aid in the innate homology directed repair mechanisms by acting as a repair template. In effect, the entire sequence between the left and right AAVS1 homology arms is inserted into the safe-harbor site. For both the DEP and RFP

repair templates, the inserted region also includes the ORF for a green fluorescent protein, and puromycin n-acetyl transferase.

All transfections and co-transfections were carried out in 12-well plates, in Opti-MEM media (Gibco; 31985088) using Lipofectamine 3000 (Thermo Fisher Scientific; L3000001). MCF7 cells were seeded onto two 12-well plates at approximately 0.1 x 106 per well and allowed to rest for 24 hours. Approximately 24 hours after seeding, cells were subjected to co-transfections of Cas9/DEPTOR, and Cas9/RFP, as well as individual transfections of one element of each vector pair as negative controls. In addition, subsets of cells were transfected without exogenous DNA as additional negative controls. Transfections were performed as a modified protocol of a previously described protocol (47). Co-transfections were performed as titrations by delivering 0.25, 0.5, and 1.0 ug of total plasmid DNA to cells, with each amount delivered in a 1:1, 1:2, and 1:3 combination with lipofectamine 3000. Cell media was replaced with Opti-MEM and lipid/DNA complexes were added and incubated for a full 24 hours at 37°C and 5% CO2 before returning to DMEM growth media.

5.2.3. Identification of DEPTOR Overexpressing MCF7 Cell Lines

Stable transgene expression was confirmed in the MCF7 cells in multiple ways. Firstly, following a 24-hour recovery in standard DMEM, cultured cells were subjected to puromycin selection lasting for 14 days in DMEM enriched with 1 ug/ml puromycin, as indicated by wild-type MCF7 puromycin toxicity dose-response kill curve (unpublished data). Cellular growth was monitored daily via brightfield microscopy and

the puromycin enriched media was changed every 24-hours for 14 days. Secondly, live cell fluorescence microscopy was performed on cells surviving the puromycin selection for confirmation of appropriate fluorescent protein expression. Finally, cells were analyzed by immunoblot analysis for confirmation of DEPTOR overexpression.

5.2.4. Disruption of the DEPTOR/mTOR Axis Using Small Molecule Interference

The present study was designed to assess the impact of DEPTOR overexpression on growth rates of MCF7 cells. To establish whether potential changes in MCF7 growth was directly attributed the inhibitory impact of DEPTOR on mTOR and not a result of an unintended off-target consequence, we mechanistically assessed the role of DEPTOR on mTOR inhibition utilizing the small molecule inhibitor NSC126405 (84). This molecule directly alleviates DEPTOR's inhibitory effect on mTOR through a competitive inhibition of the protein-protein binding site. In theory, any impact that was directly attributed to the DEPTOR inhibition of mTOR should be completely reversed in the presence of this molecule but would not necessarily impact potential off target consequences.

5.2.5. Immunoblotting, Rates of Protein Synthesis, and Proliferation Assay

To assess the expression of proteins and their phosphorylation status, equal quantities of total protein obtained from whole cell lysates were analyzed as described previously (20, 60, 61), and normalized to the whole lane total protein content as measured by Ponceau S staining (71). Assessment of specific protein content was

accomplished with the following antibodies: 4E-BP1 (Cell Signaling Technology, Danvers, MA #9644), Phospho-4E-BP1$^{Thr37/46}$ (Cell Signaling #2855), P70S6K1 (Cell signaling #2708), Phospho-p70S6K1^{Thr389} (Cell Signaling #9234), and DEPTOR (Millipore Signa, Burlington, MA, #ABS222).

Proliferation assay was carried out initially as a 4-day time course, with harvests every 24 hours. DEP and RFP cells were seeded onto 24-well plates with $2x10^4$ cells/well. A second proliferation assay was performed as an 8-day time course, with harvests at 1, 2, 4, and 8 days. MCF7 cells (DEP, RFP, with and without 1 µM NSC126405 treatment) were also grown in 24-well plates, but at a seeding density of $4x10^4$ cells/well. Cells in both assays were fed daily with GM and harvested at the indicated time points with indicated treatments. Cellular proliferation was based on measures of total cellular protein content. This measure was accomplished by aspirating media, washing twice with ice cold PBS, and lysing the entire contents of the culture well by the direct addition of lysing buffer with Triton X-100 detergent. Cell lysates were collected and analyzed via a BCA protein content assay (Thermo Fischer, #23225) in triplicate.

Twenty-four-hour fractional rates (FSR) of protein synthesis were measured in the DEP (n=6) and RFP (n=6) groups grown on 10 cm plates, using the previously described deuterium stable isotope labeling methodology (2). In addition, FSR was determined on the DEP and RFP groups (with and without NSC126405) from each timepoint of the 8-day proliferation assay.

5.2.6. Statistical Analyses

The effect of CRISPR/Cas9 mediated overexpression of DEPTOR gene on the rates of protein synthesis, and in measures of relative protein content by immunoblotting in MCF7 epithelial breast cancer cells was assessed by independent t tests. For evaluation of the effect of DEPTOR overexpression and NSC-126405 treatment on proliferation rates, a 2-way ANOVA was used, followed by Tukey's multiple comparisons test. For evaluation of differences in rates of protein synthesis within a timepoint, a one-way ANOVA was performed, followed by a Tukey's multiple comparisons test. Statistical significance was set at $P \leq 0.05$ (denoted in all figures by *). In addition, a single independent t test was performed as a preselected comparison between RFP and a previous cohort of WT MCF7 cells. All data are presented as means ± standard error.

5.3. Results

5.3.1. Puromycin Selection and Fluorescence Microscopy

Of the MCF7 epithelial cells that underwent co-transfections and single transfections, only the DEP and RFP groups contained cells that survived the 14-day puromycin selection. All groups experienced massive cell death at the onset of puromycin selection (<48 hours), but the DEP and RFP groups both contained colonies of surviving cells that were not only able to survive in the 1 µg/ml puromycin enriched media, but proliferate under the adverse conditions.

Following the Puromycin selection, surviving cells grown on glass coverslips were assessed for appropriate fluorescent protein expression. As shown in Figure 5.1, Figure 5.2, Figure 5.3, and Figure 5.4, the DEP group appropriately exhibits GFP expression, but no RFP expression, while the RFP group appropriately exhibits both GFP and RFP expression.

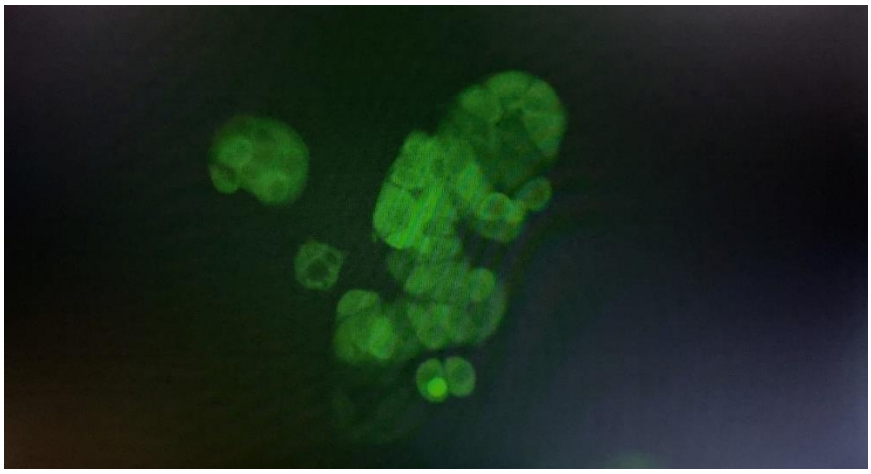

Figure 5.1 MCF7 DEP Cells Expressing GFP.

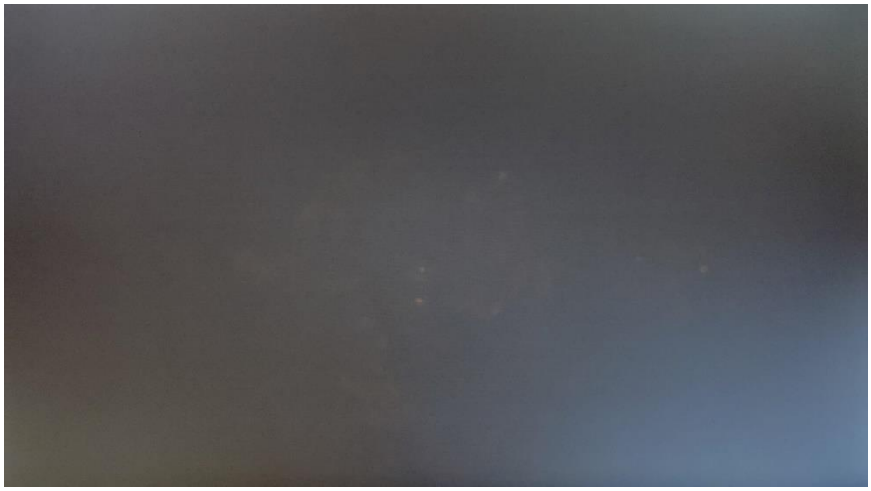

Figure 5.2 MCF7 DEP Cells with No RFP Expression.

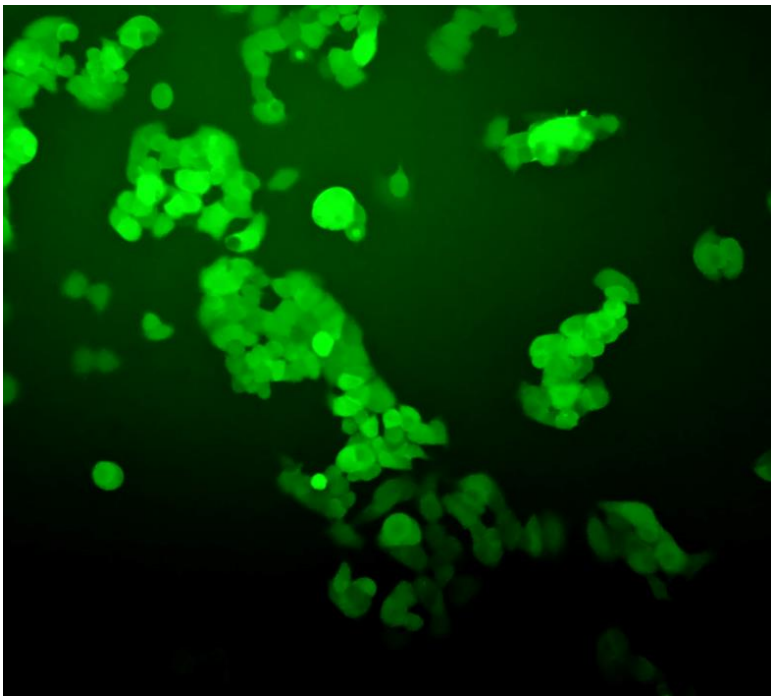

Figure 5.3 MCF7 RFP Cells Expressing GFP.

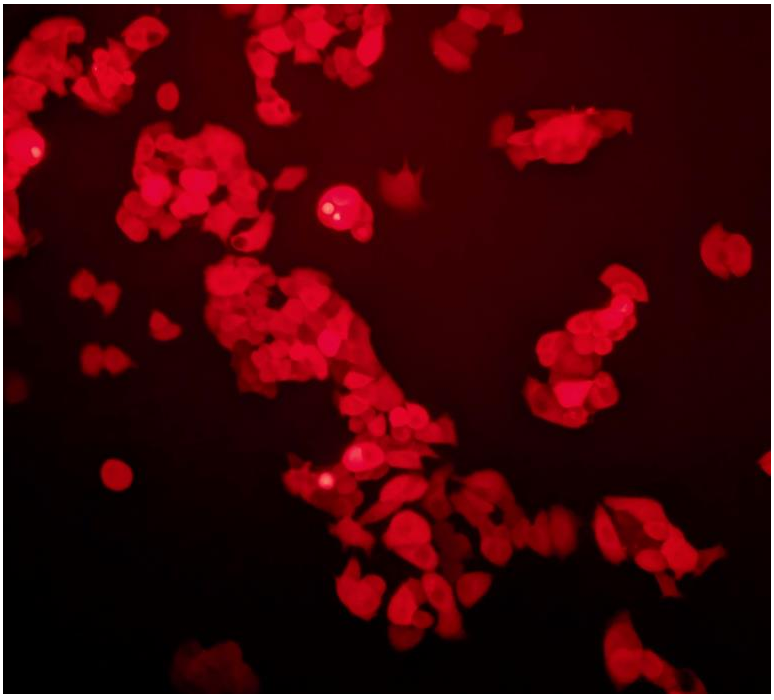

Figure 5.4 MCF7 RFP Cells Expressing RFP.

5.3.2. Immunoblotting and FSR of DEPTOR Overexpressing MCF7 Cells

Immunoblot analysis of DEP and RFP groups indicated no statistical differences in the relative expression of phosphorylated p70S6 Kinase at Threonine 389, or total p70S6 Kinase (Figure 5.5 – A, and Figure 5.5 – B). However, the ratio of phosphorylated to total p70S6 Kinase was significantly lower in the DEP group compared to the RFP group, P=0.0276, (Figure 5.5 – C). Conversely, Phosphorylated 4E-BP1 at Threonine 37 and 46, as well as total 4E-BP1, was found to be significantly higher in the DEP group compared to the RFP group (Figure 5.5 – D, and Figure 5.5 – E), P=0.0163, and P=0.0001 respectively, but the ratio of phosphorylated to total 4E-BP1 was not statistically different.

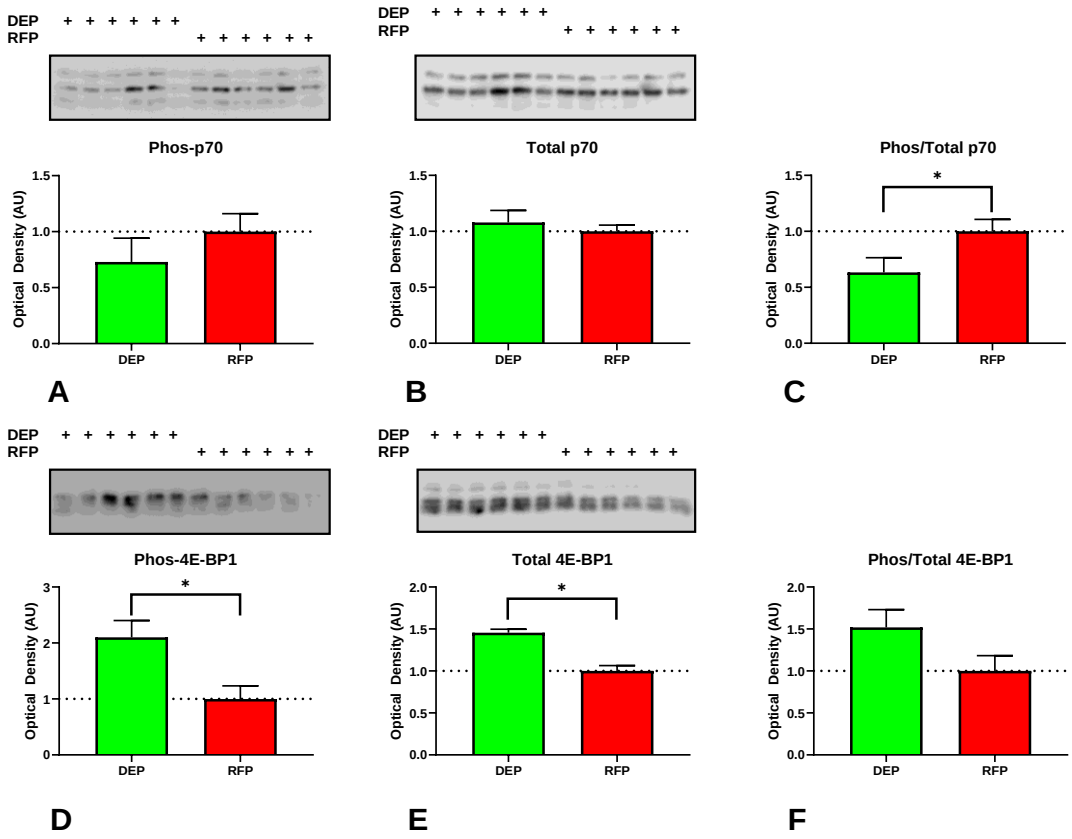

Figure 5.5 MCF7 24-Hour Western Blot Analysis (n=6 per group). (A) Phosphorylated p70 S6 Kinase ^{Thr389} (DEP, 0.7291 ± 0.2129; RFP, 1.000 ± 0.1602, P=0.1667). (B) Total p70 S6 Kinase (DEP, 1.080 ± 0.1074; RFP, 1.000 ± 0.0553, P=0.2621). (C) Phosphorylated to total ratio of p70 S6 Kinase (DEP, 0.6329 ± 0.1315; RFP, 1.000 ± 0.1065, *P=0.0276). (D) Phosphorylated 4E-BP1 $^{Thr37/46}$ (DEP, 2.101 ± 0.3012; RFP, 1.000 ± 0.2347, *P=0.0163). (E) Total 4E-BP1 (DEP, 1.455 ± 0.0418; RFP, 1.000 ± 0.0647, *P=0.0001). (F) Phosphorylated to total ratio of 4E-BP1 (DEP, 1.518 ± 0.2128; RFP, 1.000 ± 0.1831, P=0.945).

Immunoblot analysis of the relative DEPTOR protein content indicated a 9.4-fold greater DEPTOR content in the DEP group compared to the RFP group (Figure 5.6), P <0.0001. In addition, as shown in Figure 5.7, assessment of protein fractional synthesis

rates revealed a ~40% reduction in the DEP group compared to the RFP group (DEP, 0.954% ± 0.094% vs RFP, 1.562% ± 0.008%; P<0.0001).

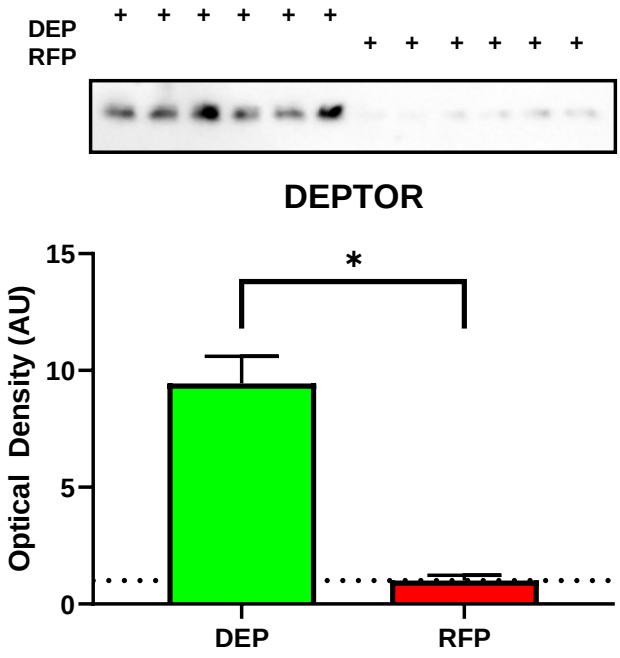

Figure 5.6 MCF7 24-Hour Western Blot Analysis for DEPTOR (n=6 per group). DEP significantly higher than RFP. ~9.4x difference (DEP, 9.443 ± 1.165; RFP, 1.000 ± 0.2257, *P <0.0001). Dotted line represents an AU value of "1.00" for reference.

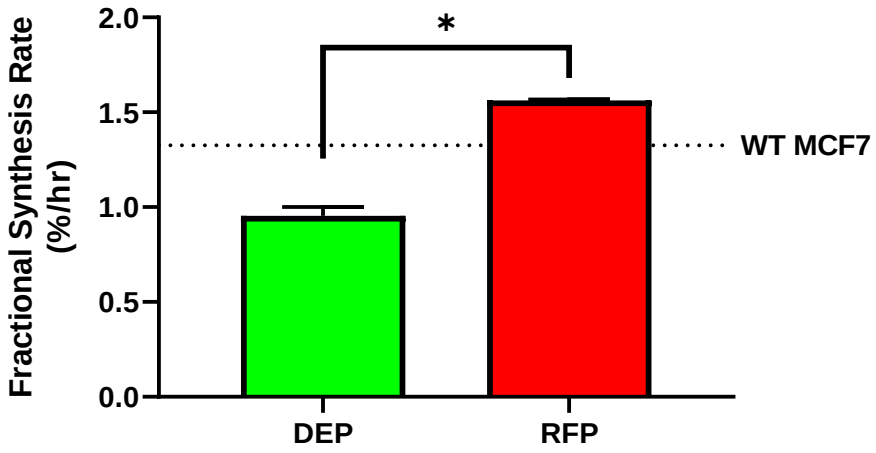

Figure 5.7 MCF7 24-Hour Fractional Synthesis Rate of DEP (n=4) and RFP (n=4) Groups (* DEP, 0.954% ± 0.094% vs RFP, 1.562% ± 0.008%; P<0.0001). Dotted line represents a previously assessed average FSR in wild-type MCF7 cells.

5.3.3. 4-day and 8-Day Proliferation Assay and FSR of DEPTOR Overexpressing MCF7 Cells

The 4-day proliferation assay between DEP and RFP groups were not different for days 1, 2, and 3, but the differences between groups became statistically significant on day 4 as shown in Figure 5.8 (DEP, 0.0709 ± 0.0097 mg/ml vs RFP, 0.1251 ± 0.0188 mg/ml; P=0.0114).

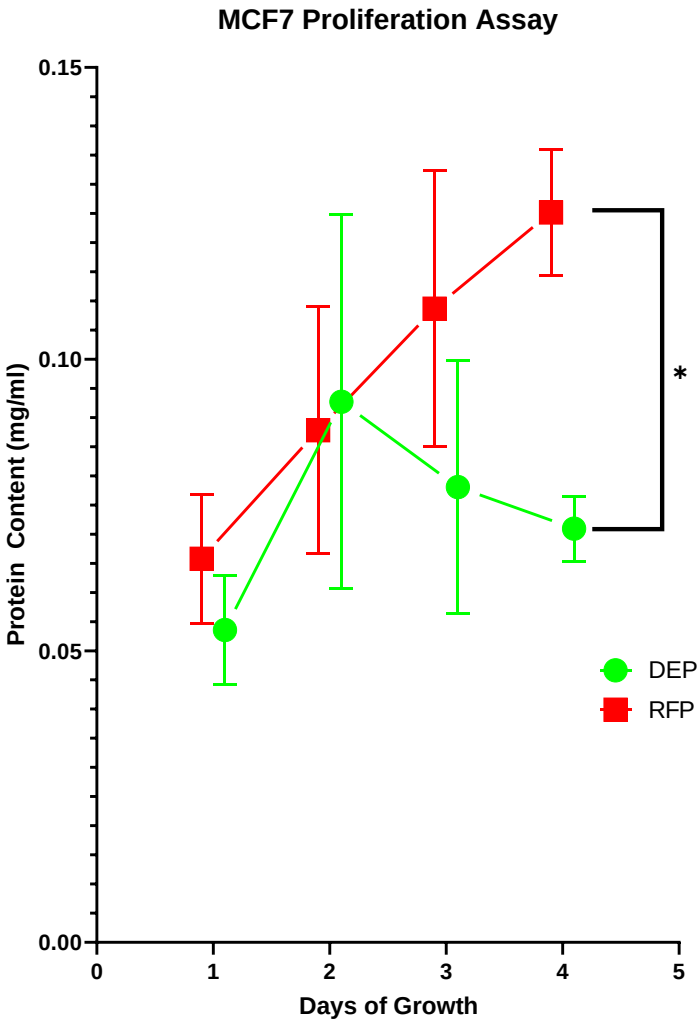

Figure 5.8 MCF7 Four-Day Proliferation Assay of DEP (n=3) and RFP (n=3) Groups. (* DEP, 0.0709 ± 0.0097 mg/ml vs RFP, 0.1251 ± 0.0188 mg/ml; P=0.0114)

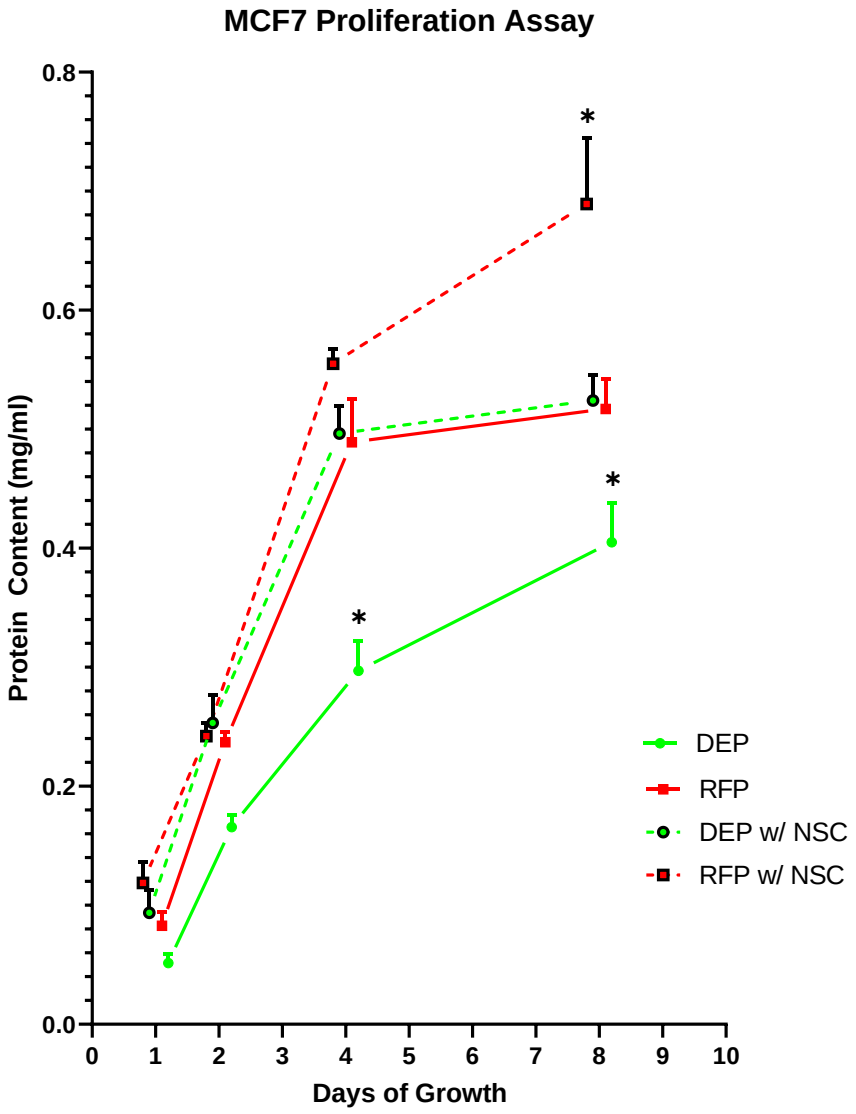

Figure 5.9 MCF7 Extended Proliferation Assay of DEP (n=6), RFP (n=6), DEP w/ NSC (n=6), and RFP w/ NSC (n=6) Groups. NSC-126405 delivered at 1 µM. Day 4, DEP group significantly lower than all other groups (* DEP, 0.297 ± 0.062 mg/ml; vs RFP, 0.489 ± 0.090 mg/ml, P<0.0001; vs DEP w/ NSC, 0.496 ± 0.056 mg/ml, P<0.0001; and vs RFP w/ NSC 0.555 ± 0.031 mg/ml, P<0.0001). Day 8, DEP group (DEP, 0.517 ± 0.062 mg/ml) remained significantly lower than all other groups (vs RFP, 0.517 ± 0.062 mg/ml, P=0.0436; vs DEP w/ NSC, 0.524 ± 0.052 mg/ml, P=0.0231; vs RFP w/ NSC, 0.689 ± 0.136 mg/ml, P<0.0001). RFP w/ NSC group was found to be significantly higher than all other groups (vs DEP, P<0.0001; vs RFP, P<0.0001; vs DEP w/ NSC, P=0.0002).

However, in the extended 8-day proliferation assay, not only do we observe a similar reduction in total protein content in the DEP group by day 4 (DEP, 0.297 ± 0.062 mg/ml; vs RFP, 0.489 ± 0.090 mg/ml, P<0.0001; vs DEP w/ NSC, 0.496 ± 0.056 mg/ml, P<0.0001; and vs RFP w/ NSC 0.555 ± 0.031 mg/ml, P<0.0001), we also observe multiple differences at the 8 day time point (Figure 5.9). The DEP group (DEP, 0.517 ± 0.062 mg/ml) remained significantly lower than all other groups (vs RFP, 0.517 ± 0.062 mg/ml, P=0.0436; vs DEP w/ NSC, 0.524 ± 0.052 mg/ml, P=0.0231; vs RFP w/ NSC, 0.689 ± 0.136 mg/ml, P<0.0001). However, the RFP w/ NSC group was also found to be significantly higher than all other groups (vs DEP, P<0.0001; vs RFP, P<0.0001; vs DEP w/ NSC, P=0.0002).

Fractional synthesis rates of the extended proliferation assay day 2 time point (Figure 5.10) indicate that the DEP group had a significantly lower 24-hour rate of protein synthesis when compared to RFP (DEP, 0.4438 ± 0.1686%; vs RFP, 1.000 ± 0.4534%, P=0.0014). To assess role of the DEPTOR-mTOR interaction, we introduced the small molecule inhibitor NSC126405 that abolishes the DEPTOR-mTOR interaction. This led to an increase in protein synthesis in the DEP w/ NSC group when compared to DEP (DEP w/ NSC, 1.072 ± 0.1667%; DEP, 0.4438 ± 0.1686%, P=0.0002). While the addition of NSC126405 did not increase FSR in the RFP w/ NSC group compared to RFP (RFP w/ NSC, 0.8907 ± 0.1198%; RFP, 1.000 ± 0.4534%, P=0.8212), it was similarly higher than the DEP group (P=0.0095).

By day 4 (Figure 5.10), however, the DEP w/ NSC group (1.570 ± 0.3802%) was found to have a significantly higher FSR than the RFP group (1.000 ± 0.1678%,

P=0.0012) and DEP group (1.042 ± 0.3037%, P=0.0029). There was no difference between the RFP w/ NSC group and any other group. However, by day 8 (Figure 5.10), the FSR of the DEP group (1.267 ± 0.0976%) was significantly higher than the RFP group (1.000 ± 0.0848%, P=0.0144), and approaching significance when compared to the DEP w/ NSC group (1.084 ± 0.0298%, P=0.1423), and the RFP w/ NSC group (1.060 ± 0.0492%, P=0.0782).

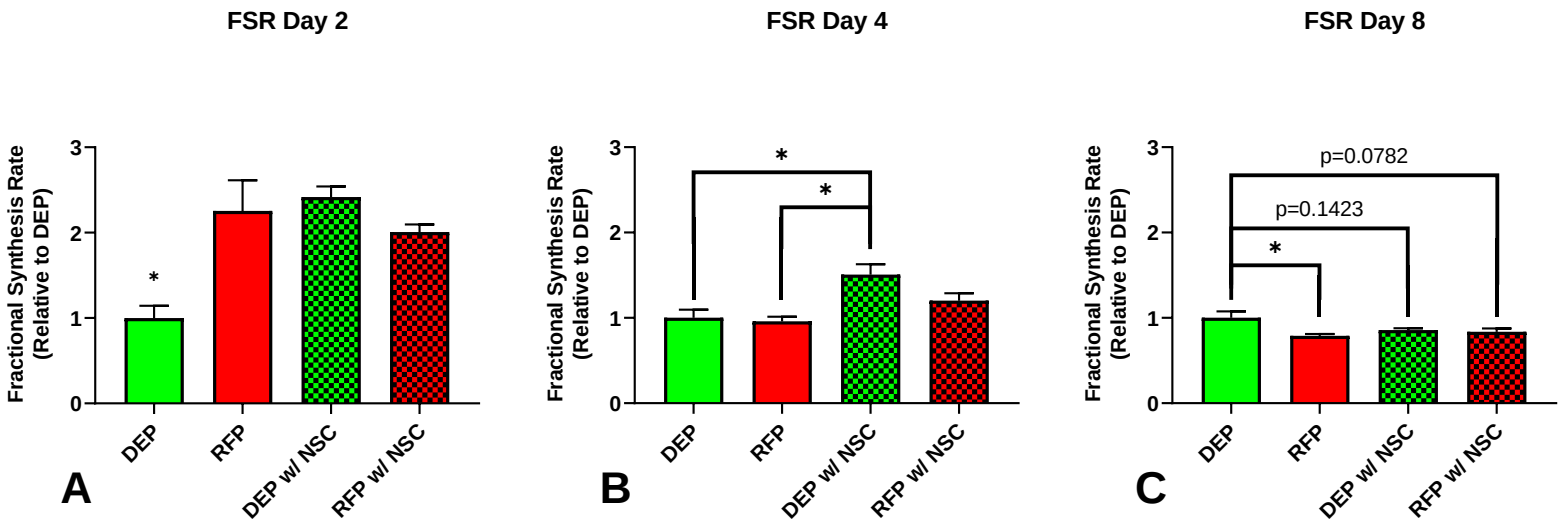

Figure 5.10 MCF7 Extended Proliferation Assay FSR by Day. (A) Day 2, DEP group significantly lower than all other groups. DEP, 1.000 ± 0.1436%; vs RFP, 2.253 ± 0.3612%, P=0.0014; vs DEP w/ NSC, 2.415 ± 0.1252%, P=0.0002; vs RFP w/ NSC, 2.007 ± 0.0900%, P=0.0095. (B) Day 4, DEP w/ NSC group (1.506 ± 0.1216%) significantly higher than RFP (0.9596 ± 0.0537%, P=0.0012), and DEP (1.000 ± 0.0972%, P=0.0029). (C) Day 8, DEP (1.000 ± 0.0770%) significantly higher than RFP (0.7894 ± 0.02231%, P=0.0144).

5.4. Discussion

While the inhibitory effect of DEPTOR on mTOR has been well-established (10, 16, 39, 45, 67, 99), much of the dynamic interactions between the two proteins are less understood. By stably and constitutively overexpressing DEPTOR protein independently of canonical regulatory mechanisms, we have been able to provide evidence for a causal relationship of DEPTOR expression leading directly to the suppression of mTOR activity and the subsequent suppression of both 24-hour protein synthesis rates and multi-day rates of proliferation. This is in contrast to previous speculation that changes in DEPTOR protein content may be a result of changes in mTOR activity, rather than a driving force of those changes. While this is still likely true to an extent, this study has demonstrated a direct relationship between DEPTOR protein levels and the suppression of downstream anabolic activity whether measured as a 24-hour average, or over the span of multiple days.

Previous, unpublished work from this laboratory has indicated that *under expression* of DEPTOR protein and concomitant mTOR hyperactivity in MCF7 epithelial cells appears to be a driving factor in their rapid proliferation. This effect is abrogated with the use of both rapamycin, and second generation mTOR inhibitors, with the latter leading to a more potent anti-anabolic effect, and greater rescue of DEPTOR. Treatments with each mTOR inhibitor, however, leads to a rescue of DEPTOR protein content during the associated reduction in overall anabolism. It has also been demonstrated that alterations in DEPTOR protein content can be achieved via manipulation of the $SCF^{\beta\text{-}TRCP}$ E3 ubiquitin ligase complex that is responsible for

DEPTOR degradation (106). However, both of these approaches suffer from off-target effects and eventual cytotoxicity (50, 97). Many mTOR kinase inhibitors have significant overlap with other serine-threonine kinases, particularly those that also belong to the PIKK family, and the $SCF^{\beta\text{-}TRCP}$ E3 ubiquitin ligase complex is also responsible for the degradation of a number of other extremely biologically relevant proteins, including IκB, β-Catenin, and PDCD4 (97). For these reasons, we have sought a more direct approach to mTOR-kinase inhibition through overexpression of an intrinsic inhibitor.

In the present study, initial investigations to characterize directed DEPTOR overexpression in the MCF7 cancer cells found that FSR was significantly diminished when compared to the RFP controls (Figure 5.6), while the RFP controls exhibited rates of protein synthesis consistent with previous measures of wild type MCF7 cells. This reduction in FSR was concomitant with a dramatic increase in the expression of DEPTOR protein content. This is consistent with the previously described double-negative feedback loop that exists between DEPTOR and mTOR. While direct inhibition of mTOR via pharmacological inhibitors such as rapamycin or Torin 1 are capable of rescuing DEPTOR content and reducing FSR, we have shown in this study that overexpression of DEPTOR is capable of producing a similar reduction in FSR, indicating that the complex relationship between DEPTOR and mTOR may be driven by the expression of DEPTOR protein, rather than post-translational modifications to DEPTOR relating to its degradation.

The most remarkable findings from this study are the marked reduction in measures of cellular anabolism with DEPTOR overexpression, coupled with what appears to be a total reversal with the NSC126405 treatment. Not only do these cancer cells overexpressing DEPTOR exhibit significant reductions in their anabolic and proliferative rates, but DEP cells treated with the NSC126405 drug appear to completely abrogate the effect of DEPTOR overexpression, making them virtually indistinguishable from the control RFP expressing cells. Interestingly, when the RFP cells were treated with the NSC126405 drug, they experienced a further increase in growth when compared to the DEP w/ NSC and RFP groups, suggesting a DEPTOR content-dependent response. This appears to indicate the possibility of manipulating long-term anabolic rates in a titratable fashion. In addition, this finding appears to be consistent with the notion that DEPTOR expression is likely a causative factor in determining the total inhibition levied against mTOR. However, the temporal nature of this relationship is currently unclear. It is entirely plausible that the net effect of DEPTOR inhibition on mTOR is determined by the rate of DEPTOR synthesis balanced against the rate of degradation by the $SCF^{\beta\text{-}TRCP}$ E3 ubiquitin ligase complex. It is also currently unclear what effect unbound DEPTOR has on the anabolic signaling environment independent of mTOR, or if a newly synthesized DEPTOR molecule is capable of suppressing the activity of an mTOR kinase that has been activated by upstream input and freed from DEPTOR. Based on our current investigation, it seems likely that a free DEPTOR molecule is capable of binding and inhibiting an active mTOR molecule, but more work is required to elucidate the dynamics of the DEPTOR-mTOR relationship which could

prove invaluable in the development of targeted therapies designed to increase, or decrease cellular anabolism in a variety of situations.

While reductions in the ratio of phosphorylated to total p70 S6 kinase were anticipated outcomes based on our previous work (60) and work by others (41), the increases in both phosphorylated and total 4E-BP1 were not. Not only was 4E-BP1 activation and total content not reduced in the presence of DEPTOR protein overexpression, it was actually increased. While it is entirely possible that altered activation and expression of 4E-BP1 is a result of chronic mTORC1 inhibition, it appears that these findings, coupled with the reductions of protein synthesis rates and cellular proliferation, indicate a need for a more thorough time course sampling of anabolic signal transduction, rather than the single 24-time point reported here. In addition, while the FSR measured on day 2 of the 8-day proliferation assay is in agreement with previous measures of FSR in the DEP and RFP groups, the changes observed at days 4 and 8 provide interesting insight into the relationship of cellular proliferation, confluency, and protein synthesis rates. As the measures of FSR only take into account the preceding 24 hour period prior to tissue harvest, these values do not necessarily align perfectly with the changes observed in the 48-hour period between days 2 and 4, or the 96 hour period between days 4 and 8. It is likely that the changes in FSR observed on days 4 and 8 are indicative of changes in cellular confluency on the relatively small 12-well culture dish. By day 8, the RFP, DEP w/ NSC, and RFP w/ NSC groups had achieved significant confluency, while the DEP group had not, allowing for higher rates of FSR directed toward cellular division.

In summary, we have shown that DEPTOR protein content has a causative effect on cellular anabolism through reductions in 24-hour protein synthesis rates, and in multi-day measures of cellular proliferation. Not only did DEPTOR overexpression decrease cellular anabolism in these human cancer cells, but these changes were effectively reversed following treatment with the NSC126405 pharmacological agent, strongly supporting the notion that the attenuated growth of the MCF7 cancer cell lines were a direct result of DEPTOR through its interaction with mTOR. Our study indicates that not only is DEPTOR protein a potential therapeutic target in the modulation of some types of cancer, but its inhibitory effect on mTOR may be titratable to produce varying levels of inhibition. This has profound implications for the treatment of cancer, but also indicates that manipulation of DEPTOR-mTOR may be utilized as a potent general regulator of cellular anabolism in a variety of experimental models, such as cancer cachexia and type 2 diabetes. While this study provides some exciting data related to a potential target to slow cancer, it must be noted that the present investigation has a number of limitations. For example, we were unable to utilize western blot analysis in either of the cellular proliferation assays due to limited amounts of protein content. Future investigations will require additional immunoblot time points, as well as an expanded list of immunoblotting targets, such as AKT, IRS-1, and various members of cellular translational machinery.

6. FINAL CONCLUSIONS

This dissertation was designed to ascertain if chronic and constitutively active expression of DEPTOR was possible, and if there is a causative role of DEPTOR expression on reduced activation of mTOR and downstream cellular metabolism. Our results indicate that not only is chronic overexpression of DEPTOR possible in the MCF7 human epithelial breast cancer cells (and very likely the C2C12 myotubes), but that its interaction with mTOR is directly responsible for alterations in downstream anabolic function. While the confirmation of DEPTOR overexpression in the C2C12 cells was complicated by a lack of effective primary antibodies against *Mus musculus* DEPTOR protein, the dual confirmation of transgene expression through puromycin selection and fluorescence microscopy lends credence to the validity of altered rates of protein synthesis. However, outcomes in the MCF7 epithelial cancer cells are particularly compelling and provide evidence for the direct and causative role of DEPTOR inhibiting mTOR, leading to changes in downstream cellular anabolic processes. The ~9.4 fold increase in DEPTOR protein expression and concomitant ~40% decrease in 24-hour rates of protein synthesis is compelling evidence of this relationship, but the observation that this decrease in cellular proliferation is eliminated with the addition of the NSC126405 DEPTOR-mTOR binding inhibitor, leaves little doubt that DEPTOR protein content plays an incredibly important role in the regulation of downstream metabolic functions.

This dissertation work has also provided evidence that directed increases in DEPTOR protein content through Cas9 mediated transgene integration at safe-harbor loci has the potential to be adapted for therapeutic use, given that certain hurdles can be overcome. Specifically, for this approach to be viable as a therapy, it will require a more precise tissue-specific delivery. Possibly through the use of Virus Like Particles to provide tissue specific gene delivery (48) of Cas9 protein pre-coupled to site specific sgRNA, and a linear dsDNA repair template (59). Given the prominence of anabolically aggressive, DEPTOR deficient diseases, these studies may represent a powerful new strategy for their management.

During the early phases of executing this dissertation project, it was discovered that of all of the commercially available primary antibodies against *Mus musculus* DEPTOR protein, none were particularly reliable for detection in C2C12 myoblasts or myotubes, with the most "effective" being polyclonal antibodies producing bands at multiple molecular weights, none of which could be confirmed to be of reasonably similar molecular weight to DEPTOR protein. Unfortunately, it appears that many of the publications that utilize immunoblotting for DEPTOR in mice or mouse tissue culture utilize mTOR immunoprecipitations as a purifying pulldown step before immunoblotting specifically for DEPTOR. In addition, many others do not provide molecular weight confirmation on their specific DEPTOR immunoblots without IP pulldown. This has made it particularly difficult to confirm DEPTOR protein overexpression in the C2C12s through immunoblotting.

In addition, as mentioned in Chapter 5, tissues collected for the 8-day proliferation assay in MCF7 cells were prioritized for analysis of rates of cellular proliferation and protein synthesis, and therefore were not analyzed for specific protein expression via immunoblot analysis. These measures will be of critical importance for the determination of DEPTOR overexpression on changes in the negative feedback of upstream signaling through IRS-1, AKT, and mTORC2, as well as changes to downstream protein translation with and without the NSC126405 inhibitor.

As a slightly anecdotal observation from having worked with these cells very closely over many months, both the DEPTOR overexpressing C2C12 and MCF7 cells are extremely slow growing cell lines. Figure 5.9 especially highlights this fact for the MCF7 cells. By day 8, the DEP group had not yet achieved half of the total protein content achieved by any other group by day 4. The slow growth exhibited by the DEPTOR overexpressing cell lines is, almost ironically, inconveniently slow. While this is a fantastic outcome for demonstrating the effect of DEPTOR overexpression on mTOR activity in a rapidly growing cancer, it has been a limitation for the execution of very short- and long-term experiments in these cell lines, as it is impossible to simultaneously control for the initial seeding density, growth duration, and cell confluency at harvest. As a result, the experiments in this dissertation were carried out by beginning with equal seeding densities.

In summary, these studies indicate that DEPTOR protein expression can be a potential therapeutic target in the modulation of MCF7 cancer and C2C12 myotube growth. This direct and causal relationship of DEPTOR and mTOR has profound

implications for the development of pharmacological and targeted gene therapies for the treatment of anabolically aggressive diseases such as cancer, type 2 diabetes, certain neurodegenerative diseases, and possibly aging (7, 50). Although further experimentation is required, substantial evidence exists that the stable and chronic manipulation of this same relationship in the opposite direction (i.e., directed DEPTOR knockdown) has the potential to be of therapeutic use in the fight against cancer cachexia, disuse atrophy, and even microgravity induced muscle loss (7, 41, 60). Future investigations utilizing this technique in animal models could set the stage for the development of inducible and titratable models of anabolic regulation to aid in the investigation of a variety of diseases with roots in metabolic dysregulation.

REFERENCES

1. **Adkins JN**, **Varnum SM**, **Auberry KJ**, **Moore RJ**, **Angell NH**, **Smith RD**, **Springer DL**, **Pounds JG**. Toward a human blood serum proteome: analysis by multidimensional separation coupled with mass spectrometry. *Mol Cell Proteomics MCP* 1: 947–955, 2002. doi: 10.1074/mcp.m200066-mcp200.

2. **Beretta L**, **Gingras AC**, **Svitkin YV**, **Hall MN**, **Sonenberg N**. Rapamycin blocks the phosphorylation of 4E-BP1 and inhibits cap-dependent initiation of translation. *EMBO J* 15: 658–664, 1996. doi: 10.1002/j.1460-2075.1996.tb00398.x.

3. **Bodine SC**, **Stitt TN**, **Gonzalez M**, **Kline WO**, **Stover GL**, **Bauerlein R**, **Zlotchenko E**, **Scrimgeour A**, **Lawrence JC**, **Glass DJ**, **Yancopoulos GD**. Akt/mTOR pathway is a crucial regulator of skeletal muscle hypertrophy and can prevent muscle atrophy in vivo. *Nat Cell Biol* 3: 1014–1019, 2001. doi: 10.1038/ncb1101-1014.

4. **Brown EJ**, **Albers MW**, **Bum Shin T**, **Ichikawa K**, **Keith CT**, **Lane WS**, **Schreiber SL**. A mammalian protein targeted by G1-arresting rapamycin–receptor complex. *Nature* 369: 756–758, 1994. doi: 10.1038/369756a0.

5. **Brunkard JO**. Exaptive Evolution of Target of Rapamycin Signaling in Multicellular Eukaryotes. *Dev Cell* 54: 142–155, 2020. doi: 10.1016/j.devcel.2020.06.022.

6. **Cai Z**, **Chen G**, **He W**, **Xiao M**, **Yan L-J**. Activation of mTOR: a culprit of Alzheimer's disease? *Neuropsychiatr Dis Treat* 11: 1015–1030, 2015. doi: 10.2147/NDT.S75717.

7. **Caron A**, **Briscoe DM**, **Richard D**, **Laplante M**. DEPTOR at the Nexus of Cancer, Metabolism, and Immunity. *Physiol Rev* 98: 1765–1803, 2018. doi: 10.1152/physrev.00064.2017.

8. **Caron A**, **Labbé SM**, **Lanfray D**, **Blanchard P-G**, **Villot R**, **Roy C**, **Sabatini DM**, **Richard D**, **Laplante M**. Mediobasal hypothalamic overexpression of DEPTOR protects against high-fat diet-induced obesity. *Mol Metab* 5: 102–112, 2016. doi: 10.1016/j.molmet.2015.11.005.

9. **Catena V**, **Fanciulli M**. Deptor: not only a mTOR inhibitor. *J Exp Clin Cancer Res CR* 36: 12, 2017. doi: 10.1186/s13046-016-0484-y.

10. **Chen X**, **Xiong X**, **Cui D**, **Yang F**, **Wei D**, **Li H**, **Shu J**, **Bi Y**, **Dai X**, **Gong L**, **Sun Y**, **Zhao Y**. DEPTOR is an in vivo tumor suppressor that inhibits prostate

tumorigenesis via the inactivation of mTORC1/2 signals. *Oncogene* 39: 1557–1571, 2020. doi: 10.1038/s41388-019-1085-y.

11. **Clausen JO**, **Hansen T**, **Bjørbaek C**, **Echwald SM**, **Urhammer SA**, **Rasmussen S**, **Andersen CB**, **Hansen L**, **Almind K**, **Pedersen O**, **Clausen JO**, **Borch-Johnsen K**, **Winther K**, **Haraldsdòttir J**. Insulin resistance: interactions between obesity and a common variant of insulin receptor substrate-1. *The Lancet* 346: 397–402, 1995. doi: 10.1016/S0140-6736(95)92779-4.

12. **Cong L**, **Ran FA**, **Cox D**, **Lin S**, **Barretto R**, **Habib N**, **Hsu PD**, **Wu X**, **Jiang W**, **Marraffini LA**, **Zhang F**. Multiplex Genome Engineering Using CRISPR/Cas Systems. *Science* 339: 819–823, 2013. doi: 10.1126/science.1231143.

13. **Davies J**, **Zachariades E**, **Rogers-Broadway K-R**, **Karteris E**. Elucidating the role of DEPTOR in Alzheimer's disease. *Int J Mol Med* 34: 1195–1200, 2014. doi: 10.3892/ijmm.2014.1895.

14. **de la Parra C**, **Ernlund A**, **Alard A**, **Ruggles K**, **Ueberheide B**, **Schneider RJ**. A widespread alternate form of cap-dependent mRNA translation initiation. *Nat Commun* 9, 2018. doi: 10.1038/s41467-018-05539-0.

15. **DeFronzo RA**, **Tripathy D**. Skeletal Muscle Insulin Resistance Is the Primary Defect in Type 2 Diabetes. *Diabetes Care* 32: S157–S163, 2009. doi: 10.2337/dc09-S302.

16. **Ding Y**, **Shan L**, **Nai W**, **Lin X**, **Zhou L**, **Dong X**, **Wu H**, **Xiao M**, **Zhou X**, **Wang L**, **Li T**, **Fu Y**, **Lin Y**, **Jia C**, **Dai M**, **Bai X**. DEPTOR Deficiency-Mediated mTORc1 Hyperactivation in Vascular Endothelial Cells Promotes Angiogenesis. *Cell Physiol Biochem* 46: 520–531, 2018. doi: 10.1159/000488619.

17. **Dong X**, **Wang L**, **Han Z**, **Zhou L**, **Shan L**, **Ding Y**, **Xu W**, **Li J**, **Su Y**, **Cai R**, **Xiong G**, **Diao D**, **Dai M**, **Jia C**, **Zheng H**. Different functions of DEPTOR in modulating sensitivity to chemotherapy for esophageal squamous cell carcinoma. *Exp Cell Res* 353: 35–45, 2017. doi: 10.1016/j.yexcr.2017.03.003.

18. **Duan S**, **Skaar JR**, **Kuchay S**, **Toschi A**, **Kanarek N**, **Ben-Neriah Y**, **Pagano M**. mTOR Generates an Auto-Amplification Loop by Triggering the βTrCP- and CK1α-Dependent Degradation of DEPTOR. *Mol Cell* 44: 317–324, 2011. doi: 10.1016/j.molcel.2011.09.005.

19. **Ebner M**, **Sinkovics B**, **Szczygieł M**, **Ribeiro DW**, **Yudushkin I**. Localization of mTORC2 activity inside cells. *J Cell Biol* 216: 343–353, 2017. doi: 10.1083/jcb.201610060.

20. **Fluckey JD**, **Pohnert SC**, **Boyd SG**, **Cortright RN**, **Trappe TA**, **Dohm GL**. Insulin stimulation of muscle protein synthesis in obese Zucker rats is not via a rapamycin-sensitive pathway. *Am J Physiol-Endocrinol Metab* 279: E182–E187, 2000.

21. **Fonseca BD**, **Zakaria C**, **Jia J-J**, **Graber TE**, **Svitkin Y**, **Tahmasebi S**, **Healy D**, **Hoang H-D**, **Jensen JM**, **Diao IT**, **Lussier A**, **Dajadian C**, **Padmanabhan N**, **Wang W**, **Matta-Camacho E**, **Hearnden J**, **Smith EM**, **Tsukumo Y**, **Yanagiya A**, **Morita M**, **Petroulakis E**, **González JL**, **Hernández G**, **Alain T**, **Damgaard CK**. La-related Protein 1 (LARP1) Represses Terminal Oligopyrimidine (TOP) mRNA Translation Downstream of mTOR Complex 1 (mTORC1). *J Biol Chem* 290: 15996–16020, 2015. doi: 10.1074/jbc.M114.621730.

22. **Gao D**, **Inuzuka H**, **Tan M-KM**, **Fukushima H**, **Locasale JW**, **Liu P**, **Wan L**, **Zhai B**, **Chin YR**, **Shaik S**, **Lyssiotis CA**, **Gygi SP**, **Toker A**, **Cantley LC**, **Asara JM**, **Harper JW**, **Wei W**. mTOR Drives Its Own Activation via SCFβTrCP-Dependent Degradation of the mTOR Inhibitor DEPTOR. *Mol Cell* 44: 290–303, 2011. doi: http://dx.doi.org/10.1016/j.molcel.2011.08.030.

23. **Gasier HG**, **Fluckey JD**, **Previs SF**. The application of 2H2O to measure skeletal muscle protein synthesis. *Nutr Metab* 7: 31, 2010. doi: 10.1186/1743-7075-7-31.

24. **Gasier HG**, **Riechman SE**, **Wiggs MP**, **Previs SF**, **Fluckey JD**. A comparison of 2H2O and phenylalanine flooding dose to investigate muscle protein synthesis with acute exercise in rats. *Am J Physiol - Endocrinol Metab* 297: E252–E259, 2009. doi: 10.1152/ajpendo.90872.2008.

25. **Gentilella A**, **Morón-Duran FD**, **Fuentes P**, **Zweig-Rocha G**, **Riaño-Canalias F**, **Pelletier J**, **Ruiz M**, **Turón G**, **Castaño J**, **Tauler A**, **Bueno C**, **Menéndez P**, **Kozma SC**, **Thomas G**. Autogenous Control of 5′TOP mRNA Stability by 40S Ribosomes. *Mol Cell* 67: 55-70.e4, 2017. doi: 10.1016/j.molcel.2017.06.005.

26. **Gest H**. Evolutionary roots of the citric acid cycle in prokaryotes. *Biochem Soc Symp* 54: 3–16, 1987.

27. **Gingras A-C**, **Gygi SP**, **Raught B**, **Polakiewicz RD**, **Abraham RT**, **Hoekstra MF**, **Aebersold R**, **Sonenberg N**. Regulation of 4E-BP1 phosphorylation: a novel two-step mechanism. *Genes Dev* 13: 1422–1437, 1999.

28. **Gingras A-C**, **Raught B**, **Gygi SP**, **Niedzwiecka A**, **Miron M**, **Burley SK**, **Polakiewicz RD**, **Wyslouch-Cieszynska A**, **Aebersold R**, **Sonenberg N**. Hierarchical phosphorylation of the translation inhibitor 4E-BP1. *Genes Dev* 15: 2852–2864, 2001. doi: 10.1101/gad.912401.

29. **Goodenough C**, **Therrien D**, **Nguyen B**, **Cardin J**, **Riechman S**, **Kochan K**, **Riggs P**, **Fluckey J**. Muscular Contractions Facilitate Systemic Circulation of MicroRNA that Impact Cancer [Online]. *Int J Exerc Sci Conf Proc* 2, 2019. https://digitalcommons.wku.edu/ijesab/vol2/iss11/70.

30. **Greber BJ**, **Bieri P**, **Leibundgut M**, **Leitner A**, **Aebersold R**, **Boehringer D**, **Ban N**. The complete structure of the 55S mammalian mitochondrial ribosome. *Science* 348: 303–308, 2015. doi: 10.1126/science.aaa3872.

31. **Haar EV**, **Lee S**, **Bandhakavi S**, **Griffin TJ**, **Kim D-H**. Insulin signalling to mTOR mediated by the Akt/PKB substrate PRAS40. *Nat Cell Biol* 9: 316–323, 2007. doi: 10.1038/ncb1547.

32. **Hall MN**. mTOR-What does it do? *Transplant Proc* 40: S5-8, 2008. doi: 10.1016/j.transproceed.2008.10.009.

33. **Hara K**, **Maruki Y**, **Long X**, **Yoshino K**, **Oshiro N**, **Hidayat S**, **Tokunaga C**, **Avruch J**, **Yonezawa K**. Raptor, a Binding Partner of Target of Rapamycin (TOR), Mediates TOR Action. *Cell* 110: 177–189, 2002. doi: 10.1016/S0092-8674(02)00833-4.

34. **Harwood FC**, **Geltink RIK**, **O'Hara BP**, **Cardone M**, **Janke L**, **Finkelstein D**, **Entin I**, **Paul L**, **Houghton PJ**, **Grosveld GC**. ETV7 is an essential component of a rapamycin-insensitive mTOR complex in cancer. *Sci Adv* 4: eaar3938, 2018. doi: 10.1126/sciadv.aar3938.

35. **Hay N**, **Sonenberg N**. Upstream and downstream of mTOR. *Genes Dev* 18: 1926–1945, 2004. doi: 10.1101/gad.1212704.

36. **Hers I**, **Vincent EE**, **Tavaré JM**. Akt signalling in health and disease. *Cell Signal* 23: 1515–1527, 2011. doi: 10.1016/j.cellsig.2011.05.004.

37. **Hsing M**, **Wang Y**, **Rennie PS**, **Cox ME**, **Cherkasov A**. ETS transcription factors as emerging drug targets in cancer. *Med Res Rev* 40: 413–430, 2020. doi: 10.1002/med.21575.

38. **Jackson RJ**, **Hunt SL**, **Reynolds JE**, **Kaminski A**. Cap-Dependent and Cap-Independent Translation: Operational Distinctions and Mechanistic Interpretations. In: *Cap-Independent Translation*, edited by Sarnow P. Springer Berlin Heidelberg, p. 1–29.

39. **Ji Y-M**, **Zhou X-F**, **Zhang J**, **Zheng X**, **Li S-B**, **Wei Z-Q**, **Liu T**, **Cheng D-L**, **Liu P**, **Song K**, **Tan T**, **Zhu H**, **Guo J-L**. DEPTOR suppresses the progression of esophageal squamous cell carcinoma and predicts poor prognosis. *Oncotarget* 7: 14188–14198, 2016. doi: 10.18632/oncotarget.7420.

40. **Katanik J**, **McCabe BJ**, **Brunengraber DZ**, **Chandramouli V**, **Nishiyama FJ**, **Anderson VE**, **Previs SF**. Measuring gluconeogenesis using a low dose of2H2O: advantage of isotope fractionation during gas chromatography. *Am J Physiol-Endocrinol Metab* 284: E1043–E1048, 2003. doi: 10.1152/ajpendo.00485.2002.

41. **Kazi AA**, **Hong-Brown L**, **Lang SM**, **Lang CH**. Deptor Knockdown Enhances mTOR Activity and Protein Synthesis in Myocytes and Ameliorates Disuse Muscle Atrophy. *Mol Med* 17: 925–936, 2011. doi: 10.2119/molmed.2011.00070.

42. **Keiper BD**. Cap-Independent mRNA Translation in Germ Cells. *Int J Mol Sci* 20, 2019. doi: 10.3390/ijms20010173.

43. **Keith CT**, **Schreiber SL**. PIK-Related Kinases: DNA Repair, Recombination, and Cell Cycle Checkpoints. *Science* 270: 50–50, 1995. doi: 10.1126/science.270.5233.50.

44. **Kozak M**. The scanning model for translation: an update. *J Cell Biol* 108: 229–241, 1989. doi: 10.1083/jcb.108.2.229.

45. **Laplante M**, **Horvat S**, **Festuccia WT**, **Birsoy K**, **Prevorsek Z**, **Efeyan A**, **Sabatini DM**. DEPTOR Cell-Autonomously Promotes Adipogenesis, and Its Expression Is Associated with Obesity. *Cell Metab* 16: 202–212, 2012. doi: 10.1016/j.cmet.2012.07.008.

46. **Laplante M**, **Sabatini DM**. mTOR Signaling in Growth Control and Disease. *Cell* 149: 274–293, 2012. doi: 10.1016/j.cell.2012.03.017.

47. **Lee DE**, **Brown JL**, **Rosa ME**, **Brown LA**, **Perry RA**, **Wiggs MP**, **Nilsson MI**, **Crouse SF**, **Fluckey JD**, **Washington TA**, **Greene NP**. microRNA-16 Is Downregulated During Insulin Resistance and Controls Skeletal Muscle Protein Accretion. *J Cell Biochem* 117: 1775–1787, 2016. doi: 10.1002/jcb.25476.

48. **Lee EB**, **Kim J-H**, **Hur W**, **Choi JE**, **Kim SM**, **Park DJ**, **Kang B-Y**, **Lee GW**, **Yoon SK**. Liver-specific Gene Delivery Using Engineered Virus-Like Particles of Hepatitis E Virus. *Sci Rep* 9: 1616, 2019. doi: 10.1038/s41598-019-38533-7.

49. **Li L**, **Zhao G-D**, **Shi Z**, **Qi L-L**, **Zhou L-Y**, **Fu Z-X**. The Ras/Raf/MEK/ERK signaling pathway and its role in the occurrence and development of HCC. *Oncol Lett* 12: 3045–3050, 2016. doi: 10.3892/ol.2016.5110.

50. **Liu GY**, **Sabatini DM**. mTOR at the nexus of nutrition, growth, ageing and disease. *Nat Rev Mol Cell Biol* 21: 183–203, 2020. doi: 10.1038/s41580-019-0199-y.

51. **Livingstone M**, **Bidinosti M**. Rapamycin-insensitive mTORC1 activity controls eIF4E:4E-BP1 binding. *F1000Research* 1, 2012. doi: 10.12688/f1000research.1-4.v1.

52. **López-Lastra M**, **Rivas A**, **Barría MI**. Protein synthesis in eukaryotes: The growing biological relevance of cap-independent translation initiation. *Biol Res* 38, 2005. doi: 10.4067/S0716-97602005000200003.

53. **Marques-Ramos A**, **Candeias MM**, **Menezes J**, **Lacerda R**, **Willcocks M**, **Teixeira A**, **Locker N**, **Romão L**. Cap-independent translation ensures mTOR expression and function upon protein synthesis inhibition. *RNA* 23: 1712–1728, 2017. doi: 10.1261/rna.063040.117.

54. **Marraffini LA**, **Sontheimer EJ**. CRISPR Interference Limits Horizontal Gene Transfer in Staphylococci by Targeting DNA. *Science* 322: 1843–1845, 2008. doi: 10.1126/science.1165771.

55. **Meléndez-Hevia E**, **Waddell TG**, **Cascante M**. The puzzle of the Krebs citric acid cycle: Assembling the pieces of chemically feasible reactions, and opportunism in the design of metabolic pathways during evolution. *J Mol Evol* 43: 293–303, 1996. doi: 10.1007/BF02338838.

56. **Meng ZX**, **Wang L**, **Xiao Y**, **Lin JD**. The Baf60c/Deptor pathway links skeletal muscle inflammation to glucose homeostasis in obesity. *Diabetes* 63: 1533–45, 2014. doi: 10.2337/db13-1061.

57. **Menon S**, **Manning BD**. Common corruption of the mTOR signaling network in human tumors. *Oncogene* 27: S43–S51, 2008. doi: 10.1038/onc.2009.352.

58. **Miao L**, **Yao H**, **Li C**, **Pu M**, **Yao X**, **Yang H**, **Qi X**, **Ren J**, **Wang Y**. A dual inhibition: microRNA-552 suppresses both transcription and translation of cytochrome P450 2E1. *Biochim Biophys Acta BBA - Gene Regul Mech* 1859: 650–662, 2016. doi: 10.1016/j.bbagrm.2016.02.016.

59. **Nguyen DN**, **Roth TL**, **Li PJ**, **Chen PA**, **Apathy R**, **Mamedov MR**, **Vo LT**, **Tobin VR**, **Goodman D**, **Shifrut E**, **Bluestone JA**, **Puck JM**, **Szoka FC**, **Marson A**. Polymer-stabilized Cas9 nanoparticles and modified repair templates increase genome editing efficiency. *Nat Biotechnol* 38: 44–49, 2020. doi: 10.1038/s41587-019-0325-6.

60. **Nilsson MI**, **Dobson JP**, **Greene NP**, **Wiggs MP**, **Shimkus KL**, **Wudeck EV**, **Davis AR**, **Laureano ML**, **Fluckey JD**. Abnormal protein turnover and anabolic resistance to exercise in sarcopenic obesity. *FASEB J* 27: 3905–3916, 2013. doi: 10.1096/fj.12-224006.

61. **Nilsson MI**, **Greene NP**, **Dobson JP**, **Wiggs MP**, **Gasier HG**, **Macias BR**, **Shimkus KL**, **Fluckey JD**. Insulin resistance syndrome blunts the mitochondrial anabolic response following resistance exercise. *Am J Physiol-Endocrinol Metab* 299: E466–E474, 2010. doi: 10.1152/ajpendo.00118.2010.

62. **O'Brien J**, **Hayder H**, **Zayed Y**, **Peng C**. Overview of MicroRNA Biogenesis, Mechanisms of Actions, and Circulation. *Front Endocrinol* 9, 2018. doi: 10.3389/fendo.2018.00402.

63. **Papapetrou EP**, **Lee G**, **Malani N**, **Setty M**, **Riviere I**, **Tirunagari LMS**, **Kadota K**, **Roth SL**, **Giardina P**, **Viale A**, **Leslie C**, **Bushman FD**, **Studer L**, **Sadelain M**. Genomic safe harbors permit high β-globin transgene expression in thalassemia induced pluripotent stem cells. *Nat Biotechnol* 29: 73–78, 2011. doi: 10.1038/nbt.1717.

64. **Papapetrou EP**, **Schambach A**. Gene Insertion Into Genomic Safe Harbors for Human Gene Therapy. *Mol Ther* 24: 678–684, 2016. doi: 10.1038/mt.2016.38.

65. **Patterson BW**, **Zhao G**, **Klein S**. Improved accuracy and precision of gas chromatography/mass spectrometry measurements for metabolic tracers. *Metabolism* 47: 706–712, 1998. doi: 10.1016/S0026-0495(98)90035-X.

66. **Perticone JI**. Protein Degradative Processes Associated with Anabolic Dysregulation in Diabetic Skeletal Muscle [Online]. 2014. https://oaktrust.library.tamu.edu/handle/1969.1/153245 [10 Sep. 2020].

67. **Peterson TR**, **Laplante M**, **Thoreen CC**, **Sancak Y**, **Kang SA**, **Kuehl WM**, **Gray NS**, **Sabatini DM**. DEPTOR Is an mTOR Inhibitor Frequently Overexpressed in Multiple Myeloma Cells and Required for Their Survival. *Cell* 137: 873–886, 2009. doi: 10.1016/j.cell.2009.03.046.

68. **Ramanathan A**, **Robb GB**, **Chan S-H**. mRNA capping: biological functions and applications. *Nucleic Acids Res* 44: 7511–7526, 2016. doi: 10.1093/nar/gkw551.

69. **Ran FA**, **Hsu PD**, **Wright J**, **Agarwala V**, **Scott DA**, **Zhang F**. Genome engineering using the CRISPR-Cas9 system. *Nat Protoc* 8: 2281–2308, 2013. doi: 10.1038/nprot.2013.143.

70. **Richter JD**, **Sonenberg N**. Regulation of cap-dependent translation by eIF4E inhibitory proteins. *Nature* 433: 477–480, 2005. doi: 10.1038/nature03205.

71. **Romero-Calvo I**, **Ocón B**, **Martínez-Moya P**, **Suárez MD**, **Zarzuelo A**, **Martínez-Augustin O**, **de Medina FS**. Reversible Ponceau staining as a loading control alternative to actin in Western blots. *Anal Biochem* 401: 318–320, 2010. doi: 10.1016/j.ab.2010.02.036.

72. **Roux PP**, **Shahbazian D**, **Vu H**, **Holz MK**, **Cohen MS**, **Taunton J**, **Sonenberg N**, **Blenis J**. RAS/ERK Signaling Promotes Site-specific Ribosomal Protein S6 Phosphorylation via RSK and Stimulates Cap-dependent Translation. *J Biol Chem* 282: 14056–14064, 2007. doi: 10.1074/jbc.M700906200.

73. **Sabatini DM**. mTOR and cancer: insights into a complex relationship. *Nat Rev Cancer* 6: 729–734, 2006. doi: 10.1038/nrc1974.

74. **Sabatini DM**, **Erdjument-Bromage H**, **Lui M**, **Tempst P**, **Snyder SH**. RAFT1: A mammalian protein that binds to FKBP12 in a rapamycin-dependent fashion and is homologous to yeast TORs. *Cell* 78: 35–43, 1994. doi: 10.1016/0092-8674(94)90570-3.

75. **Sabers CJ**, **Martin MM**, **Brunn GJ**, **Williams JM**, **Dumont FJ**, **Wiederrecht G**, **Abraham RT**. Isolation of a Protein Target of the FKBP12-Rapamycin Complex in Mammalian Cells. *J Biol Chem* 270: 815–822, 1995. doi: 10.1074/jbc.270.2.815.

76. **Sarbassov DD**, **Ali SM**, **Sengupta S**, **Sheen J-H**, **Hsu PP**, **Bagley AF**, **Markhard AL**, **Sabatini DM**. Prolonged Rapamycin Treatment Inhibits mTORC2 Assembly and Akt/PKB. *Mol Cell* 22: 159–168, 2006. doi: 10.1016/j.molcel.2006.03.029.

77. **Sarbassov DD**, **Guertin DA**, **Ali SM**, **Sabatini DM**. Phosphorylation and Regulation of Akt/PKB by the Rictor-mTOR Complex. *Science* 307: 1098–1101, 2005. doi: 10.1126/science.1106148.

78. **Scholl FA**, **Dumesic PA**, **Barragan DI**, **Harada K**, **Bissonauth V**, **Charron J**, **Khavari PA**. Mek1/2 MAPK Kinases Are Essential for Mammalian Development, Homeostasis, and Raf-Induced Hyperplasia. *Dev Cell* 12: 615–629, 2007. doi: 10.1016/j.devcel.2007.03.009.

79. **Schult P**, **Roth H**, **Adams RL**, **Mas C**, **Imbert L**, **Orlik C**, **Ruggieri A**, **Pyle AM**, **Lohmann V**. microRNA-122 amplifies hepatitis C virus translation by shaping the structure of the internal ribosomal entry site. *Nat Commun* 9: 2613, 2018. doi: 10.1038/s41467-018-05053-3.

80. **Segalés J**, **Perdiguero E**, **Serrano AL**, **Sousa-Victor P**, **Ortet L**, **Jardí M**, **Budanov AV**, **Garcia-Prat L**, **Sandri M**, **Thomson DM**, **Karin M**, **Hee Lee J**, **Muñoz-Cánoves P**. Sestrin prevents atrophy of disused and aging muscles by integrating anabolic and catabolic signals. *Nat Commun* 11: 189, 2020. doi: 10.1038/s41467-019-13832-9.

81. **Sehgal SN**, **Baker H**, **Vézina C**. Rapamycin (AY-22,989), a new antifungal antibiotic. II. Fermentation, isolation and characterization. *J Antibiot (Tokyo)* 28: 727–732, 1975. doi: 10.7164/antibiotics.28.727.

82. **Sen ND**, **Zhou F**, **Harris MS**, **Ingolia NT**, **Hinnebusch AG**. eIF4B stimulates translation of long mRNAs with structured 5′ UTRs and low closed-loop potential but weak dependence on eIF4G. *Proc Natl Acad Sci* 113: 10464, 2016. doi: 10.1073/pnas.1612398113.

83. **Shatsky IN**, **Terenin IM**, **Smirnova VV**, **Andreev DE**. Cap-Independent Translation: What's in a Name? *Trends Biochem Sci* 43: 882–895, 2018. doi: 10.1016/j.tibs.2018.04.011.

84. **Shi Y**, **Daniels-Wells TR**, **Frost P**, **Lee J**, **Finn RS**, **Bardeleben C**, **Penichet ML**, **Jung ME**, **Gera J**, **Lichtenstein A**. Cytotoxic Properties of a DEPTOR-mTOR Inhibitor in Multiple Myeloma Cells. *Cancer Res* 76: 5822–5831, 2016. doi: 10.1158/0008-5472.CAN-16-1019.

85. **Shimkus KL**, **Shirazi-Fard Y**, **Wiggs MP**, **Ullah ST**, **Pohlenz C**, **Gatlin DM**, **Carroll CC**, **Hogan HA**, **Fluckey JD**. Responses of skeletal muscle size and anabolism are reproducible with multiple periods of unloading/reloading. *J Appl Physiol* 125: 1456–1467, 2018. doi: 10.1152/japplphysiol.00736.2017.

86. **Smith LM**, **Kelleher NL**, **Consortium for Top Down Proteomics**. Proteoform: a single term describing protein complexity. *Nat Methods* 10: 186–187, 2013. doi: 10.1038/nmeth.2369.

87. **Sonenberg N**, **Hinnebusch AG**. Regulation of Translation Initiation in Eukaryotes: Mechanisms and Biological Targets. *Cell* 136: 731–745, 2009. doi: 10.1016/j.cell.2009.01.042.

88. **Soo RM**, **Hemp J**, **Parks DH**, **Fischer WW**, **Hugenholtz P**. On the origins of oxygenic photosynthesis and aerobic respiration in Cyanobacteria. *Science* 355: 1436–1440, 2017. doi: 10.1126/science.aal3794.

89. **Tcherkezian J**, **Cargnello M**, **Romeo Y**, **Huttlin EL**, **Lavoie G**, **Gygi SP**, **Roux PP**. Proteomic analysis of cap-dependent translation identifies LARP1 as a key regulator of 5′TOP mRNA translation. *Genes Dev* 28: 357–371, 2014. doi: 10.1101/gad.231407.113.

90. **Tremblay F**, **Brûlé S**, **Um SH**, **Li Y**, **Masuda K**, **Roden M**, **Sun XJ**, **Krebs M**, **Polakiewicz RD**, **Thomas G**, **Marette A**. Identification of IRS-1 Ser-1101 as a target of S6K1 in nutrient- and obesity-induced insulin resistance. *Proc Natl Acad Sci* 104: 14056–14061, 2007. doi: 10.1073/pnas.0706517104.

91. **Tremblay F**, **Marette A**. Amino Acid and Insulin Signaling via the mTOR/p70 S6 Kinase Pathway A NEGATIVE FEEDBACK MECHANISM LEADING TO INSULIN RESISTANCE IN SKELETAL MUSCLE CELLS. *J Biol Chem* 276: 38052–38060, 2001.

92. **Ueda Y**, **Hirai S**, **Osada S**, **Suzuki A**, **Mizuno K**, **Ohno S**. Protein Kinase C δ Activates the MEK-ERK Pathway in a Manner Independent of Ras and Dependent on Raf. *J Biol Chem* 271: 23512–23519, 1996. doi: 10.1074/jbc.271.38.23512.

93. **Ueno M**, **Carvalheira JBC**, **Tambascia RC**, **Bezerra RMN**, **Amaral ME**, **Carneiro EM**, **Folli F**, **Franchini KG**, **Saad MJA**. Regulation of insulin signalling by hyperinsulinaemia: role of IRS-1/2 serine phosphorylation and the mTOR/p70 S6K pathway. *Diabetologia* 48: 506–518, 2005. doi: 10.1007/s00125-004-1662-6.

94. **User:Mariuswalter**. English: Colour-friendly reupload of User:Mariuswalter's image showing DNA Repair after CRISPR-Cas9 double strand break, adapted to be accessible to those with red-green colourblindness [Online]. https://commons.wikimedia.org/wiki/File:DNA_Repair-colourfriendly.png [14 Jul. 2020].

95. **van Dam TJP**, **Zwartkruis FJT**, **Bos JL**, **Snel B**. Evolution of the TOR Pathway. *J Mol Evol* 73: 209–220, 2011. doi: 10.1007/s00239-011-9469-9.

96. **Varusai TM**, **Nguyen LK**. Dynamic modelling of the mTOR signalling network reveals complex emergent behaviours conferred by DEPTOR. *Sci Rep* 8: 1–14, 2018. doi: 10.1038/s41598-017-18400-z.

97. **Wang Z**, **Zhong J**, **Gao D**, **Inuzuka H**, **Liu P**, **Wei W**. DEPTOR ubiquitination and destruction by SCFβ-TrCP. *Am J Physiol-Endocrinol Metab* 303: E163–E169, 2012. doi: 10.1152/ajpendo.00105.2012.

98. **Wang Z**, **Zhong J**, **Inuzuka H**, **Gao D**, **Shaik S**, **Sarkar FH**, **Wei W**. An Evolving Role for DEPTOR in Tumor Development and Progression. *Neoplasia N Y N* 14: 368–375, 2012.

99. **Xie Q**, **Liang Y**, **Yang M**, **Yang Y**, **Cen X**, **Yin G**. DEPTOR-mTOR Signaling Is Critical for Lipid Metabolism and Inflammation Homeostasis of Lymphocytes in Human PBMC Culture. *J. Immunol. Res.* 2017 Hindawi: e5252840, 2017.

100. **Yang H**, **Jiang X**, **Li B**, **Yang HJ**, **Miller M**, **Yang A**, **Dhar A**, **Pavletich NP**. Mechanisms of mTORC1 activation by RHEB and inhibition by PRAS40. *Nature* 552: 368–373, 2017. doi: 10.1038/nature25023.

101. **Yang Y**, **Wang Z**. IRES-mediated cap-independent translation, a path leading to hidden proteome. *J Mol Cell Biol* 11: 911–919, 2019. doi: 10.1093/jmcb/mjz091.

102. **Yang Z-Z**, **Tschopp O**, **Hemmings-Mieszczak M**, **Feng J**, **Brodbeck D**, **Perentes E**, **Hemmings BA**. Protein Kinase Bα/Akt1 Regulates Placental Development and Fetal Growth. *J Biol Chem* 278: 32124–32131, 2003. doi: 10.1074/jbc.M302847200.

103. **Yen C-H**, **Lu Y-C**, **Li C-H**, **Lee C-M**, **Chen C-Y**, **Cheng M-Y**, **Huang S-F**, **Chen K-F**, **Cheng A-L**, **Liao L-Y**, **Lee Y-HW**, **Chen Y-MA**. Functional Characterization of Glycine N-Methyltransferase and Its Interactive Protein DEPDC6/DEPTOR in Hepatocellular Carcinoma. *Mol Med* 18: 286–296, 2012. doi: 10.2119/molmed.2011.00331.

104. **Yuan H-X**, **Guan K-L**. The SIN1-PH Domain Connects mTORC2 to PI3K. *Cancer Discov* 5: 1127–1129, 2015. doi: 10.1158/2159-8290.CD-15-1125.

105. **Zhang C**, **Cortez N g.**, **Berns K i.** Characterization of a Bipartite Recombinant Adeno-Associated Viral Vector for Site-Specific Integration. *Hum Gene Ther* 18: 787–797, 2007. doi: 10.1089/hum.2007.056.

106. **Zhao Y**, **Sun Y**. Targeting the mTOR-DEPTOR Pathway by CRL E3 Ubiquitin Ligases: Therapeutic Application. *Neoplasia* 14: 360–367, 2012. doi: https://doi.org/10.1593/neo.12532.

107. **Zhu Z**, **Yang C**, **Iyaswamy A**, **Krishnamoorthi S**, **Sreenivasmurthy SG**, **Liu J**, **Wang Z**, **Tong BC-K**, **Song J**, **Lu J**, **Cheung K-H**, **Li M**. Balancing mTOR Signaling and Autophagy in the Treatment of Parkinson's Disease. *Int J Mol Sci* 20: 728, 2019. doi: 10.3390/ijms20030728.

APPENDIX A

PLASMID DATASHEETS

SH150 Datasheet

Clone Information

Catalog No.: SH150
Description: Custom clone
Whole Plasmid Size: 10442 bp
Vector: MCP-ROSA26-CG01

Vector Information for SH150

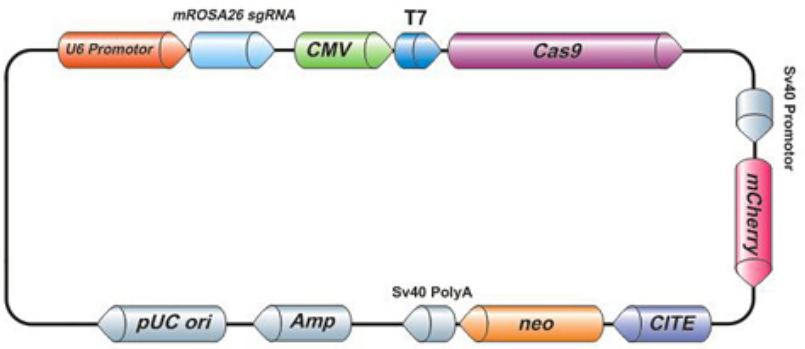

Figure A.1 MCP-ROSA26-CG01 (Rosa26/Cas9)

OmicsLink™ Expression Clone Datasheet of DC-Mm25645-SH02

Clone Information

Catalog No.: DC-Mm25645-SH02
Accession No.: NM_145470 **ORF Length:** 1230 bp
Whole Plasmid Size: 9970 bp
Description: Mus musculus DEP domain containing MTOR-interacting protein (Deptor), transcript variant 1, mRNA.
Vector: pDonor-SH02 **Antibiotic:** Ampicillin
Stable Selection Marker: Puromycin

Suggested Sequencing Primers:
Forward: 5'-CGGTGGGAGGTCTATATAAGCAG-3'
Reverse: 5'-GACAGTGGGAGTGGCACCTTC-3'

Vector Information for DC-Mm25645-SH02

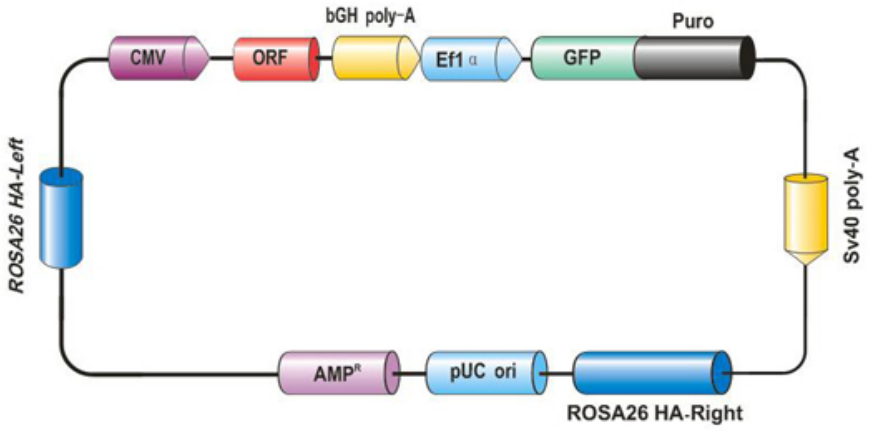

Figure A.2 DC-Mm25645-SH02 (Rosa26 *Mus musculus* DEPTOR donor)

SH358 Datasheet

Clone Information

Catalog No.: SH358
Description: ROSA26 RFP control
Whole Plasmid Size: 9354 bp

Vector Information for SH358

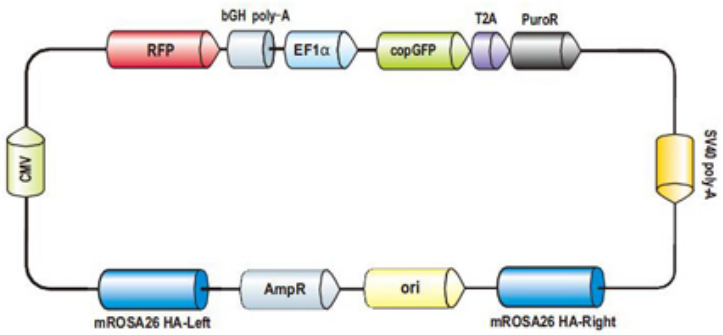

Figure A.3 DC-SH358-SH02 (Rosa26 RFP donor positive control)

SH100 Datasheet

Clone Information

Catalog No.: SH100
Description: All-in-one sgRNA/Cas9 expression clone for human AAVS1 safe harbor site
Target site: GGGGCCACTAGGGACAGGAT
Whole Plasmid Size: 8508 bp
Resistance: Ampicillin

Vector Information

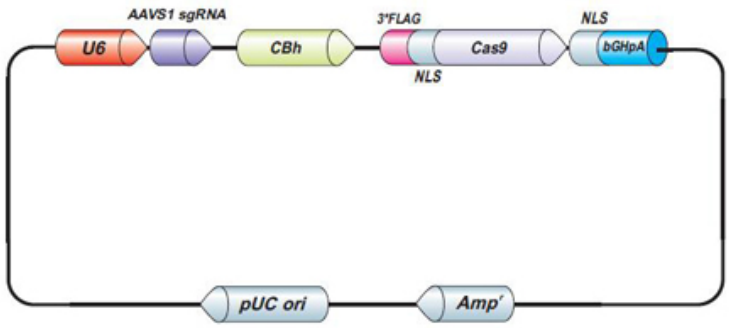

Figure A.4 HCP-AAVS1-CG02 (AAVS1/Cas9)

OmicsLink™ Expression Clone Datasheet of DC-A4329-SH01

Clone Information

Catalog No.: DC-A4329-SH01
Accession No.: NM_022783 **ORF Length:** 1230 bp
Whole Plasmid Size: 10050 bp
Description: Homo sapiens DEP domain containing MTOR interacting protein (DEPTOR), transcript variant 1, mRNA.
Vector: pDonor-SH01 **Antibiotic:** Ampicillin
Stable Selection Marker: Puromycin

Suggested Sequencing Primers:
Forward: 5'-CGGTGGGAGGTCTATATAAGCAG-3'
Reverse: 5'-GACAGTGGGAGTGGCACCTTC-3'

Vector Information for DC-A4329-SH01

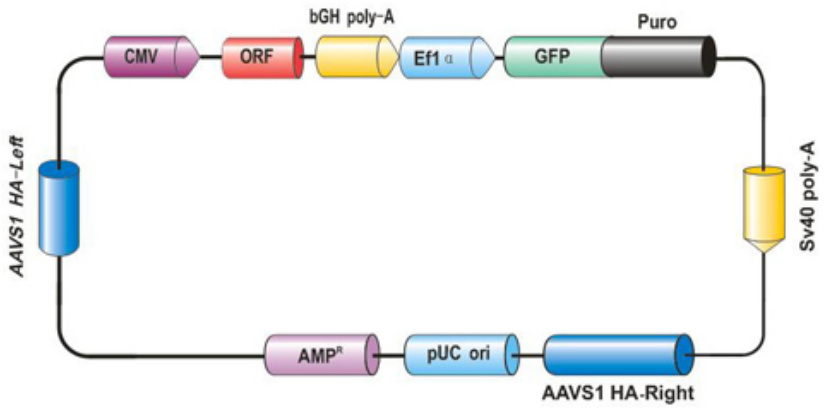

Figure A.5 DC-A4329-SH01 (AAVS1 *Homo sapiens* DEPTOR donor)

SH308 Datasheet

Clone Information

Catalog No.: SH308
Description: AAVS1 RFP control
Whole Plasmid Size: 9431 bp
Resistance: Ampicillin

Vector Information for SH308

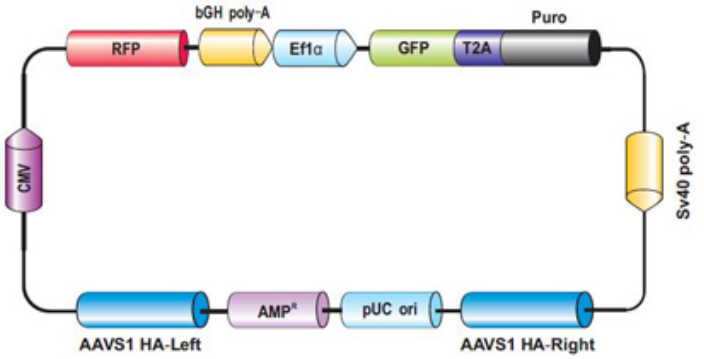

Figure A.6 DC-RFP-SH01 (AAVS1 RFP donor positive control)

APPENDIX B

GCMS METHODS PARAMETERS

^{2}H-Alanine Pulsed Splitless Scan Mode Analysis Method

INSTRUMENT CONTROL PARAMETERS: GCMS

C:\MSDCHEM\1\METHODS\WILL'S METHODS\2H-ALANINE_2UL_PULSEDSPLITLESS_SCANMODE.M
Sat Jun 20 12:56:16 2020

Control Information
------- -----------

Sample Inlet : GC
Injection Source : GC ALS
Mass Spectrometer : Enabled

Oven
Equilibration Time 0.5 min
Oven Program On
90 °C for 5 min
then 5 °C/min to 130 °C for 0 min
then 40 °C/min to 260 °C for 5 min
Run Time 21.25 min

Front Injector
Syringe Size 10 µL
Injection Volume 2 µL
Injection Repetitions 1
Injection Delay 0 sec
Solvent A Washes (PreInj) 2
Solvent A Washes (PostInj) 4
Solvent A Volume 8 µL
Solvent B Washes (PreInj) 2
Solvent B Washes (PostInj) 4
Solvent B Volume 8 µL
Sample Washes 0
Sample Wash Volume 8 µL
Sample Pumps 6
Dwell Time (PreInj) 0 min
Dwell Time (PostInj) 0 min
Solvent Wash Draw Speed 300 µL/min
Solvent Wash Dispense Speed 6000 µL/min
Sample Wash Draw Speed 300 µL/min
Sample Wash Dispense Speed 6000 µL/min
Injection Dispense Speed 6000 µL/min
Viscosity Delay 0 sec
Sample Depth Disabled

Sample Overlap
Sample overlap is not enabled

Front SS Inlet He

Mode	Pulsed Splitless
Heater	On 250 °C
Pressure	On 9.954 psi
Total Flow	On 54 mL/min
Septum Purge Flow	On 3 mL/min
Gas Saver	On 20 mL/min After 2 min
Injection Pulse Pressure	20 psi Until 0.5 min
Purge Flow to Split Vent	50 mL/min at 2 min

Thermal Aux 2 {MSD Transfer Line}

Heater	On
Temperature Program	On
230 °C for 0 min	
Run Time	21.25 min

Column #1
DB-5ms: 1
DB-5ms
325 °C: 30 m x 250 µm x 0.25 µm
In: Front SS Inlet He
Out: Vacuum

(Initial)	90 °C
Pressure	9.954 psi
Flow	1 mL/min
Average Velocity	37.132 cm/sec
Holdup Time	1.3466 min
Flow Program	On
1 mL/min for 0 min	
Run Time	21.25 min

Signals

Test Plot	Save Off
	50 Hz
Test Plot	Save Off
	50 Hz
Test Plot	Save Off
	50 Hz
Test Plot	Save Off
	50 Hz

MS ACQUISITION PARAMETERS

General Information
------- -----------

Tune File : atune.u
Acquistion Mode : Scan

MS Information
-- -----------

Solvent Delay : 3.00 min

EMV Mode : Gain Factor
Gain Factor : 1.00
Resulting EM Voltage : 1153

[Scan Parameters]

Low Mass : 10.0
High Mass : 550.0
Threshold : 150
Sample # : 2 A/D Samples 4

[MSZones]

MS Source : 230 C maximum 250 C
MS Quad : 150 C maximum 200 C

Timed Events
----- ------

[Timed MS Detector Table Entries]

Time (min)	State (MS On/Off)
3.00	On
20.00	Off

END OF MS ACQUISITION PARAMETERS

TUNE PARAMETERS for SN: US71216291

Trace Ion Detection is ON.

EMISSION : 34.610
ENERGY : 69.922
REPELLER : 24.594
IONFOCUS : 90.157
ENTRANCE_LE : 32.000
EMVOLTS : 1082.353
Actual EMV : 1152.94
GAIN FACTOR : 0.99
AMUGAIN : 1691.000
AMUOFFSET : 123.813

FILAMENT : 2.000
DCPOLARITY : 0.000
ENTLENSOFFS : 17.569
MASSGAIN : -716.000
MASSOFFSET : -37.000

END OF TUNE PARAMETERS

END OF INSTRUMENT CONTROL PARAMETERS

---

^{2}H-Alanine Scan Mode Analysis Method

INSTRUMENT CONTROL PARAMETERS: GCMS

C:\MSDCHEM\1\METHODS\WILL'S METHODS\2H-ALANINE_1ul_20to1_SCANMODE.M
Wed Jan 08 11:58:52 2020

Control Information

Sample Inlet : GC
Injection Source : GC ALS
Mass Spectrometer : Enabled

Oven
Equilibration Time 0.5 min
Oven Program On
90 °C for 5 min
then 5 °C/min to 130 °C for 0 min
then 40 °C/min to 240 °C for 5 min
Run Time 20.75 min

Front Injector
Syringe Size 10 µL
Injection Volume 1 µL
Injection Repetitions 1
Injection Delay 0 sec
Solvent A Washes (PreInj) 2
Solvent A Washes (PostInj) 4
Solvent A Volume 8 µL
Solvent B Washes (PreInj) 2
Solvent B Washes (PostInj) 4
Solvent B Volume 8 µL
Sample Washes 0
Sample Wash Volume 8 µL
Sample Pumps 6
Dwell Time (PreInj) 0 min
Dwell Time (PostInj) 0 min
Solvent Wash Draw Speed 300 µL/min
Solvent Wash Dispense Speed 6000 µL/min
Sample Wash Draw Speed 300 µL/min
Sample Wash Dispense Speed 6000 µL/min
Injection Dispense Speed 6000 µL/min
Viscosity Delay 0 sec
Sample Depth Disabled

Sample Overlap
Sample overlap is not enabled

Front SS Inlet He
Mode Split

Heater On 250 °C
Pressure On 9.954 psi
Total Flow On 24 mL/min
Septum Purge Flow On 3 mL/min
Gas Saver On 20 mL/min After 2 min
Split Ratio 20 :1
Split Flow 20 mL/min

Thermal Aux 2 {MSD Transfer Line}
Heater On
Temperature Program On
230 °C for 0 min
Run Time 20.75 min

Column #1
DB-5ms: 1
DB-5ms
325 °C: 30 m x 250 µm x 0.25 µm
In: Front SS Inlet He
Out: Vacuum

(Initial) 90 °C
Pressure 9.954 psi
Flow 1 mL/min
Average Velocity 37.132 cm/sec
Holdup Time 1.3466 min
Flow Program On
1 mL/min for 0 min
Run Time 20.75 min

Signals
Test Plot Save Off
50 Hz
Test Plot Save Off
50 Hz
Test Plot Save Off
50 Hz
Test Plot Save Off
50 Hz

MS ACQUISITION PARAMETERS

General Information
------- -----------

Tune File : atune.u
Acquistion Mode : Scan

MS Information
-- -----------

Solvent Delay : 3.50 min

EMV Mode : Gain Factor
Gain Factor : 1.00
Resulting EM Voltage : 988

[Scan Parameters]

Low Mass : 10.0
High Mass : 550.0
Threshold : 150
Sample # : 2 A/D Samples 4

[MSZones]

MS Source : 230 C maximum 250 C
MS Quad : 150 C maximum 200 C

Timed Events
----- ------

[Timed MS Detector Table Entries]

Time (min)	State (MS On/Off)
3.50	On
20.00	Off

END OF MS ACQUISITION PARAMETERS

TUNE PARAMETERS for SN: US71216291

Trace Ion Detection is ON.

EMISSION : 34.610
ENERGY : 69.922
REPELLER : 24.092
IONFOCUS : 90.157
ENTRANCE_LE : 32.000
EMVOLTS : 894.118
Actual EMV : 894.118
GAIN FACTOR : 0.47
AMUGAIN : 1689.000
AMUOFFSET : 122.875
FILAMENT : 2.000
DCPOLARITY : 0.000
ENTLENSOFFS : 17.569
MASSGAIN : -716.000
MASSOFFSET : -37.000

END OF TUNE PARAMETERS

END OF INSTRUMENT CONTROL PARAMETERS

---

^{2}H-Alanine Pulsed Splitless Analysis Method

INSTRUMENT CONTROL PARAMETERS: GCMS

C:\MSDCHEM\1\METHODS\WILL'S METHODS\2H-ALANINE_2UL_PULSEDSPLITLESS_LONGWINDOW.M
Sat Jun 20 16:51:55 2020

Control Information
------- -----------

Sample Inlet : GC
Injection Source : GC ALS
Mass Spectrometer : Enabled

Oven
Equilibration Time 0.5 min
Oven Program On
90 °C for 5 min
then 5 °C/min to 115 °C for 0 min
then 40 °C/min to 260 °C for 5 min
Run Time 18.625 min

Front Injector
Syringe Size 10 µL
Injection Volume 2 µL
Injection Repetitions 1
Injection Delay 0 sec
Solvent A Washes (PreInj) 2
Solvent A Washes (PostInj) 4
Solvent A Volume 8 µL
Solvent B Washes (PreInj) 2
Solvent B Washes (PostInj) 4
Solvent B Volume 8 µL
Sample Washes 0
Sample Wash Volume 8 µL
Sample Pumps 6
Dwell Time (PreInj) 0 min
Dwell Time (PostInj) 0 min
Solvent Wash Draw Speed 300 µL/min
Solvent Wash Dispense Speed 6000 µL/min
Sample Wash Draw Speed 300 µL/min
Sample Wash Dispense Speed 6000 µL/min
Injection Dispense Speed 6000 µL/min
Viscosity Delay 0 sec
Sample Depth Disabled

Sample Overlap
Sample overlap is not enabled

Front SS Inlet He
Mode Pulsed Splitless
Heater On 250 °C
Pressure On 9.954 psi
Total Flow On 54 mL/min
Septum Purge Flow On 3 mL/min
Gas Saver On 20 mL/min After 2 min
Injection Pulse Pressure 20 psi Until 0.5 min
Purge Flow to Split Vent 50 mL/min at 0.5 min

Thermal Aux 2 {MSD Transfer Line}
Heater On
Temperature Program On
230 °C for 0 min
Run Time 18.625 min

Column #1
DB-5ms: 1
DB-5ms
325 °C: 30 m x 250 µm x 0.25 µm
In: Front SS Inlet He
Out: Vacuum

(Initial) 90 °C
Pressure 9.954 psi
Flow 1 mL/min
Average Velocity 37.132 cm/sec
Holdup Time 1.3466 min
Flow Program On
1 mL/min for 0 min
Run Time 18.625 min

Signals
Test Plot Save Off
50 Hz
Test Plot Save Off
50 Hz
Test Plot Save Off
50 Hz
Test Plot Save Off
50 Hz

MS ACQUISITION PARAMETERS

General Information
------- -----------

Tune File : atune.u
Acquistion Mode : SIM

MS Information
-- -----------

Solvent Delay : 3.00 min

EMV Mode : Gain Factor
Gain Factor : 1.00
Resulting EM Voltage : 1129

[Sim Parameters]

GROUP 1
Group ID : 1
Resolution : High
Plot 1 Ion : 99.00
Ions/Dwell In Group (Mass, Dwell) (Mass, Dwell)
(99.00, 10) (100.00, 10)

[MSZones]

MS Source : 230 C maximum 250 C
MS Quad : 150 C maximum 200 C

Timed Events
----- ------

[Timed MS Detector Table Entries]

Time (min)	State (MS On/Off)
6.00	On
14.00	Off

END OF MS ACQUISITION PARAMETERS

TUNE PARAMETERS for SN: US71216291

Trace Ion Detection is ON.

EMISSION : 34.610
ENERGY : 69.922
REPELLER : 24.594
IONFOCUS : 90.157
ENTRANCE_LE : 32.000
EMVOLTS : 1035.294
Actual EMV : 1129.41
GAIN FACTOR : 1.01
AMUGAIN : 1689.000
AMUOFFSET : 124.313
FILAMENT : 2.000
DCPOLARITY : 0.000

ENTLENSOFFS : 16.565
MASSGAIN : -716.000
MASSOFFSET : -37.000

END OF TUNE PARAMETERS

END OF INSTRUMENT CONTROL PARAMETERS
